Journal of Algebra 517 (2019) 457–512

Contents lists available at ScienceDirect

Journal of Algebra

www.elsevier.com/locate/jalgebra

Tropical geometry of genus two curves

Maria Angelica Cueto [a], Hannah Markwig [b,*]

[a] *Mathematics Department, The Ohio State University, 231 W 18th Ave, Columbus, OH 43210, USA*
[b] *Eberhard Karls Universität Tübingen, Fachbereich Mathematik, Auf der Morgenstelle 10, 72108 Tübingen, Germany*

ARTICLE INFO

Article history:
Received 15 January 2018
Available online 24 September 2018
Communicated by Seth Sullivant

MSC:
primary 14T05, 14H45
secondary 14Q05, 14G22

Keywords:
Tropical geometry
Tropical modifications
Faithful tropicalizations
Berkovich spaces
Hyperelliptic covers
Igusa invariants

ABSTRACT

We exploit three classical characterizations of smooth genus two curves to study their tropical and analytic counterparts. First, we provide a combinatorial rule to determine the dual graph of each algebraic curve and the metric structure on its minimal Berkovich skeleton. Our main tool is the description of genus two curves via hyperelliptic covers of the projective line with six branch points. Given the valuations of these six points and their differences, our algorithm provides an explicit harmonic 2-to-1 map to a metric tree on six leaves. Second, we use tropical modifications to produce a faithful tropicalization in dimension three starting from a planar hyperelliptic embedding.

Finally, we consider the moduli space of abstract genus two tropical curves and translate the classical Igusa invariants characterizing isomorphism classes of genus two algebraic curves into the tropical realm. While these tropical Igusa functions do not yield coordinates in the tropical moduli space, we propose an alternative set of invariants that provides new length data.

* Corresponding author.
E-mail addresses: cueto.5@osu.edu (M.A. Cueto), hannah@math.uni-tuebingen.de (H. Markwig).

https://doi.org/10.1016/j.jalgebra.2018.08.034
0021-8693/

1. Introduction

Algebraic smooth genus two curves defined over an algebraically closed non-Archimedean valued field K, with residue field $\widetilde{K}$ of $\operatorname{char}\widetilde{K} \neq 2$ can be studied from three perspectives:

(i) as a planar curve defined by a (dehomogeneized) hyperelliptic equation:

$$y^2 = u\prod_{i=1}^{6}(x-\alpha_i)\,; \tag{1.1}$$

(ii) as a K-point of the space M_2 of smooth genus two curves;
(iii) as a hyperelliptic cover of $\mathbb{P}^1_K$ with six simple branch points $\alpha_1,\dots,\alpha_6 \in \mathbb{P}^1_K$.

The hyperelliptic cover is determined, up to isomorphism, by a choice of six branch points, i.e., by a K-point in the space $M_{0,6}$ of smooth rational curves with six marked points.

The top row in Fig. 1.1 contains the three relevant spaces and maps between them. The first and third characterizations are related by a projection to the x-coordinate and a forgetful map that disregards the planar embedding of the curve induced by (1.1).

The present paper exploits the aforementioned description to characterize the tropical and Berkovich non-Archimedean analytic counterparts of smooth genus two curves. It relies on known comparison methods between the moduli of (stable) algebraic and abstract tropical curves via the vertical tropicalization maps from Fig. 1.1 [1,14,18]. Such curves come in seven combinatorial types, and they form a poset under degenerations. Their associated Berkovich skeleta are obtained as dual metric graphs to the central fiber of a semistable regular model of each input curve over the valuation ring K° of K [5,51]. Each vertex in the graph is assigned the genus of the corresponding irreducible component as its weight. The induced poset of skeleta is depicted on the left of Fig. 1.2. The good reduction case is the only smooth one and it corresponds to Type (VII). The *tropical moduli space* of abstract genus two tropical curves M_2^{trop} is obtained as the image of $M_2(K)$ under the tropicalization map [1, Theorem 1.2.1]. It has the structure of a stacky fan with seven cones, each labeled by a type and isomorphic to an orthant of dimension equal to the number of edges on the skeleton [1,16,18]. We discuss this space in more detail in Section 2.

The tropical moduli space $M_{0,6}^{\mathrm{trop}}$ of rational tropical curves with six marked points is the space of phylogenetic trees on six leaves of Billera–Holmes–Vogtmann [7]. It is realized as the image of $M_{0,6}(K)$ under the vertical tropicalization map in Fig. 1.1, i.e., by taking coordinatewise negative valuations of all K-points of $M_{0,6}$ embedded in the toric variety defined by the pointed fan $M_{0,6}^{\mathrm{trop}} \subset \mathbb{R}^9$. This map and the combinatorial structure of $M_{0,6}^{\mathrm{trop}}$ are also discussed in Section 2.

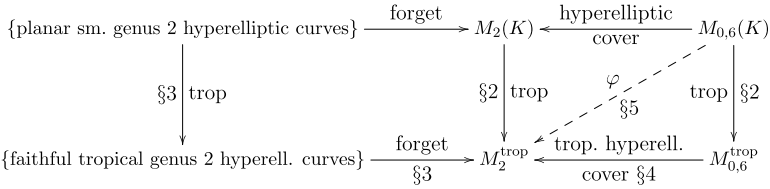

Fig. 1.1. Three ways to represent genus two curves, their relations, and their tropical analogues.

As in the algebraic case, abstract genus two tropical curves are hyperelliptic: they admit a tropical hyperelliptic cover of a metric tree with six markings, given by a 2-to-1 harmonic map branched at all six legs of the tree [3,18]. We review this construction in Section 4. The tropical covers turn the right square of Fig. 1.1 into a commuting diagram, but the assignment is not explicit: it requires prior knowledge of each Berkovich skeleton. We bypass this difficulty by factoring the right square of the diagram through the map φ. The assignment depends on the valuations of the points $\alpha_1, \ldots, \alpha_6 \in K^*$ and their differences:

$$\omega_i := -\operatorname{val}(\alpha_i) \text{ for } i = 1, \ldots, 6, \text{ and } d_{ij} := -\operatorname{val}(\alpha_i - \alpha_j) \text{ for } i < j, \text{ if } \omega_i = \omega_j. \quad (1.2)$$

Here is our first main result, which we discuss in Section 5:

Theorem 1.1. *Each point in M_2^{trop} together with an explicit harmonic 2-to-1 map to a metric tree in $M_{0,6}^{trop}$ is determined by the ordering of the quantities ω_i and d_{ij} (see Table 5.1).*

For example, the two maximal cells in M_2^{trop} correspond to the orders $\omega_1 < \omega_2 < \omega_3 < \omega_4 < \omega_5 < \omega_6$ (the dumbbell graph (I)) and $\omega_1 < \omega_2 < \omega_3 \leq \omega_4 < \omega_5 < \omega_6$ with $d_{34} < \omega_3$ (the theta graph (II)). They are realized as 2-to-1 harmonic covers of the caterpillar and snowflake trees as shown in Fig. 1.2. Similar results were obtained earlier by Ren–Sam–Sturmfels [46, Table 3] but with very different methods.

Our proof of Theorem 1.1 is sketched in the right of Fig. 1.2. Starting from $\mathbb{TP}^1$, tropical modifications of $\mathbb{TP}^1$ at the locations of the points ω_i dictated by the quantities d_{ij} allow us to construct the target metric trees. The source curve and the map are determined by the tropical Riemann–Hurwitz formula [13]. Proposition 5.2 provides a list of seven regions in $M_{0,6}(K)$ that surject onto M_2^{trop}. Algorithms 5.1 and 5.2 take six arbitrary points in $(K^*)^6$ and return a linear change of coordinates of $\mathbb{P}^1$ that sends these six points to one of these seven witness regions. The same techniques will lead to a natural extension of Theorem 1.1 to the tropical hyperelliptic locus in M_g^{trop} for any $g \geq 2$.

The left side of Fig. 1.1 involves embedded tropicalizations. Given the hyperelliptic equation (1.1) defining a smooth genus two curve $\mathcal{X}$, the tropical plane curve $\operatorname{Trop}\mathcal{X} \subset \mathbb{R}^2$ is the dual complex of the Newton subdivision of $\mathcal{X}$. An explicit calculation shown in Table 6.1 proves that the planar tropicalization is always a tree, so it

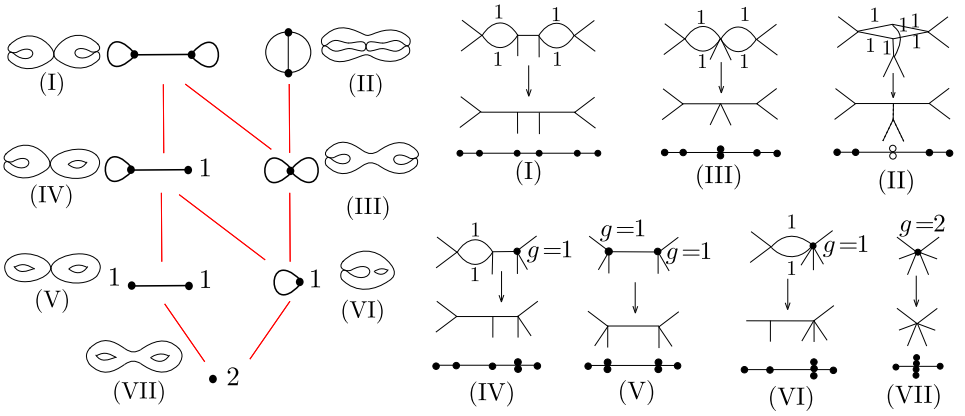

Fig. 1.2. From left to right: poset of stable genus two curves, and their weighted dual graphs encoding the genus and intersections of all components; harmonic 2-to-1 covers of tropical lines with six legs for each type, and ordering of the valuations of the six branch points. All edge weights in the source curve equal two or one (indicated). All vertices in the source curves have genus zero, unless otherwise indicated. The unfilled points in type (II) share initial terms and yield a dashed branch on the metric tree.

does not reflect the genus of our algebraic curve. Thus, outside Types (V) and (VII), the minimal Berkovich skeleton of $\mathcal{X}^{\mathrm{an}}$ will not map isometrically to a subgraph of $\operatorname{Trop}\mathcal{X}$ under the hyperelliptic tropicalization map $\operatorname{trop}\colon \mathcal{X}^{\mathrm{an}} \to \operatorname{Trop}\mathcal{X}$. The forgetful map on the bottom left of Fig. 1.1 is analogous to the retraction map of $\mathcal{X}^{\mathrm{an}}$ onto the minimal Berkovich skeleton: it shrinks all unbounded edges of the tropical curve and contracts edges adjacent to one-valent vertices if they correspond to a rational initial degeneration of $\mathcal{X}$. The map is further described in Section 3, and it will only be defined if the tropicalization is faithful.

Faithful tropicalizations are a powerful tool to study non-Archimedean curves through combinatorial means [5]. In [20], we proposed a program for effectively producing faithfulness for curves over non-Archimedean fields, starting in genus one. Our second main result shows that similar methods can be used to faithfully re-embed genus two curve in three-space in a uniform fashion. The explicit construction is the subject of Section 6 and it relies on the notion of tropical modifications, which we review in Section 3.

Theorem 1.2. *Outside Types (V) and (VII), the naïve tropicalization induced by the hyperelliptic equation can be repaired in dimension three by adding one equation of the form $z - f(x,y)$ where f is linear in y and quadratic in x. The re-embedded tropical curve contains an isometric copy of the minimal Berkovich skeleton (see Table 6.1 and Fig. 6.9).*

A precise formula for $f(x,y)$ can be found in (6.2). An alternative refinement of this polynomial, denoted by $\tilde{f}(x,y)$ in (6.5) will sometimes be used to simplify the combinatorics.

In concrete computations, it is always desirable to bound the ambient dimension required to achieve faithful tropicalizations on minimal skeleta. In genus two, Wagner [52] showed that, under certain length restrictions, any Mumford curve (curves with totally

degenerate reduction, namely Types (I), (II) and (III)) can be embedded faithfully in dimension three. Starting from the Schottky uniformization [25] of the given Mumford curve, his techniques involve tropical Jacobians, together with an explicit description of the Abel–Jacobi map and they apply not only to the minimal Berkovich skeleta but also to unbounded subgraphs of extended skeleta.

Theorem 1.2 recovers the same dimension bound for every curve of genus two where the curve is given by its hyperelliptic equation. In addition to contributing a larger class of curves where the same bound can be attained, our techniques have the additional advantage of extending to the whole hyperelliptic locus in any genus. Generalizations of this result to extended skeleta are also treated in Section 6.

Remark 1.3 *(**Algorithmic faithful tropicalization in genus** 2).* Theorems 1.1 and 1.2 can be combined with Algorithms 5.1 and 5.2 to produce an explicit algorithm that inputs a hyperelliptic equation of the curve $\mathcal{X}$ and outputs a faithful tropicalization. Indeed, starting from the six branch points $\alpha_1, \ldots, \alpha_6$ of the cover, we use Algorithms 5.1 and 5.2 to construct an automorphism of the projective line that places the branch points in one of the seven special configurations described in Table 5.1. This step recovers the type of the Berkovich skeleton of $\mathcal{X}^{\mathrm{an}}$. With this knowledge, after shifting two of the branch points to be the origin and the point at infinity via Lemma 6.1, we can pick the appropriate function $f(x, y)$ (which depends on the branch points) that gives the faithful embedding for the minimal Berkovich skeleton by Theorem 1.2. As a result, we obtain an explicit projective model for the input curve $\mathcal{X}$ in dimension three where we detect the topological type of its Berkovich analytification through its embedded tropicalization. In case we wish to recover faithfulness on the extended skeleta we must refine our choice of $f(x, y)$ and perform further linear re-embeddings. These refined methods are type-dependent. We explain them in detail in Subsections 6.1–6.6.

A second motivation for Theorems 1.1 and 1.2 and the explicit description of the diagonal map φ from Fig. 1.1 originates in the invariant theory of M_2 [33] and the search for a coordinate system for M_2^{trop}. Defining complete sets of tropical invariants for each cell in the tropical hyperelliptic locus from their algebraic counterparts is challenging already in small genera. The genus one case is well-understood. The j-invariant has its tropical analog: the tropical j-invariant. It arises as the expected negative valuation of the j-invariant by using the conductor-discriminant formula for Weierstrass equations [37]. This tropical invariant defines a piecewise linear function on the space of smooth tropical plane cubics (i.e., the identity on M_1^{trop}) and it is crucial in tropical enumerative geometry of genus one curves [38].

In the algebraic setting, the isomorphism classes of curves of genus two are determined by the three (absolute) *Igusa invariants* [33]. They can be expressed as rational functions on all pairwise differences of the six ramification points [27]. From a computational perspective, they can be viewed as a coordinate-dependent interpretation of the top row in Fig. 1.1. We refer to Section 7 for the precise definitions.

Any point on a maximal cell in M_2^{trop} is determined by three edge lengths: L_0, L_1 and L_2 in Fig. 2.1. In analogy with recent work of Helminck [32], our third main result relates these three numbers to the tropicalization of the Igusa invariants, but confirms that these classical invariants are not well suited for tropicalization:

Theorem 1.4. *The tropicalization of the Igusa invariants j_1, j_2 and j_3 are piecewise linear functions in M_2^{trop}, with domains of linearity given by the seven cones in M_2^{trop}. They do not form a complete set of invariants in M_2^{trop} since $j_{i\,\bigcirc\!\!\!\!\bigcirc}^{trop} = L_1+L_0+L_2$ for all $i = 1, 2, 3$, whereas $j_{1\,\circ\!-\!\circ}^{trop} = L_1+12L_0+L_2$, and $j_{2\,\circ\!-\!\circ}^{trop} = j_{3\,\circ\!-\!\circ}^{trop} = L_1+8L_0+L_2$ whenever* $\operatorname{char} \widetilde{K} \neq 2, 3$.

Replacing j_3 by the new invariant $j_4 = j_2 - 4j_3$ induces a piecewise linear function on M_2^{trop} with $j_{4\,\bigcirc\!\!\!\!\bigcirc}^{trop} = L_0 + L_1 + L_2 - \min\{L_0, L_1, L_2\}$, and $j_{4\,\circ\!-\!\circ}^{trop} = L_1 + 8L_0 + L_2$ when $\operatorname{char} \widetilde{K} \neq 2, 3$. *The tropicalization of the invariants $\{j_1, j_2, j_4\}$ recovers two of the three edge lengths on each point in the tropical moduli space. Similar formulas hold if* $\operatorname{char} \widetilde{K} = 3$.

The ill-behavior of the Igusa invariants under tropicalizations is similar to a phenomenon occurring in the ring of symmetric polynomials: power sums will never yield a complete set of tropical invariants. Indeed, their valuation only captures the root with lowest valuation. In turn, the elementary symmetric functions enable us to recover the valuation of all roots. Theorem 1.4 manifests again the non-faithfulness of the hyperelliptic embedding and shows that faithfulness should be viewed as the natural replacement for the tropical Igusa invariants. It remains an interesting challenge to find three new algebraic invariants on M_2 inducing tropical coordinates on each cell of M_2^{trop}.

Supplementary material

Many results in this paper rely on calculations performed with `Singular` [21] (including its `tropical.lib` library [36]), `Macaulay2` [28], `Polymake` [24] and `Sage` [49]. We have created supplementary files so that the reader can reproduce all the claimed assertions done via explicit computations and numerical examples. The files are available at:

https://people.math.osu.edu/cueto.5/tropicalGeometryGenusTwoCurves/

In addition to all `Sage` scripts, the website contains all input and output files both as `Sage` object files and in plain text. We have also included the supplementary files on the latest `arXiv` submission of this paper. They can be obtained by downloading the source.

2. Tropical moduli spaces

In this section, we introduce the objects in the center and right of Fig. 1.1 involving abstract tropical curves and their moduli spaces.

Definition 2.1. An *abstract tropical curve* is a connected metric graph consisting of the data of a triple $\Gamma = (G, g, \ell)$ where $G = (V, E, L)$ is a connected graph G with vertices V, edges E and unbounded legs L (called *markings*), together with a weight function $g\colon V \to \mathbb{Z}_{\geq 0}$ on vertices and a length function $\ell\colon E \to \mathbb{R}_{>0}$ on edges. Legs are considered to have infinite length. In the absence of legs, we say the curve has no markings. The genus of a metric graph Γ equals

$$\operatorname{genus}(\Gamma) := b_1(\Gamma) + \sum_{v \in V} g(v), \tag{2.1}$$

where $b_1(\Gamma) = |E| - |V| + 1$ is the first Betti number of the graph G. A genus zero curve is called *rational*: it corresponds to a metric tree with constant weight function $g \equiv 0$.

An *isomorphism* of a tropical curve is an automorphism of the underlying graph G that respects both the length and weight functions. The *combinatorial type* of a tropical curve is obtained by disregarding the metric structure, i.e. it is given by (G, g).

The set of all tropical curves with a given a combinatorial type (G, g) can be parameterized by the quotient of an open cone $\mathbb{R}^E_{>0}$ under the action of automorphisms of G that preserve the weight function g. Cones corresponding to different combinatorial types can be glued together by collapsing edges and adjusting the genus function accordingly. Such operations keep track of possible degenerations of the algebraic curves. Fig. 1.2 describes this process for unmarked genus two curves. In this way, the tropical moduli space $M^{\mathrm{trop}}_{g,n}$ (respectively, M^{trop}_g) of n-marked (respectively, unmarked) curves of genus g inherits the structure of an abstract cone complex. For more details on tropical moduli spaces of curves, we refer to [1,16,18,23,44].

In this paper, we focus on two examples: $M^{\mathrm{trop}}_{0,6}$ and M^{trop}_2. The first is the space of rational tropical curves with six markings. Up to relabeling of the markings, the moduli space $M^{\mathrm{trop}}_{0,6}$ has two top-dimensional cells, corresponding to the snowflake and caterpillar trees on six leaves. The second object of interest is the space of genus two tropical curves with no marked legs. Fig. 1.2 shows the labeling of the two top-dimensional cones: the dumbbell and theta graphs, indicated by Types (I) and (II).

The connection between moduli spaces of stable marked curves and their counterparts in tropical geometry has been studied on various occasions [1,26,46]. The spaces $M_{0,n}$ can be identified with a quotient of the open orbit of the cone over the Grassmannian of planes by the torus $(K^*)^n$ and tropicalized thereafter, as in [46]. In turn, $M^{\mathrm{trop}}_{0,n}$ becomes the space of trees on n leaves [48,50] where we assign length zero to all leaf edges, as we now explain.

Up to an automorphism of $\mathbb{P}^1$ we may assume that our marked points exclude $(1:0)$ and $(0:1)$, so we identify them with a tuple in $\underline{\alpha} \in (K^*)^n$. The torus $(K^*)^n$ acts on $\mathbb{G}\mathrm{r}_0(2,n)$ by $\underline{t} \star (p_{ij})_{i,j} = (t_i t_j p_{ij})_{i,j}$. In particular, we get an isomorphism

$$\Phi\colon M_{0,n} \xrightarrow{\simeq} \mathbb{G}\mathrm{r}_0(2,n)/(K^*)^n \subset (K^*)^{\binom{n}{2}}/(K^*)^n \qquad \Phi(\underline{\alpha}) = (\alpha_i - \alpha_j)_{1 \leq i < j \leq n}, \tag{2.2}$$

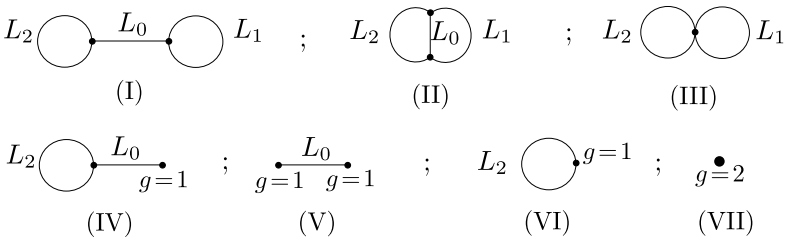

Fig. 2.1. Minimal skeleta of genus two curves obtained by applying the forgetful map to the double covers in the right of Fig. 1.2.

The space $\overline{M}_{0,n}$ of stable rational curves with n marked points is the tropical compactification of $M_{0,n}$ induced by $M_{0,n}^{\mathrm{trop}} := \mathrm{Trop}\ \mathbb{G}\mathrm{r}_0(2,n)/\mathbb{R}^n \subset \mathbb{R}^{\binom{n}{2}}/\mathbb{R}^n$ [50, Theorem 5.5]. Here, $\mathbb{R}^n \subset \mathbb{R}^{\binom{n}{2}}$ is the image of the linear map $\underline{\alpha} \mapsto (\alpha_i + \alpha_j)_{i,j}$. This is precisely the lineality space of $\mathrm{Trop}\ \mathbb{G}\mathrm{r}_0(2,n)$. It is generated by the n cut-metrics [48].

The lattice spanned by the cut-metrics has index two in its saturation in $\mathbb{Z}^{\binom{n}{2}}$. For this reason, a factor of $1/2$ must be added when considering lattice lengths on the space of trees (see [29, Section 3.1].) In particular, when $n = 6$, the tropicalization map sends a tuple $\underline{\alpha}$ of six distinct points in K^* to the pairwise *half*-distances between the legs of the corresponding tree on six leaves:

$$\mathrm{trop}\colon M_{0,6}(K) \to M_{0,6}^{\mathrm{trop}} \subset \mathbb{R}^{15}/\mathbb{R}^6 \qquad \mathrm{trop}(\underline{\alpha}) = (-\operatorname{val}(\alpha_i - \alpha_j))_{1\leq i<j\leq 6}. \tag{2.3}$$

All seven combinatorial types of trees with six leaves are depicted in the right of Fig. 1.2. The poset structure of all labeled seven cells matches that of stable genus two curves and their tropical counterparts. Furthermore, the space M_2^{trop} can be constructed from $M_{0,6}^{\mathrm{trop}}$ via tropical hyperelliptic covers as in Section 4. Indeed, starting from a metric tree T with six leaves, there is a unique tropical hyperelliptic cover of it by a tropical curve Γ of genus two with six legs. Our genus two abstract tropical curve will be obtained as the image of Γ under the *tropical forgetful map* that contracts all legs and, in turn, all edges adjacent to one-valent vertices of genus zero [10]. This identification describes the commuting right square of Fig. 1.1, as proved in [46, Theorem 5.3].

The tropicalization map $\mathrm{trop}\colon M_2(K) \to M_2^{\mathrm{trop}}$ factors through $\mathrm{trop}\colon {M_2}^{\mathrm{an}} \twoheadrightarrow M_2^{\mathrm{trop}}$ [1, Theorem 1.2.1]. Under this map, abstract tropical curves correspond to the minimal Berkovich skeleta: metrized dual graphs of central fibers of semistable regular models of a smooth curve over the valuation ring K° [5,51].

3. Faithful tropicalization, skeleta and tropical modifications

In this section, we discuss embedded tropicalizations of curves and their relation to abstract tropical curves and their moduli. Embedded tropical curves are determined by the negative valuations of all K-points on a curve $\mathcal{X}$ inside the multiplicative split torus $(K^*)^n$ [41, Chapter 3]: they are balanced weighted graphs in $\mathbb{R}^n$ with rational slopes.

While this approach is computationally advantageous due to its connection to Gröbner degenerations [35] it also poses a major challenge: tropicalization in this setting strongly depends on the embedding. Furthermore, certain features of an abstract tropical curve can be lost under a given choice of coordinates. For example, the naïve tropicalization of a genus two hyperelliptic plane curve induced by (1.1) is a graph $\Gamma \subset \mathbb{R}^2$ with $b_1(\Gamma) = 0$.

The connection to Berkovich non-Archimedean spaces [6] initiated by Payne [45] hands us a way to overcome this coordinate-dependency: a faithful tropicalization is the best candidate to reflect relevant geometric properties of the algebraic curve [5]. An embedding $\mathcal{X} \subset (K^*)^n$ induces a *faithful tropicalization* if $\operatorname{Trop}\mathcal{X}$ contains an isometric copy of the minimal Berkovich skeleton of $\mathcal{X}^{\mathrm{an}}$ under the tropicalization map $\operatorname{trop}\colon \mathcal{X}^{\mathrm{an}} \to \operatorname{Trop}\mathcal{X}$. The latter can be obtained from a given (extended) skeleton by contracting it to its minimal expression [4].

Just as in the abstract setting, faithful tropicalizations induced by $\mathcal{X} \subset (K^*)^n$ admit a tropical forgetful map to M_g^{trop}, where g is the arithmetic genus of $\mathcal{X}$. In order to do so, we must endow the rational weighted balanced graph $\Gamma = \operatorname{Trop}\mathcal{X}$ in $\mathbb{R}^n$ with a weight function on its vertices. This can be achieved by means of an extended Berkovich skeleton $\Sigma(\mathcal{X})$ coming from a semistable model of $\mathcal{X}$ with a horizontal divisor (i.e. the closure of a divisor of the generic fiber in the model) that is compatible with Γ [30,31]. Indeed, to each vertex v in Γ we assign the sum of the genera of all semistable vertices of $\Sigma(\mathcal{X})$ mapping to v under $\operatorname{trop}\colon \Sigma(\mathcal{X}) \to \operatorname{Trop}\mathcal{X}$. The semistable vertices correspond exactly to the components of the central fiber [4], so we weigh them with the genus of the associated component.

For planar tropicalizations, a similar ad-hoc rule can be put in practice. If we let Γ be the dual complex of the Newton subdivision of the corresponding curve, each vertex of Γ gets assigned the number of interior lattice points of its dual polygon. This quantity is the genus of the initial degeneration of the curve induced by the vertex minus the number of nodes (assuming it is nodal). However, unless our planar embedding is faithful (which only occurs for Types (V) and (VII)), we will not be able to define a forgetful map on the tropical side (by collapsing all legs and weight zero one-valent vertices, as we did in the abstract case) that recovers the image of the Berkovich skeleton under tropicalization.

In the algebraic setting, the forgetful map sending planar genus two smooth hyperelliptic curves to points in $M_2(K)$ is surjective if we allow the curves to be defined over valued field extensions $L|K$. Since the forgetful map on the associated tropical plane curves is only defined for Types (V) and (VII), faithfulness becomes an essential property to define the left square in Fig. 1.1. A similar behavior in genus three and four was encountered by Brodsky–Joswig–Morrison–Sturmfels [10, Theorems 5.1 and 7.1]. Section 6 and Table 6.1 give explicit effective methods for producing *faithful re-embeddings* of smooth planar genus two curves in a suitable torus. The main technique involved is tropical modifications of $\mathbb{R}^n$ along tropical divisors [12,34,43], which we now recall.

Definition 3.1. Fix a tropical polynomial F defining a piecewise linear function

$$F\colon \mathbb{R}^n \to \mathbb{T} = \mathbb{R} \cup \{-\infty\} \quad F(\underline{X}) = \max_{\beta \in \mathbb{Z}^n_{\geq 0}} \{C_\beta + \beta_1 X_1 + \ldots + \beta_n X_n\} \text{ in } \mathbb{T}[X_1, \ldots, X_n].$$

The graph of F is a rational polyhedral complex of pure dimension n. Unless F is linear, the bend locus of F has codimension 1. At each break codimension-one cell σ, we attach a new cell $\widetilde{\sigma}$ spanned by σ and $-e_{n+1} := (0, \ldots, 0, -1)$. The result is a pure rational polyhedral complex in $\mathbb{R}^{n+1}$. We call it the *tropical modification of* $\mathbb{R}^n$ *along* F.

It will often be useful to consider *polynomial lifts* of F, namely

$$f(\underline{x}) = \sum_{\beta \in \operatorname{supp}(F)} c_\beta \underline{x}^\beta \in K[x_1, \ldots, x_n] \qquad \text{where} \qquad \operatorname{supp}(F) := \{\beta\colon C_\beta \neq -\infty\} \quad (3.1)$$

satisfies $\operatorname{trop}(f)(\underline{X}) := \max_\beta\{-\operatorname{val}(c_\beta) + \beta_1 X_1 + \ldots + \beta_n X_n\} = F(\underline{X})$ as functions on $\mathbb{R}^n$.

By the Structure Theorem [41, Proposition 3.1.6], any polynomial lift f of F will allow us to turn the tropical modification of $\mathbb{R}^n$ along F into a weighted balanced complex, since it will be supported on the tropical hypersurface $\operatorname{Trop} V(f)$. In turn, any tropical hypersurface $\operatorname{Trop} V(g)$ in $\mathbb{R}^n$ can be modified along F in a similar fashion and the attached cells can be endowed with suitable multiplicities to turn the resulting complex into a balanced one. For precise multiplicity formulas, we refer to [2, Construction 3.3].

Example 3.2. The leftmost map in Fig. 5.1 describes the tropical modification of $\mathbb{R}$ along the tropical function $F = \max\{X, -\operatorname{val}(\alpha_2)\} = \operatorname{trop}(x - \alpha_2)$. The result is a tropical line in $\mathbb{R}^2$ with vertex $(-\operatorname{val}(\alpha_2), -\operatorname{val}(\alpha_2))$. All its tropical multiplicities equal 1. A higher dimensional analog can be found in Example 3.4. $\diamond$

Tropical modifications can be used to define re-embeddings of irreducible plane curves $\mathcal{X}$ [12,20,34]. This technique is also known as tropical refinement in parts of the literature. Consider a tropical polynomial $F \in \mathbb{T}[X, Y]$ and a lift f. Given a defining equation $g(x, y)$ for $\mathcal{X}$, the tropicalization of the ideal

$$I_{g,f} := \langle g, z - f \rangle \subset K[x^{\pm}, y^{\pm}, z^{\pm}] \quad (3.2)$$

is a tropical curve in the modification of $\mathbb{R}^2$ along F. For almost all lifts f, $\operatorname{Trop} V(I_{g,f})$ coincides with the modification of $\operatorname{Trop} V(g)$ along F, i.e. we only bend $\operatorname{Trop} V(g)$ so that it fits the graph of F and attach suitable weighted downward legs. However, for some special choices of lifts f, the cells of $\operatorname{Trop} V(I_{g,f})$ in the downward cells of the modification of $\mathbb{R}^n$ along F become more interesting. Such choices are determined by the initial degenerations of g along the bend locus of F. More details can be found in Section 6.

In addition to linear tropical polynomials, which were the main players in [20], our main focus in Section 6 will be modifications of $\mathbb{R}^2$ along tropical polynomials of the form

$$F = \max\{Y, A + X, B + 2X\} = \operatorname{trop}(f) \qquad \text{for } A, B \in \mathbb{R}. \tag{3.3}$$

The tropical surface $\operatorname{Trop} V(f)$ consists of six two-dimensional cells $\sigma_1, \ldots, \sigma_6$, as depicted in Fig. 3.1. They are defined by the following systems of linear equations and inequalities:

$$\begin{aligned}
\sigma_1 &:= \{Z = X + A \geq Y, X \leq A - B\}, & \sigma_4 &:= \{Z, Y \leq 2A - B, X = A - B\},\\
\sigma_2 &:= \{Z = 2X + B \geq Y, X \geq A - B\}, & \sigma_5 &:= \{Y = 2X + B \geq Z, X \geq A - B\},\\
\sigma_3 &:= \{Z = Y \geq X + A, 2X + B\}, & \sigma_6 &:= \{Y = X + A \geq Z, X \leq A - B\}.
\end{aligned} \tag{3.4}$$

Just as it happened in the linear case [20, Lemma 2.2], the choice of F in (3.3) allows us to recover $\operatorname{Trop} V(I_{g,f})$ in $\mathbb{R}^3$ from the three coordinate projections. This property will be exploited in Section 6 to certify faithfulness by planar computations.

Lemma 3.3. *Given an irreducible curve $\mathcal{X} \subset (K^*)^2$ defined by a polynomial $g \in K[x, y]$ and a polynomial lift $f(x, y) = y - ax - bx^2 \in K[x, y]$ of the tropical polynomial F from (3.3), the tropicalization induced by the ideal $I_{g,f} = \langle g, z - f\rangle \subset K[x^{\pm}, y^{\pm}, z^{\pm}]$ is completely determined by the tropical plane curves $\operatorname{Trop} V(g)$, $\operatorname{Trop} V(I_{g,f} \cap K[x^{\pm}, z^{\pm}])$, and $\operatorname{Trop} V(I_{g,f} \cap K[y^{\pm}, z^{\pm}])$.*

Proof. Since coordinate projections are monomial maps, functoriality ensures that the three coordinate projections of $\operatorname{Trop} V(I_{g,f})$ are supported on the three tropical plane curves in the statement. The tropical space curve is completely determined by its intersection with the relative interiors of the six maximal cells of $\operatorname{Trop} V(f)$. By construction, each open cell σ_i° maps to a two-dimensional open region under two out of the three projections. The precise choices are indicated on Fig. 3.1. Note that overlaps occur only in the YZ-projection between two pairs of cells: (σ_1, σ_4) and (σ_4, σ_6).

The tropical multiplicities in all coordinate projections let us recover the support of $\operatorname{Trop} V(I_{g,f})$ along the bend locus from the generalized push-forward formula for multiplicities of Sturmfels–Tevelev in the non-constant coefficients case [5, Corollary 7.3]. □

Example 3.4. Consider the smooth genus two curve in $(K^*)^2$ defined over $\mathbb{C}\{\{t\}\}$ by

$$g(x, y) = y^2 - x(x - (3t^5)^2)(x - (11t^2 + 5t^7)^2)(x - (11t^2)^2)(x + (1 + t^2)^2),$$

the tropical polynomial $F = \max\{Y, -4 + X, 2X\}$ and its lift $f(x, y) = y - (1 + t^2)(11t^2 + 5t^7)(11t^2)\, x + (1 + t^2)\, x^2$. The tropicalization induced by $I_{g,f} \subset K[x^{\pm}, y^{\pm}, z^{\pm}]$ is depicted in the left of Fig. 3.1 and it lies in the tropical surface in $\mathbb{R}^3$ obtained by modifying

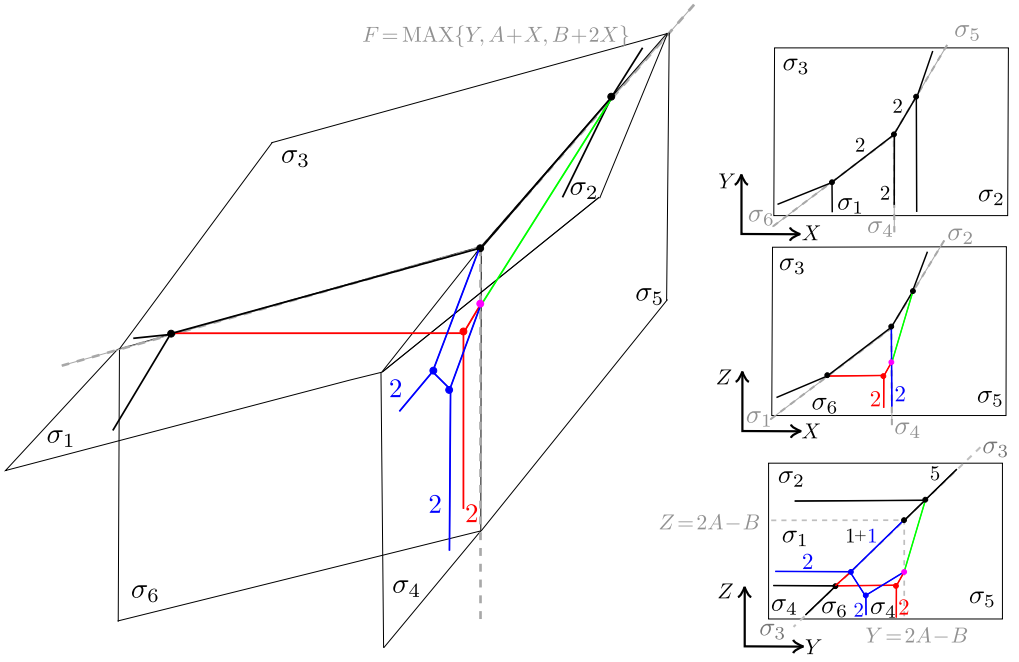

Fig. 3.1. A tropical modification of $\mathbb{R}^2$ and its coordinate projections.

$\mathbb{R}^2$ along F. We reconstruct the tropical curve from the three coordinate projections shown on the right of the picture, accounting for additivity of multiplicities and the two *false crossings* on the YZ-projection. The naïve plane tropicalization agrees with the XY-projection. The Berkovich skeleton is a theta graph. For further details we refer to Example 6.12. ◇

4. Tropical hyperelliptic covers of metric trees

Algebraic genus two curves are hyperelliptic and hence can be realized as the source curve of a 2-to-1 cover of the projective line branched at six points. The analogous results for tropical hyperelliptic genus g curves and metric trees with $n = 2g + 2$ legs and genus zero vertices was first established by Baker–Norine [3] and Chan [19], and later generalized to admissible covers and harmonic morphisms by Caporaso [15] and Cavalieri–Markwig–Ranganathan [17]. We restrict the exposition to our case of interest.

Definition 4.1. A map $\pi\colon \Gamma \to \Gamma'$ is a morphism of metric graphs if π sends the vertices of Γ to vertices of Γ', and the edges (respectively, legs) of Γ to edges (respectively, legs) of Γ' in a piecewise fashion with integral slopes.

Remark 4.2. Assume the morphism π sends an edge e of Γ with length $\ell(e)$ onto an edge e' of Γ' of length $\ell(e')$. We may write the map $\pi_{|_e}$ as $h\colon [0, \ell(e)] \twoheadrightarrow [0, \ell(e')]$ with

$h(t) = w(e)t$ for some $w(e) \in \mathbb{Z}_{>0}$. By construction, $w(e) = \ell(e')/\ell(e)$. Similarly, the map π restricted to a leg e of Γ equals $h\colon [0,\infty) \twoheadrightarrow [0,\infty)$ with $h(t) = w(e)t$ for some $w(e) \in \mathbb{Z}_{>0}$.

Definition 4.3. A map $\pi\colon \Gamma \to \Gamma'$ of metric graphs is *harmonic* if for each vertex v of Γ and any edge e' adjacent to $\pi(v)$, the number

$$d_v := \sum_{\substack{e \in E(\Gamma) \\ v \in e, \pi(e) = e'}} w(e) \tag{4.1}$$

does not depend on the choice of edge e'. We call d_v the *local degree* of the map π at v. The *degree* of π is the sum over all local degrees in the fiber of any vertex $v' \in \Gamma'$.

Definition 4.4. A *tropical hyperelliptic cover* of a metric tree T by a metric graph Γ is a surjective degree two harmonic map $\pi\colon \Gamma \to T$ of metric graphs satisfying the local Riemann–Hurwitz conditions at each v vertex of Γ:

$$2 - 2g(v) = 2d_v - \#\{e \ni v : \omega(e) = 2\}. \tag{4.2}$$

Definition 4.5. A *branch point* of a hyperelliptic cover $\pi\colon \Gamma \to T$ of a genus zero metric tree T is a leg or edge of T which is covered by a leg or edge e of Γ with weight $w(e) = 2$.

Since we are interested in metric graphs Γ of genus two, we are restricted to covers of trees T with precisely six leaves. Each vertex of T has valency between three and six. The following technical lemma describes the local behavior of a hyperelliptic cover $\Gamma \to T$.

Lemma 4.6. *There are precisely five tropical hyperelliptic covers of a single genus zero vertex with valency between three and six with source curve a vertex of genus at most two.*

Proof. We let v' be the vertex in the target curve and fix a covering vertex v on the source curve. The result follows by analyzing all possible combinations of genus $g(v)$ and valency of v'. Replacing each value of $g_v = 0, 1,$ or 2 in (4.2) yields all cases in Fig. 4.1. □

Our main result in this section describes the combinatorics of hyperelliptic covers of trees on six leaves. It implies that the poset structures on $M_{0,6}^{\mathrm{trop}}$ and M_2^{trop} agree, as shown in [46, Theorem 5.3]. Unlike the latter, our proof is elementary and uses the local tropical Riemann–Hurwitz conditions (4.2). The general hyperelliptic case is treated in [8, Lemma 2.4]. Superhyperelliptic curves are discussed in [9]:

Proposition 4.7. *Each tree on six leaves is covered by exactly one genus two graph with six legs via a harmonic 2-to-1 map branched at all six leaf edges as in Fig. 1.2.*

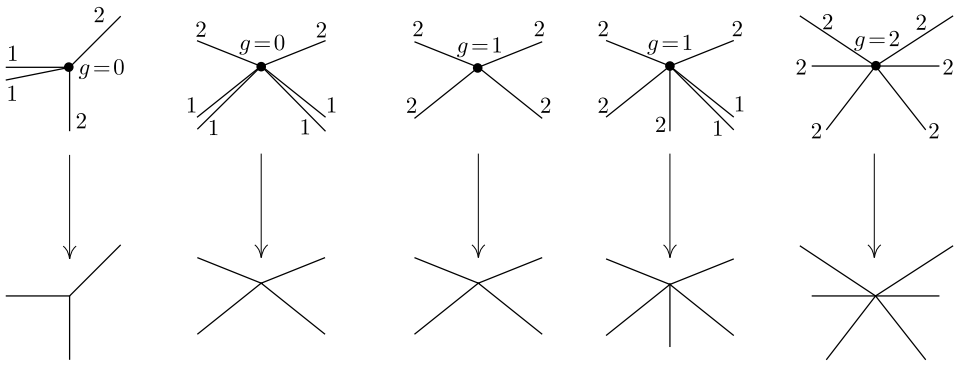

Fig. 4.1. All possible degree two covers of a single genus zero vertex with valency between three and six by a single vertex of genus up to two.

Proof. The leaf edges on the trees are branch points, hence they must be covered by legs of weight two. Lemma 4.6 characterizes the local behavior at each vertex of the tree. These two facts uniquely determine the combinatorial type of the graph and the cover itself. □

Remark 4.8. Following Remark 4.2, the length of an edge e in Γ covering an edge e' in Γ' satisfies $\ell(e) = \ell(e')/\omega(e)$. In particular, when two weight-one edges in Γ form a loop that covers a single edge e' in Γ', then the loop has length $2\,\ell(e')$.

5. The Classification Theorem and the diagonal map $M_{0,6}(K) \to M_2^{\mathrm{trop}}$

Throughout this section, we let $\alpha_1, \ldots, \alpha_6$ be six distinct points in K^* defining an element of $M_{0,6}(K)$ via the six marking $(1 : \alpha_1), \ldots, (1 : \alpha_6)$ in $\mathbb{P}^1$. We consider the diagonal map

$$\varphi\colon M_{0,6}(K) \to M_2^{\mathrm{trop}} \tag{5.1}$$

from Fig. 1.1 sending a smooth rational curve $\mathcal{X} \in M_{0,6}(K)$ to the minimal Berkovich skeleton $\varphi(\mathcal{X})$ of the unique hyperelliptic curve covering $\mathcal{X}$ with branching at $(1 : \alpha_1), \ldots, (1 : \alpha_6)$, as in Fig. 1.2. This map is well-defined since it only depends on the equivalence class of $\underline{\alpha} := (\alpha_1, \ldots, \alpha_6)$ in $(K^*)^6$ up to isomorphism. Combining Table 5.1 with Algorithms 5.1 and 5.2 will completely determine φ. Furthermore, this characterization depends solely on the relative order of the negative valuations of the entries of $\underline{\alpha}$ and some of their differences, as in (1.2). As discussed in Remark 1.3, results in this section can be used to take an arbitrary genus two curve given by a hyperelliptic equation to one of the seven forms corresponding to the seven cones in M_2^{trop}.

Since $K = \overline{K}$ is non-trivially valued by assumption, it follows that the valued group of K is dense in $\mathbb{R}$ [41, Lemma 2.1.12]. As a consequence, we can construct a splitting of

the valuation map [41, Lemma 2.1.15]. Inspired by the canonical splitting for the Puiseux series field, we write it as $\gamma \mapsto t^\gamma$. We use this notion to define initial forms in K^*:

Definition 5.1. Given a splitting $\gamma \mapsto t^\gamma$ of the valuation on K, we define the *initial form* $\mathrm{in}(\alpha)$ of any $\alpha \in K^*$ as the class of $\alpha\, t^{-\operatorname{val}(\alpha)}$ in the residue field $\widetilde{K}$ of K obtained as the quotient of the valuation ring by its maximal ideal.

We let $\underline{\omega} := (\omega_1, \ldots, \omega_6) \in \mathbb{R}^6$ be the weight vector from (6.13) associated to $\underline{\alpha}$ and assume $\omega_1 \leq \omega_2 \leq \ldots \leq \omega_6$. Whenever there is a tie between ω_i and ω_{i+1} and the corresponding initial forms of α_i and α_{i+1} agree, we consider the valuation of the difference $\alpha_i - \alpha_{i+1}$ and notice that $d_{i,i+1} := -\operatorname{val}(\alpha_i - \alpha_{i+1}) < \omega_i = \omega_{i+1}$ if $\mathrm{in}(\alpha_i) = \mathrm{in}(\alpha_{i+1})$. In this situation, we replace the $(i+1)$-st. entry of $\underline{\omega}$ by $d_{i,i+1}$.

As a first step towards a complete classification of the image of φ and its domains of linearity, we construct seven regions in the space of branch points whose associated trees have different combinatorial types:

$$\Omega^{(i)} := \{\underline{\alpha} \in M_{0,6}(K) \colon \text{weight } \underline{\omega} \in \mathbb{R}^6 \text{ satisfies conditions (i) in Table 5.1}\}, \tag{5.2}$$

for $i \in \{\mathrm{I}, \ldots, \mathrm{VII}\}$. Even though these sets do not cover all tuples of distinct points in $(K^*)^6$ we show that they parameterize all seven cones in M_2^{trop} and the harmonic maps from the metric graphs in M_2^{trop} to $M_{0,6}^{\mathrm{trop}}$ given in Fig. 1.2. Here is the precise statement:

Proposition 5.2. *For each $i \in \{\mathrm{I}, \ldots, \mathrm{VII}\}$, the diagonal map φ from (5.1) restricted to $\Omega^{(i)}$ parameterizes the cone of Type (i) in M_2^{trop} and induces a hyperelliptic cover of a tree in $M_{0,6}^{trop}$ by an abstract tropical curve of Type (i) in M_2^{trop}. Furthermore, the metrics on both objects are completely determined by piecewise functions on the weight vectors $\underline{\omega}$ of points in each $\Omega^{(i)}$ as in the second and fourth column of Table 5.1.*

Proof. Starting from a tuple $\underline{\alpha} \in \Omega^{(i)}$ viewed as a marking on $\mathbb{P}^1$, we consider the smooth rational curve $\mathcal{X}$ in $M_{0,6}$ and the associated weight vector $\underline{\omega} \in \mathbb{R}^6$. Our goal is to determine the combinatorial type of the tree $\operatorname{Trop}\mathcal{X}$ and to express its metric structure in terms of $\underline{\omega}$. We do so by analyzing each of the seven sets $\Omega^{(i)}$ separately. By Proposition 4.7 we can label each tree by the type of the genus two metric graph Γ covering it. The edge length formulas on Γ indicated on the last column of Table 5.1 are obtained directly from the metric structure on each tree using Remark 4.8. It is important to emphasize that the tropical Plücker map will give the half-distance vector on the tree, as we saw in Section 2.

In what remains, we discuss the second column of the table. The combinatorial type of each tree is determined by the isomorphism $\Phi\colon M_{0,6} \xrightarrow{\simeq} \mathbb{G}\mathrm{r}_0(2,6)/(K^*)^6 \subset (K^*)^{15}/(K^*)^6$ from (2.2) and the four-point conditions (i.e., the tropical 3-term Plücker relations [41, Lemma 4.3.6]) on $-\operatorname{val}(\Phi(\underline{\alpha})) \in \mathbb{R}^{15}/\mathbb{R}^6$. We use the lexicographic order on $\mathbb{R}^{15}$.

Type (I): We claim Trop $\mathcal{X}$ is a trivalent caterpillar tree on six leaves with internal edge lengths $\omega_3-\omega_2$, $\omega_4-\omega_3$ and $\omega_5-\omega_4$. Indeed, since $-\operatorname{val}(\alpha_i-\alpha_j)=\omega_j$ for $i<j$ we have

$$-\operatorname{val}(\Phi(\underline{\alpha})):=(\omega_2,\omega_3,\omega_4,\omega_5,\omega_6,\omega_3,\omega_4,\omega_5,\omega_6,\omega_4,\omega_5,\omega_6,\omega_5,\omega_6,\omega_6)\in\text{Trop }\mathbb{G}\text{r}_0(2,6)/\mathbb{R}^6.$$

By construction, the half-distance vector equals $-\operatorname{val}(\Phi(\underline{\alpha}))$. The four-point condition implies that the corresponding line in $\mathbb{P}^5$ is a trivalent caterpillar tree. Linear algebra recovers the expected lengths on its three bounded edges [41, Remark 4.3.7]. Note that the lengths assigned to the six legs in the second column of Table 5.1 play no role here: the associated half-distance vector in $\mathbb{R}^{15}$ is in the same class modulo the lineality space in Trop $\mathbb{G}\text{r}_0(2,6)$. The claim follows.

Type (II): By construction, $\Phi(\underline{\alpha})$ has negative valuation vector

$$-\operatorname{val}(\Phi(\underline{\alpha})):=(\omega_2,\omega_3,\omega_4,\omega_5,\omega_6,\omega_3,\omega_4,\omega_5,\omega_6,d_{34},\omega_5,\omega_6,\omega_5,\omega_6,\omega_6)\in\text{Trop }\mathbb{G}\text{r}_0(2,6)/\mathbb{R}^6,$$

where the ω_i and d_{34} are as in (6.13). The four-point conditions imply that the tropical line in $\mathbb{P}^5$ is a snowflake tree with internal edges $\omega_3-\omega_2$, $\omega_5-\omega_3$ and ω_3-d_{34}, as indicated on the second column of the table.

Types (III) through (VII): The tropicalization induced by the Plücker embedding shows that the metric trees on these lower-dimensional cells of $M_{0,6}^{\text{trop}}$ are obtained by specializing the trees for Type (I) or Type (II): both the combinatorial type and the metric are obtained by coarsening either the caterpillar or the snowflake trees. The edge length formulas match those given in Table 5.1. □

In the remainder of this section we discuss why these seven regions $\Omega^{(i)}$ suffice to classify all smooth genus two tropical curves. Indeed, Algorithms 5.1 and 5.2 describe an explicit combinatorial procedure that takes six distinct points $\alpha_1,\dots,\alpha_6$ in K^* and provides linear changes of coordinates in $\mathbb{P}^1$ producing a tuple of points in one of the sets $\Omega^{(i)}$, after iteratively combining two steps:

(A) Separate points: We take a coordinate ω_k of $\underline{\omega}$ and two points α_i and α_j of valuation $-\omega_k$ where $\operatorname{val}(\alpha_i-\alpha_j)$ is maximal, and make a linear change of coordinates that turns the tuple $\underline{\alpha}\in(K^*)^6$ into $\underline{\alpha'}\in(K^*)^6$, where $-\operatorname{val}(\alpha_i')$ is the unique smallest element of ω'. The method is described in Lemma 5.3.

(B) Turn around: We change coordinates from one open affine chart of $\mathbb{P}^1$ to another by replacing x by $1/x$. As a result, $-\operatorname{val}(\alpha_i')=\operatorname{val}(\alpha_i)$ and the relative order of the valuations on the tuple $\underline{\alpha}$ is reversed on the new tuple $\underline{\alpha'}$.

As was mentioned earlier in this section, our assumptions on K ensures the density of the value group of K in $\mathbb{R}$ and the existence of a splitting $\gamma\mapsto t^\gamma$ to the valuation. We use these to properties to separate branch points:

Table 5.1
Combinatorial types with the corresponding defining valuation conditions, and length data for $M_{0,6}^{\mathrm{trop}}$ and M_2^{trop}. Here, $\omega_i = -\operatorname{val}(\alpha_i)$, $d_{34} = -\operatorname{val}(\alpha_3 - \alpha_4)$, and the edge lengths L_0, L_1 and L_2 refer to Fig. 2.1.

Type	Cover with lengths on $M_{0,6}^{\mathrm{trop}}$	Defining conditions	Lengths on M_2^{trop}
(I)	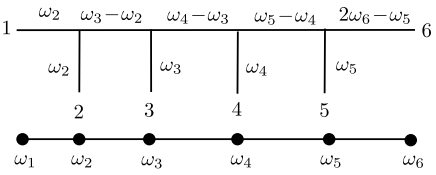	$\omega_1 < \omega_2 < \omega_3 < \omega_4 < \omega_5 < \omega_6$	$L_0 = (\omega_4 - \omega_3)/2$ $L_1 = 2(\omega_5 - \omega_4)$ $L_2 = 2(\omega_3 - \omega_2)$
(II)	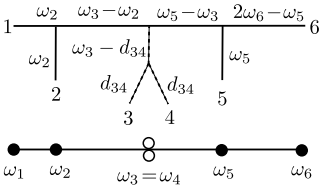	$\omega_1 < \omega_2 < \omega_3 < \omega_5 < \omega_6$ $\omega_3 = \omega_4$ $\operatorname{in}(\alpha_3) = \operatorname{in}(\alpha_4)$	$L_0 = 2(\omega_3 - d_{34})$ $L_1 = 2(\omega_5 - \omega_3)$ $L_2 = 2(\omega_3 - \omega_2)$
(III)	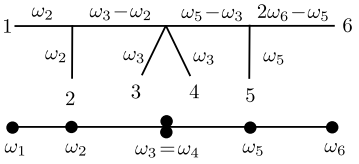	$\omega_1 < \omega_2 < \omega_4 < \omega_5 < \omega_6$ $\omega_3 = \omega_4$ $\operatorname{in}(\alpha_3) \neq \operatorname{in}(\alpha_4)$	$L_0 = 0$ $L_1 = 2(\omega_5 - \omega_3)$ $L_2 = 2(\omega_3 - \omega_2)$
(IV)	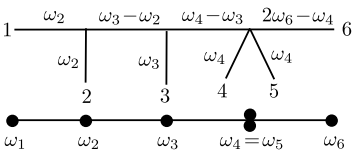	$\omega_1 < \omega_2 < \omega_3 < \omega_4 < \omega_6$ $\omega_4 = \omega_5$ $\operatorname{in}(\alpha_4) \neq \operatorname{in}(\alpha_5)$	$L_0 = (\omega_4 - \omega_3)/2$ $L_1 = 0$ $L_2 = 2(\omega_3 - \omega_2)$
(V)	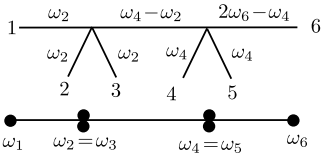	$\omega_1 < \omega_2 < \omega_4 < \omega_6$ $\omega_2 = \omega_3\,,\ \omega_4 = \omega_5$ $\operatorname{in}(\alpha_2) \neq \operatorname{in}(\alpha_3)$ $\operatorname{in}(\alpha_4) \neq \operatorname{in}(\alpha_5)$	$L_0 = (\omega_4 - \omega_2)/2$ $L_1 = 0$ $L_2 = 0$
(VI)	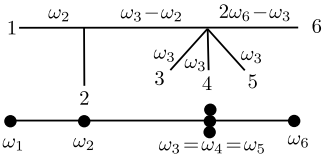	$\omega_1 < \omega_2 < \omega_3 < \omega_6$ $\omega_3 = \omega_4 = \omega_5$ $\operatorname{in}(\alpha_3) \neq \operatorname{in}(\alpha_4)$ $\operatorname{in}(\alpha_3) \neq \operatorname{in}(\alpha_5)$ $\operatorname{in}(\alpha_4) \neq \operatorname{in}(\alpha_5)$	$L_0 = 0$ $L_1 = 0$ $L_2 = 2(\omega_3 - \omega_2)$
(VII)	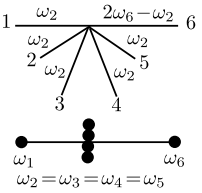	$\omega_1 < \omega_2 < \omega_6$ $\omega_2 = \omega_3 = \omega_4 = \omega_5$ $\operatorname{in}(\alpha_i) \neq \operatorname{in}(\alpha_j)$ for $1 < i < j < 6$	$L_0 = 0$ $L_1 = 0$ $L_2 = 0$

Lemma 5.3. [Separating points] *Consider a repeated coordinate ω of $\underline{\omega}$, and write*

$$\beta = \max\{\operatorname{val}(\alpha_m - \alpha_l) \colon \omega_m = \omega_l = \omega \text{ for } m \neq l\} \geq -\omega.$$

Fix two indices i, j with $\omega_i = \omega_j = \omega$ and $\beta = \operatorname{val}(\alpha_i - \alpha_j)$. If $\operatorname{in}(\alpha_i - \alpha_j) = \overline{\zeta} \in \widetilde{K}$ for some ζ with $\operatorname{val}(\zeta) = 0$, choose $\gamma \in \operatorname{val}(K^*)$ with $\beta < \gamma < \operatorname{val}(\alpha_i - \alpha_j - \zeta t^\beta)$. Then, the linear change of coordinates $\psi \colon \mathbb{P}^1 \to \mathbb{P}^1$ defined locally by

$$\psi(x) = x - \alpha_j - \zeta t^\beta - t^\gamma \tag{5.3}$$

turns the tuple $\underline{\alpha} \in (K^*)^6$ into $\underline{\alpha}' \in (K^*)^6$, where their coordinatewise negative valuations $\underline{\omega}$ and $\underline{\omega}'$ satisfy the following properties:

(1) $\omega'_s = \omega_s > \omega_i$ *if* $\omega_s > \omega_i$;
(2) $\omega'_s = \omega_i$, *and* $\operatorname{in}(\alpha'_s) = -\operatorname{in}(\alpha_i)$ *if* $\omega_s < \omega_i$;
(3) $\omega'_i = -\gamma < \omega'_s = -\operatorname{val}(\alpha_s - \alpha_i) \leq \omega_i$ *if* $\omega_s = \omega_i$ *and* $s \neq i$.

Proof. The first claim follows immediately from the strong non-Archimedean triangle inequality since $\alpha_j + \zeta t^\beta + t^\gamma$ has valuation $-\omega_i$. A similar argument proves the second claim. In particular, $\alpha'_s \neq 0$ whenever $\omega_s \neq \omega_i$.

We now prove the third item. Again, $\operatorname{val}(\alpha_i - \alpha_j - \zeta t^\beta) > \gamma$, so $\operatorname{val}(\alpha'_i) = \gamma$ and $\alpha'_i \neq 0$. Pick $s \neq i$ with $\omega_s = \omega_i$. We write

$$\alpha'_s = \underbrace{(\alpha_s - \alpha_i)}_{-\omega_i \leq \operatorname{val}(\cdot) \leq \beta} + \underbrace{(\alpha_i - \alpha_j - \zeta t^\beta) - t^\gamma}_{\operatorname{val}(\cdot) = \gamma > \beta}.$$

By the strong non-Archimedean inequality, $-\omega_i \leq \operatorname{val}(\alpha'_s) = \operatorname{val}(\alpha_s - \alpha_i) < \gamma$, so $\alpha'_s \neq 0$. □

As the next example illustrates, the effect of the coordinate change in Lemma 5.3 can easily be visualized by means of a tropical modification followed by a coordinate projection.

Example 5.4. Consider points in the Puiseux series field $K = \mathbb{C}\{\{t\}\}$:

$$\alpha_1 = t^3,\ \alpha_2 = 2 + t,\ \alpha_3 = 2 + t^2,\ \alpha_4 = t^{-2},\ \alpha_5 = t^{-3},\ \text{ and } \alpha_6 = t^{-4} \text{ in } K^*,$$

where $\omega_1 = -3$, $\omega = \omega_2 = \omega_3 = 0$, $\omega_4 = 2$, $\omega_5 = 3$, $\omega_6 = 4$, $\beta = \zeta = 1$, $1 < \gamma = 3/2 < \operatorname{val}(t^2)$.

To separate α_2 from α_3, and place $-\operatorname{val}(\alpha_2)$ to the very left of $\mathbb{R}$, we reembed the line in the plane via $y = x - (2 + t^2) - t - t^{3/2}$. The tropicalization of this planar line together with its marked points and the projection to the y-coordinate is depicted in Fig. 5.1. ◇

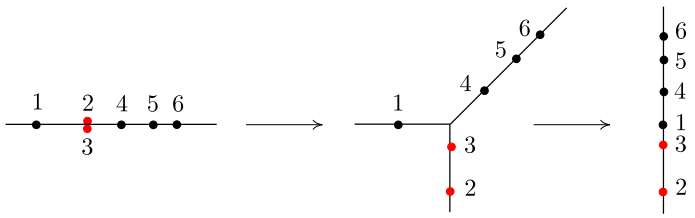

Fig. 5.1. Visualizing the coordinate change (A) via tropical modifications.

Our first combinatorial procedure uses a change of coordinates in $\mathbb{P}^1$ and a relabeling to produce a new tuple $\underline{\alpha}'$ from $\underline{\alpha}$ with the additional property that the maximum and minimum values of $\underline{\omega}'$ are attained exactly once. This is the content of Algorithm 5.1. In turn, Algorithm 5.2 transforms the output of Algorithm 5.1 into a configuration of points in a suitable region $\Omega^{(i)}$. We measure improvement by two auxiliary variables:

- the *deficiency* $\operatorname{def}(\underline{\alpha})$ of the point configuration defined as the size of the partition of $[6] = \{1, \dots, 6\}$ identifying equal coordinates of $\underline{\omega}$,
- a refined partition Λ taking both the valuation and the initial terms into account.

Our partitions will always have the singletons $\{1\}$ and $\{6\}$ since ω_1 and ω_6 remain isolated after each iteration of Step (A).

Algorithm 5.1: Separate the minimum and maximum values of $\underline{\omega}$.

Input: A tuple $\underline{\alpha} = (\alpha_1, \dots, \alpha_6)$ of six distinct labeled points in K^*.
Assumption: $\operatorname{val}(K^*)$ is dense in $\mathbb{R}$ and the valuation on K splits via $\omega \mapsto t^\omega$.
Output: A tuple $\underline{\alpha}'$ obtained from $\underline{\alpha}$ by a linear change of coordinates in $\mathbb{P}^1$ followed by a relabeling, where $-\operatorname{val}(\alpha'_1) < -\operatorname{val}(\alpha'_2) \leq \ldots \leq -\operatorname{val}(\alpha'_5) < -\operatorname{val}(\alpha'_6)$.

Relabel the points so that $-\operatorname{val}(\alpha_1) \leq -\operatorname{val}(\alpha_2) \leq \ldots \leq -\operatorname{val}(\alpha_5) \leq -\operatorname{val}(\alpha_6)$;
$\underline{\alpha}' \leftarrow \underline{\alpha}$; $\underline{\omega}' \leftarrow -\operatorname{val}(\underline{\alpha}') := (-\operatorname{val}(\alpha'_1), \dots, -\operatorname{val}(\alpha'_6))$;
$\Lambda_{\min} \leftarrow \{i \colon \omega_i = \min(\underline{\omega}')\}$; $\Lambda_{\max} \leftarrow \{i \colon \omega_i = \max(\underline{\omega}')\}$;
if $|\Lambda_{\min}| > 1$ **then**
  Relabel $\Lambda_{\min}$ so that $\{\operatorname{val}(\alpha_i - \alpha_j) \colon i, j \in \Lambda_{\min}, i \neq j\}$ is maximized at $i=1, j=2$;
  $\underline{\alpha}' \leftarrow \psi(\underline{\alpha})$ where ψ is defined as in (5.3) with $\omega = \omega_1$, $i = 1$, $j = 2$;
  $\underline{\omega}' \leftarrow -\operatorname{val}(\underline{\alpha}')$;
if $|\Lambda_{\max}| > 1$ **then**
  $\underline{\alpha}' \leftarrow$ Coordinate change **(B)** on $\mathbb{P}^1$ applied to $\underline{\alpha}'$; $\Lambda_{\max} \leftarrow \Lambda_{\min}$;
  Relabel $\Lambda_{\max}$ so that $\{\operatorname{val}(\alpha'_i - \alpha'_j) \colon i, j \in \Lambda_{\max}, i \neq j\}$ is maximized for $i=6, j=5$;
  $\underline{\alpha}' \leftarrow \psi(\underline{\alpha}')$ where ψ is defined as in (5.3) with $\omega = \omega'_6$, $i = 6$, $j = 5$;
  $\underline{\alpha}' \leftarrow$ Coordinate change **(B)** on $\mathbb{P}^1$ applied to $\underline{\alpha}'$;
return $\underline{\alpha}'$.

Proof of Algorithm 5.2. If the input $\underline{\alpha}$ is already in one of the desired regions $\Omega^{(i)}$ for i in $\{\mathrm{I}, \dots, \mathrm{VII}\}$, the algorithm outputs the pair $(\underline{\alpha}, i)$. If not, the deficiency of the partition Λ of $\underline{\alpha}'$ gives us precise rules to apply transformations (A) and (B) to improve this invariant one step at a time. Before each iteration, we use the turn around transformation (B) followed by a relabeling of $[6]$ (to satisfy $-\operatorname{val}(\alpha_j) \leq -\operatorname{val}(\alpha_{j+1})$ for all $j = 1, \dots, 6$) to

Algorithm 5.2: Finding a representative of a tuple $\underline{\alpha}$ in some $\Omega^{(i)}$ for $i \in \{\mathrm{I}, \ldots, \mathrm{VII}\}$.

Input: A tuple $\underline{\alpha} = (\alpha_1, \ldots, \alpha_6)$ of six distinct labeled points in K^* with $-\operatorname{val}(\alpha_1) < -\operatorname{val}(\alpha_2) \leq \ldots \leq -\operatorname{val}(\alpha_5) < -\operatorname{val}(\alpha_6)$.
Assumption: $\operatorname{val}(K^*)$ is dense in $\mathbb{R}$ and the valuation on K splits via $\omega \mapsto t^\omega$.
Output: A pair $(\underline{\alpha}', i)$ where $i \in \{\mathrm{I}, \ldots, \mathrm{VII}\}$ and $\underline{\alpha}'$ lies in $\Omega^{(i)}$. Here, $\underline{\alpha}'$ is obtained from $\underline{\alpha}$ by a linear change of coordinates in $\mathbb{P}^1$ followed by a relabeling of $[6] = \{1, \ldots, 6\}$ if needed.

$\underline{\alpha}' \leftarrow \underline{\alpha}$; $\underline{\omega}' \leftarrow -\operatorname{val}(\underline{\alpha}')$; $d \leftarrow \operatorname{def}(\underline{\alpha}') :=$ deficiency of $\underline{\alpha}'$;
$\Lambda \leftarrow \operatorname{part}(\underline{\alpha}') :=$ partition of $[6]$ determined by equality among $(\omega_i', \operatorname{in}(\alpha_i'))$'s;
while $d = 3$ **do**
  if $|\Lambda| = 6$ **then return** $(\underline{\alpha}', \mathit{VII})$.
  Relabel $\{2, \ldots, 5\}$ so $\max\{\operatorname{val}(\alpha_i' - \alpha_j') : \omega_i' = \omega_j' = \omega_2'\} = \operatorname{val}(\alpha_2' - \alpha_3')$;
  $\underline{\alpha}' \leftarrow \psi(\underline{\alpha}')$ where ψ is defined as in (5.3) with $\omega = \omega_2'$, $i = 2$, $j = 3$;
  Relabel $[6]$ by incr. $-\operatorname{val}(\underline{\alpha}')$; $\Lambda \leftarrow \operatorname{part}(\underline{\alpha}')$; $\underline{\omega}' \leftarrow -\operatorname{val}(\underline{\alpha}')$; $d \leftarrow \operatorname{def}(\underline{\alpha}')$;
while $d = 4$ **do**
  if $|\Lambda| = 6$, $\omega_2' = \omega_3'$, *and* $\omega_4' = \omega_5'$ **then return** $(\underline{\alpha}', V)$.
  else if $|\Lambda| = 6$, $\omega_2' < \omega_3'$ **then return** $(\underline{\alpha}', \mathit{VI})$.
  else if $(|\Lambda| = 6$ *and* $\omega_4' < \omega_5')$ *or* $(|\Lambda| < 6$, $\omega_3' < \omega_4'$ *and* $\operatorname{in}(\alpha_2') \neq \operatorname{in}(\alpha_3'))$ *or* $(|\Lambda| < 6$ *and* $\omega_2' < \omega_3')$ **then**
    $\underline{\alpha}' \leftarrow$ Coordinate change **(B)** on $\mathbb{P}^1$ applied to $\underline{\alpha}'$ with relabeling of $[6]$;
    $\underline{\omega}' \leftarrow -\operatorname{val}(\underline{\alpha}')$; $\Lambda \leftarrow \operatorname{part}(\underline{\alpha}')$; $d \leftarrow \operatorname{def}(\underline{\alpha}')$;
  else
    Relabel $\{2, \ldots, 5\}$ so that $\max\{\operatorname{val}(\alpha_i' - \alpha_j') : \omega_i' = \omega_j' = \omega_2'\} = \operatorname{val}(\alpha_2' - \alpha_3')$;
    $\underline{\alpha}' \leftarrow \psi(\underline{\alpha}')$ where ψ is defined as in (5.3) with $\omega = \omega_2'$, $i = 2$, $j = 3$;
    Relabel $[6]$ by incr. $-\operatorname{val}(\underline{\alpha}')$; $\Lambda \leftarrow \operatorname{part}(\underline{\alpha}')$; $\underline{\omega}' \leftarrow -\operatorname{val}(\underline{\alpha}')$; $d \leftarrow \operatorname{def}(\underline{\alpha}')$;
while $d = 5$ **do**
  if $\omega_3' = \omega_4'$ *and* $\operatorname{in}(\alpha_3') = \operatorname{in}(\alpha_4')$ **then return** $(\underline{\alpha}', \mathit{II})$.
  else if $\omega_3' = \omega_4'$ *and* $\operatorname{in}(\alpha_3') \neq \operatorname{in}(\alpha_4')$ **then return** $(\underline{\alpha}', \mathit{III})$.
  else if $\omega_2' = \omega_3'$ *and* $\operatorname{in}(\alpha_2') = \operatorname{in}(\alpha_3')$ **then**
    $\underline{\alpha}' \leftarrow \psi(\underline{\alpha}')$ where ψ is defined as in (5.3) with $\omega = \omega_2$, $i = 2$, $j = 3$;
    Relabel $[6]$ by incr. $-\operatorname{val}(\underline{\alpha}')$ and **return** $(\underline{\alpha}', \mathit{I})$.
  else if $\omega_4' = \omega_5'$ *and* $\operatorname{in}(\alpha_4') \neq \operatorname{in}(\alpha_5')$ **then return** $(\underline{\alpha}', \mathit{IV})$.
  else
    $\underline{\alpha}' \leftarrow$ Coordinate change **(B)** on $\mathbb{P}^1$ applied to $\underline{\alpha}'$ with relabeling of $[6]$;
    $\underline{\omega}' \leftarrow -\operatorname{val}(\underline{\alpha}')$; $\Lambda' \leftarrow \operatorname{part}(\underline{\alpha}')$;
return $(\underline{\alpha}', \mathit{I})$.

reduce ourselves to the case when $\omega_2 = \omega_3 > -\operatorname{val}(\alpha_2 - \alpha_3)$ and $\{\operatorname{val}(\alpha_i - \alpha_j) : \omega_i = \omega_j = \omega_2\}$ is maximized at $i = 2, j = 3$. In this situation, the change of coordinates (A) on $\mathbb{P}^1$ with $\omega = \omega_2$, $i = 2$, and $j = 3$ turns $\underline{\alpha}$ to $\underline{\alpha}' \in (K^*)^6$ and $\operatorname{def}(\underline{\alpha}') > \operatorname{def}(\underline{\alpha})$. After each such transformation, a relabeling of $[6]$ is performed to ensure the $-\operatorname{val}(\alpha_i)$ are ordered increasingly. The process stops in at most four steps. □

6. Faithful re-embedding of planar hyperelliptic curves

Up to this point, we have only dealt with abstract tropical curves. In this section, we turn our attention to *embedded* tropical plane curves, defined as the dual complex to Newton subdivisions of (1.1) [11,41,47]. Our objective is to prove Theorem 1.2. Along the way, we analyze the combinatorics of the re-embedded tropical curves, which will vary with the type of the input planar hyperelliptic curve. We assume throughout that the valued group of K is dense in $\mathbb{R}$ and we fix a splitting $\omega \to t^\omega$ of the valuation.

Our first result allows us to assume that the hyperelliptic cover (1.1) is branched at both 0 and ∞, and that the leading coefficient u equals 1. It ensures that the description of witness regions from Table 5.1 remains valid in this setting, for $\omega_1 = -\infty$ and $\omega_6 = \infty$:

Lemma 6.1. *After an automorphism of* $\mathbb{P}^1$ *sending* $\underline{\alpha}'$ *to* $\underline{\alpha}$*, the equation* (1.1) *becomes*

$$g(x,y) := y^2 - x\prod_{i=2}^{5}(x-\alpha_i) = 0 \qquad \alpha_2,\dots,\alpha_5 \in K^*, \tag{6.1}$$

where $\omega_i := -\operatorname{val}(\alpha_i) \in \mathbb{R}$, $\omega_i = \omega_i' - 2\omega_6' = 2\operatorname{val}(\alpha_6') - \operatorname{val}(\alpha_i')$, $\operatorname{in}\alpha_i = \operatorname{in}\alpha_i'/\operatorname{in}\alpha_6'^2$ *for all* $i = 2,\dots,5$, *and* $\omega_2 \le \omega_3 \le \omega_4 \le \omega_5$.

Proof. Equation (1.1) is obtained from (6.1) by means of the projective transformation $\varphi(x) := (x-\alpha_1')/\big((\alpha_1'-\alpha_6')(x-\alpha_6')\big)$ and replacing y with $y/\Big((x-\alpha_6')^3\sqrt{u\prod_{1\le k\le 5}(\alpha_k'-\alpha_6')}\Big)$. □

As discussed in Section 3, the naïve tropicalization $\operatorname{Trop}V(g)$ induced by (6.1) is almost never faithful. Our goal in this section is to produce faithful re-embeddings in $(K^*)^3$ for all seven witness regions, both at the level of minimal and extended Berkovich skeleta. We will make full use of the techniques developed in Section 3, in particular Lemma 3.3, which describe these re-embedded tropical curves by means of the three coordinate projections.

As we will see, except for Type (II), faithfulness can be achieved in the XZ-plane, since the relative interior of the cell σ_4 from (3.4) will contain no point from the re-embedded tropical curve $\operatorname{Trop}V(I_{g,f})$. For this reason, we postpone the treatment of Type (II) to the end of this section. Furthermore, a refined algebraic lift of the tropical polynomial $F = \max\{Y, A+X, B+2X\}$ from (3.3) will yield faithfulness on the extended skeleta for Types (I) and (III).

The rest of this section is organized as follows. We start by giving a complete description of vertices, edges and tropical multiplicities of the xy-tropicalizations, whose Newton subdivisions are shown in the middle column of Table 6.1 and in Fig. 6.1. We do so by calculating various initial forms of the input hyperelliptic equation $g(x,y)$. The explicit values will depend on the genericity of the branch points $\alpha_2,\dots,\alpha_5$ and the relation between the expected valuations of all coefficients in g and their actual valuations. These computations allow us to determine the function $f(x,y)$ from (6.2) appearing in Theorem 1.2. Lemma 6.2 confirms the validity of f as a lift of the tropical polynomial F. A refined choice $\tilde{f}(x,y)$ of this function, described in (6.5), will allow us to control the combinatorics of the re-embedded tropical curves and achieve faithfulness on the extended skeleta on certain types of curves. Propositions 6.3, 6.5 and Lemma 6.4 analyze the combinatorics of the xz-tropicalizations, visible on the right-column of Table 6.1. The description of the yz-tropicalizations for each type is done on separate subsections.

In order to find the appropriate lift $f(x,y)$ of the tropical polynomial F, we must first predict the Newton subdivision of (6.1) for each witness region. This is done by computing the expected heights of all monomials (i.e., the negative valuation of the coefficients) in the Newton polytope of $g(x,y)$ in terms of $\underline{\omega}$:

$$\mathrm{ht}(x^5)=\mathrm{ht}(y^2)=0\,,\ \mathrm{ht}(x)=\sum_{i=2}^{5}\omega_i\,,\ \mathrm{ht}(x^2)=\sum_{i=3}^{5}\omega_i\,,\ \mathrm{ht}(x^3)=\omega_5+\omega_4\ \text{ and }\ \mathrm{ht}(x^4)=\omega_5.$$

These heights determine the induced subdivision, as seen in Table 6.1 and Fig. 6.9. Notice that outside Types (I) and (II), the expected heights may not be attained. For example, the coefficient of x^3 equals $\alpha_5(\alpha_4+\alpha_3)+\sum_{i<j<5}\alpha_i\alpha_j$. Unless $\mathrm{in}(\alpha_4)=-\mathrm{in}(\alpha_3)$, its expected height in Type (III) will be achieved. We indicate these situations by red points in the Newton polytopes. Nonetheless, these special situations have no effect on the tropical world: they will only unmark the given lattice point.

The expected heights determine all vertices in $\mathrm{Trop}\,V(g)$ from Table 6.1 and Fig. 6.9:

$$v_1=(\omega_2,\omega_2+\frac{\omega_3+\omega_4+\omega_5}{2}),\ v_2=v_1+(\omega_3-\omega_2)\mathbf{1},\ v_3=(\omega_4,2\omega_4+\frac{\omega_5}{2}),\ v_4=v_3+(\omega_5-\omega_4)(1,2).$$

Unless $v_1=v_2$, the edge e_{12} joining v_1 and v_2 has tropical multiplicity 2. Similar behavior occurs for the edge e_{34} joining v_3 and v_4. Notice that the combinatorial types for $\mathrm{Trop}\,V(g)$ are all distinct, except for Types (II) and (III). However, these two differ as *tropical cycles*, since the tropical multiplicities of the vertex v_2 are distinct: it is one for Type (III) but two for Type (II). This follows by computing the initial degenerations with respect to v_2:

$$\mathrm{in}_{v_2}(g)=y^2+x^2\,\mathrm{in}(\alpha_5)(x-\mathrm{in}(\alpha_3))(x-\mathrm{in}(\alpha_4))\in\widetilde{K}[x^{\pm},y^{\pm}].$$

Indeed, $\mathrm{in}_{v_2}(g)$ is irreducible if and only if $\mathrm{in}(\alpha_3)\neq\mathrm{in}(\alpha_4)$. This holds for Type (III) but fails for Type (II) as Table 5.1 indicates. In the latter case, $\mathrm{in}_{v_2}(g)$ has two reduced components, so $m_{\mathrm{trop}}(v_2)=2$.

The tropical polynomial F from (3.3) associated to $A:=(\omega_3+\omega_4+\omega_5)/2$ and $B:=\omega_5/2$ contains all vertices of $\mathrm{Trop}\,V(g)$ and the edges between them. Our choice of lifting for F is governed by the initial degenerations of $\mathrm{Trop}\,V(g)$ along the (possibly degenerate) multiplicity two edges $e_{12}=\overline{v_1v_2}$ and $e_{34}=\overline{v_3v_4}$. Whenever these edges have positive length, the method unfolds them and produces loops in the re-embedded tropical curve, as in [20, Theorem 3.4]. We propose:

$$f(x,y):=y-\sqrt{-\alpha_3\,\alpha_4\,\alpha_5}\,x+\sqrt{-\alpha_5}\,x^2. \tag{6.2}$$

Since $\mathrm{in}_{e_{12}}(g)=y^2+\mathrm{in}(\alpha_3\alpha_4\alpha_5)\,x^2$ and $\mathrm{in}_{e_{34}}(g)=y^2+\mathrm{in}\,\alpha_5\,x^4$ we verify:

Lemma 6.2. *The polynomial f from (6.2) is a lifting of F and its initial degenerations $\mathrm{in}_{e_{12}}(f)$ and $\mathrm{in}_{e_{34}}(f)$ are irreducible components of $\mathrm{in}_{e_{12}}(g)$ and $\mathrm{in}_{e_{34}}(g)$, respectively.*

Table 6.1
Naïve tropicalization for cells (I), (II), (III), (IV) and generic (VI), and planar re-embeddings described by Newton subdivisions. All planar re-embeddings are faithful except for Type (II). The polygon $\mathcal{P}$ will be further subdivided, as in Subsection 6.5. The dashed edges correspond to the refined lift $\tilde{f}$ (6.5) of the tropical polynomial F. The red points' heights might be lower than expected for special choices of $\alpha_2, \ldots, \alpha_5$. The grey points have height $-\infty$. All vertices are described in (6.4) and (6.7). (For interpretation of the colors in the figure(s), the reader is referred to the web version of this article.)

Cells and skeleta	Naïve tropicalization	xz-tropicalization
(I) 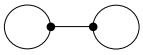	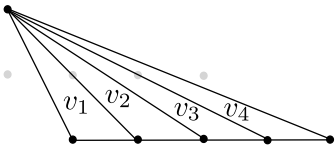	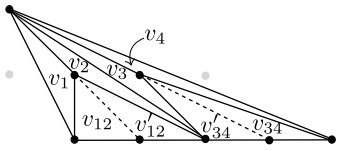
(II) 	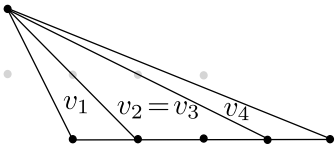	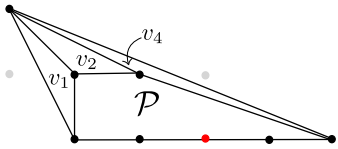
(III) 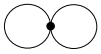	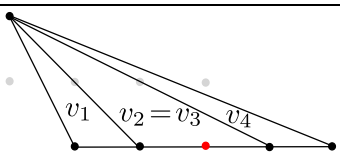	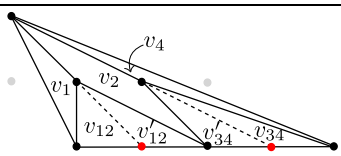
(IV) 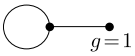	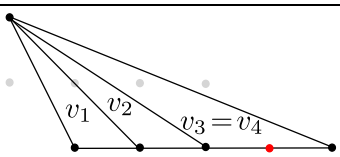	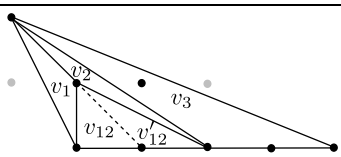
(VI) 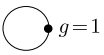	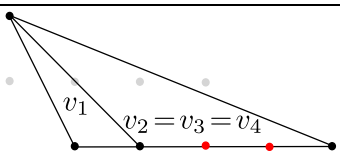	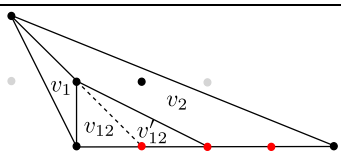

The next result recovers the Newton subdivision of the polynomial

$$\tilde{g}(x,z) := g(x, z + \beta_3\beta_4\beta_5\, x - \beta_5\, x^2) \quad \text{where } \alpha_i = \beta_i^2 \text{ for } i = 2,3,4 \text{ and } \alpha_5 = -\beta_5^2, \tag{6.3}$$

generating the ideal $I_{g,f} \cap K[x^{\pm}, z^{\pm}]$ from Table 6.1:

Proposition 6.3. *For Types (I), (III), (IV) and (VI), the expected heights of $\tilde{g}(x,z)$ are:*

$$\mathrm{ht}(z^2) = \mathrm{ht}(x^5) = 0\,, \quad \mathrm{ht}(xz) = \frac{\omega_5+\omega_4+\omega_3}{2}\,, \quad \mathrm{ht}(x^2z) = \frac{\omega_5}{2}\,, \quad \mathrm{ht}(x) = \omega_5+\omega_4+\omega_3+\omega_2,$$
$$\mathrm{ht}(x^3) = \omega_5+\omega_4\,, \quad \mathrm{ht}(x^4) = \omega_4\,, \quad \mathrm{ht}(x^2) = \omega_5+\omega_4+\omega_3.$$

The expected heights for z^2, x^5, xz and x^2z are always achieved. For the remaining monomials, genericity conditions need to be imposed for Types (III) and (VI) (see Table 6.1.)

Proof. An explicit computation with `Singular` (see the Supplementary material): reveals that the coefficients of $\tilde{g}$ from (6.3) equal:

$$\begin{aligned}
&\operatorname{coeff}(x^5) = -\operatorname{coeff}(z^2) = 1\,, \quad \operatorname{coeff}(xz) = -2\beta_3\beta_4\beta_5\,, \quad \operatorname{coeff}(x^2z) = 2\beta_5\,,\\
&\operatorname{coeff}(x^4) = -\alpha_2-\alpha_3-\alpha_4\,, \quad \operatorname{coeff}(x^3) = \alpha_5(\beta_3-\beta_4)^2+\alpha_3\alpha_4+\alpha_2(\alpha_3+\alpha_4+\alpha_5)\,,\\
&\operatorname{coeff}(x^2) = -\alpha_2((\alpha_3+\alpha_4)\alpha_5+\alpha_3\alpha_4)\,, \quad \operatorname{coeff}(x) = \alpha_2\alpha_3\alpha_4\alpha_5\,.
\end{aligned}$$

The characterization of each witness region in Table 5.1 gives both the expected heights for each relevant monomial and the genericity conditions required to achieve them:

$\mathbf{x^4}$: $\operatorname{in}(\alpha_3)+\operatorname{in}(\alpha_4)\neq 0$ for (III) or (VI),
$\mathbf{x^3}$: $\operatorname{in}(\alpha_5)(\operatorname{in}(\beta_3)-\operatorname{in}(\beta_4))^2+\operatorname{in}(\alpha_3)\operatorname{in}(\alpha_4)\neq 0$ for (VI),
$\mathbf{x^2}$: $\operatorname{in}(\alpha_3)+\operatorname{in}(\alpha_4)\neq 0$ for (III); $(\operatorname{in}(\alpha_3)+\operatorname{in}(\alpha_4))\operatorname{in}(\alpha_5)+\operatorname{in}(\alpha_3)\operatorname{in}(\alpha_4)\neq 0$ for (VI). □

The previous result, together with the characterization of all six maximal cells of $\operatorname{Trop}V(f)$ in (3.4) yield explicit formulas for all vertices of the XZ-projections depicted in Table 6.1:

$$\begin{aligned}
&v_1 = (\omega_2,\, \omega_2+\frac{\omega_3+\omega_4+\omega_5}{2},\, \omega_2+\frac{\omega_3+\omega_4+\omega_5}{2}), \quad v_3 = (\omega_4,\, 2\omega_4+\frac{\omega_5}{2},\, 2\omega_4+\frac{\omega_5}{2}),\\
&v_{12} = v'_{12} = v_1+(\omega_3-\omega_2)/2\,(1,1,0)\,, \qquad v_2 = v_1+(\omega_3-\omega_2)\mathbf{1}\,,\\
&v_{34} = v'_{34} = v_3+(\omega_5-\omega_4)/2\,(1,2,1)\,, \qquad v_4 = v_3+(\omega_5-\omega_4)(1,2,2).
\end{aligned} \tag{6.4}$$

The formulas for v_{12} and v_{34} are valid for Types (III) and (VI) only generically. Furthermore, the description of Type (VI) curves done in Table 6.1 is only generic. Fig. 6.1 shows the combinatorial types of $\operatorname{Trop}V(\tilde{g})$ for special configurations of Type (VI). In particular, for this type we can only get a triangle as the dual polygon to v_2 in the Newton subdivision of $\tilde{g}(x,y)$ when the coefficients of x^3 and x^4 are non-generic. We conclude:

Lemma 6.4. *On Type (VI), the initial form* $\operatorname{in}_{v_2-(0,0,\lambda)}(\tilde{g}(x,z))$ *for any* $\lambda>0$ *is monomial only if* $\operatorname{in}(\alpha_3) = -\operatorname{in}(\alpha_4)$ *and* $2\operatorname{in}(\alpha_5) = \operatorname{in}(\beta_3\beta_4)$.

In order to address this non-generic behavior and the combinatorics of $\operatorname{Trop}V(\tilde{g})$ for all types discussed in Proposition 6.3, it will be convenient to choose a refined lift $\tilde{f}$ of F on Types (I), (III), (IV) and (VI). We define:

$$\tilde{f}(x,y) := y-\sqrt{-\alpha_3\,\alpha_4\,\alpha_5}(1+t^{\varepsilon})\,x+\sqrt{-\alpha_5}\,(1+\delta t^{\varepsilon'})\,x^2 \quad \text{for } 0<\varepsilon,\varepsilon'\ll 1,\ \delta=0/1. \tag{6.5}$$

By construction, Lemma 6.2 holds for $\tilde{f}$ as well, and $\operatorname{Trop} V(f) = \operatorname{Trop} V(\tilde{f})$. The parameters $\varepsilon, \varepsilon'$ depend on the branch points $\alpha_2, \dots, \alpha_5$, while the choice of δ depends solely on the curve type: $\delta = 1$ for Types (I) and (III), whereas $\delta = 0$ for (IV) and (VI). Following the notation from (6.3), the generator $\tilde{g}'$ of the ideal $I_{g,\tilde{f}} \cap K[x^{\pm}, z^{\pm}]$ becomes

$$\tilde{g}'(x,z) := g(x, z + \beta_3\beta_4\beta_5\,(1+t^{\varepsilon})x - \beta_5\,(1+\delta t^{\varepsilon'})x^2). \tag{6.6}$$

Our next result shows that when ε and ε' are chosen appropriately, $\tilde{f}$ produces faithfulness on the whole extended skeleton in Types (I) and (III), as Table 6.1 indicates.

Proposition 6.5. *For Types (I), (III), (IV) and (VI), the coefficients of $\tilde{g}'(x,z)$ and $\tilde{g}(x,z)$ agree with the following five exceptions:*

$$\begin{aligned}
&\operatorname{coeff}(x^2z) = 2\beta_5(1+\delta t^{\varepsilon'}), \quad \operatorname{coeff}(x^2) = -\alpha_2(\alpha_3+\alpha_4)\alpha_5 - \alpha_2\alpha_3\alpha_4 + \alpha_3\alpha_4\alpha_5 t^{\varepsilon}(2+t^{\varepsilon}),\\
&\operatorname{coeff}(xz) = -2\beta_3\beta_4\beta_5(1+t^{\varepsilon}), \quad \operatorname{coeff}(x^4) = -\alpha_2 - \alpha_3 - \alpha_4 + \alpha_5\delta t^{\varepsilon'}(2+\delta t^{\varepsilon'}),\\
&\operatorname{coeff}(x^3) = \alpha_5(\beta_3-\beta_4)^2 + \alpha_3\alpha_4 + \alpha_2(\alpha_3+\alpha_4+\alpha_5) - 2\alpha_5\beta_3\beta_4(t^{\varepsilon} + \delta t^{\varepsilon'} + \delta t^{\varepsilon+\varepsilon'}).
\end{aligned}$$

The heights of xz and x^2z agree with those in Proposition 6.3. The expected height of x^3 is $\omega_5+\omega_4$ and it is achieved for Type (VI) only when $\operatorname{val}(\alpha_5(\beta_3-\beta_4)^2 + \alpha_3\alpha_4) = -2\omega_4$.

Moreover, if $0 < \varepsilon < (\omega_3-\omega_2)/2$ and $0 < \varepsilon' < (\omega_5-\omega_4)/2$ (if $\omega_5 \neq \omega_4$)), then

- $\operatorname{ht}(x^2) = \omega_5+\omega_4+\omega_3-\varepsilon > \omega_5+\omega_4+\omega_2$ *for all four types,*
- $\operatorname{ht}(x^4) = \omega_5 - \varepsilon'$ *for Types (I) and (III),*
- $\operatorname{ht}(x^4) = \omega_4$ *for Type (IV), and*
- $\operatorname{ht}(x^4) \leq \omega_4$ *for Type (VI). Equality is achieved if and only if* $\operatorname{in}(\alpha_3) \neq -\operatorname{in}(\alpha_4)$.

Proof. The result follows by direct computation (see the Supplementary material). The conditions on ε (and ε' for (I) and (III)) guarantee that the heights of x^2 and x^4 satisfy:

$$\operatorname{ht}(x)+\operatorname{ht}(x^3) \leq \operatorname{ht}(x)+\exp\operatorname{ht}(x^3) < 2\operatorname{ht}(x^2) \quad \text{and} \quad \operatorname{ht}(x^3)+\operatorname{ht}(x^5) \leq \exp\operatorname{ht}(x^3) < 2\operatorname{ht}(x^4).$$

Under these constraints, the point x^2 lies above the plane spanned by x, x^3 and xz in the extended Newton polygon. Therefore, the triangle in the Newton subdivision with vertices x, x^3 and xz will be subdivided by an edge joining xz and x^2. For Types (I) and (III), our choice of ε' produces the same effect for x^4 and the facet spanned by x^3, x^5 and x^2z. □

Proposition 6.5 implies that when the expected height of x^3 is attained, the refined modifications replace v_{12} and v_{34} by two pairs of vertices, as seen in Table 6.1:

$$v_{12} = v_1 + \varepsilon(1,1,0), \; v'_{12} = v_2 - \varepsilon(1,1,2), \; v_{34} = v_4 - \varepsilon'(1,2,3) \text{ and } v'_{34} = v_3 + \varepsilon'(1,2,1). \tag{6.7}$$

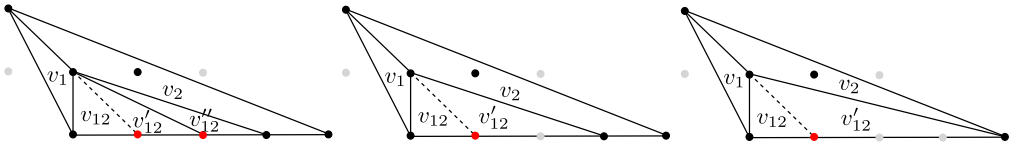

Fig. 6.1. Non-generic xz-tropicalizations for Type (VI) with respect to the height of x^3. The rightmost is non-generic with respect to x^4 as well.

Remark 6.6. The combinatorial types arising from $\tilde{g}(x,z)$ and $\tilde{g}'(x,z)$ for non-generic Type (VI) curves is more subtle. All possible Newton subdivisions are shown in Fig. 6.1 and they depend on the behavior of x^3 and x^4. Our bound for ε given in Proposition 6.5 allows us to split the vertex v_{12} into two or three vertices. There are three cases to analyze:

(1) When x^3 is non-generic but marked and the behavior of x^4 is generic (as in the leftmost picture), there will be no high-multiplicity leg in the direction $(0,0,-1)$ and the xz-tropicalization will be faithful on the whole extended skeleton. Precise formulas for v_{12}, v'_{12} and v''_{12} will depend on the heights of x^3 and x^4.
(2) When x^4 is generic and x^3 is unmarked (as in the middle picture), the vertex v_{12} splits into two vertices, with coordinates

$$v_{12} = v_1 + \varepsilon(1,1,0)\,, \qquad v'_{12} = (\omega_4 - \varepsilon/2, (5\omega_4/2 - \varepsilon)/2, (5\omega_4 - 3\varepsilon)/2).$$

A multiplicity two leg in the direction of $(0,0,-1)$ is attached to the vertex v'_{12}, so faithfulness on the extended skeleton induced by $\tilde{g}'$ is not guaranteed. If we consider $\tilde{g}$ instead, then $v_{12} = v'_{12}$ and the leg has multiplicity three. The precise coordinates of v_{12} will depend on the height of x^3.
(3) When x^4 and x^3 are both non-generic, we cannot predict the combinatorics of the Newton subdivision of $\tilde{g}$. We bypass this difficulty by choosing the refined lift $\tilde{f}$ from (6.5) with $\delta = 1$ and $\varepsilon, \varepsilon'$ satisfying:

$$0 < \varepsilon < \varepsilon' < \min\{\omega_4 - \omega_2/2, \omega_4 + \mathrm{val}(\alpha_3 + \alpha_4)\}.$$

In this case, convexity shows that the xz-tropicalization of $I_{g,\tilde{f}}$ has a unique high-multiplicity leg dual to the segment with endpoints x^2 and x^5, as in the rightmost picture. The remaining legs are adjacent to v_1 and v_4 and lie in the cells σ_1 and σ_2. The heights of x^2, x^3 and x^4 in the right-most picture in Fig. 6.1 become $3\omega_4 - \varepsilon$, $2\omega_4 - \varepsilon'$ and $\omega_4 - \varepsilon'$, respectively. Furthermore, the vertices of $\mathrm{Trop}\, V(I_{g,\tilde{f}})$ in σ_6 are $v_1 = (\omega_2, \omega_2 + 3\omega_3/2, \omega_2 + 3\omega_3/2)$, $v_4 = (\omega_3, 5\omega_3/2, 5\omega_3/2)$ and

$$v_{12} = v_1 + \varepsilon(1,1,0), \quad v'_{12} = v_4 - \varepsilon/3(1,1,4).$$

The remainder of this section is devoted to the proof of Theorem 1.2, which we do by a detailed case-by-case analysis. Following [5, Theorem 5.24] we certify faithfulness for

$I_{g,f}$ and $I_{g,\tilde{f}}$ by verifying that the tropical multiplicities of all vertices and edges on the tropical (extended) skeleton under the forgetful map equal one. The Poincaré–Lelong formula [4, Theorem 5.15] will help us analyze the tropicalizations

$$\mathrm{trop}\colon \Sigma(\mathcal{X}) \to \mathrm{Trop}\, V(I_{g,f}) \qquad \text{and} \qquad \mathrm{trop}'\colon \Sigma(\mathcal{X}) \to \mathrm{Trop}\, V(I_{g,\tilde{f}}), \tag{6.8}$$

where $\Sigma(\mathcal{X})$ denotes the extended skeleton of $\mathcal{X}^{\mathrm{an}}$ with respect to the six branch points. They correspond to the source curves on the left of Fig. 1.2. For all types except (V) and (VII), the legs in $\Sigma(\mathcal{X})$ marked with $\alpha_1 = 0$ and $\alpha_6 = \infty$ are mapped isometrically to the legs attached to v_1 and v_4 with directions $(-2,-1,-1)$ and $(2,5,5)$, respectively.

Whenever faithfulness on $\Sigma(\mathcal{X})$ cannot be achieved via f or $\tilde{f}$, we overcome this issue by employing vertical modifications along tropical polynomials of the form $\mathrm{trop}(x-\alpha_i)$. Example 6.12 provides a detailed explanation of our re-embedding methods presented briefly in Example 3.4. The Supplementary material includes a complete list of examples (with scripts) for each combinatorial type, considering generic and special branch point behaviors. The interested reader can simply change the parameters α_2, and β_i's on the script corresponding to a fixed curve type to produce new examples.

6.1. Proof for Type (I)

From the XZ-projections of both $\mathrm{Trop}\, V(I_{g,f})$ and $\mathrm{Trop}\, V(I_{g,\tilde{f}})$ given in Table 6.1 we know that the maximal cell σ_4 does not meet any of these two curves. Thus, we can ignore the YZ-projection when reconstructing the space curves using Lemma 3.3: it suffices to attach a leg in the direction $(0,-1,0)$ to the vertices v_1, v_2, v_3 and v_4 in the charts σ_1 and σ_2.

From Table 6.1, we see that all vertices and edges in $\mathrm{Trop}\, V(\tilde{g})$ and $\mathrm{Trop}\, V(\tilde{g}')$ have tropical multiplicities one, since their initial degenerations are reduced and irreducible. This shows that both xz-tropicalizations are faithful on the minimal skeleta. Furthermore, all legs in $\mathrm{Trop}\, V(\tilde{g}')$ have multiplicity one, thus the refined modification induces a faithful tropicalization on the whole tropical curve. This is not the case for $\mathrm{Trop}\, V(I_{g,f})$ since there are two multiplicity two legs in the direction $(0,0,-1)$.

The tropicalization maps in (6.8) can be read off from the combinatorics of both re-embedded curves. The legs attached to v_1, v_2, v_3 and v_4 are the isometric images of the legs marked with $\alpha_2, \alpha_3, \alpha_4$ and α_5 under the tropicalization maps. These legs get contracted under the XZ-projections. □

6.2. Proof for Type (III)

The XY- and XZ-projections reveal that σ_4 intersects both tropical curves $\mathrm{Trop}\, V(I_{g,f})$ and $\mathrm{Trop}\, V(I_{g,\tilde{f}})$ along the ray $\sigma_1 \cap \sigma_2 \cap \sigma_4$. Thus, we can use Table 6.1 to reconstruct the space curves.

All trivalent vertices in the XZ-projections of both space curves have tropical multiplicities 1. By [20, Corollary 2.14], we can confirm that v_2 has also multiplicity one by showing that the discriminants Δ of $\mathrm{in}_{v_2}(\tilde{g}(x,z))$ and $\mathrm{in}_{v2}(\tilde{g}'(x,z))$ do not vanish. The explicit descriptions of $\tilde{g}(x,z)$ and $\tilde{g}'(x,z)$ from Propositions 6.3 and 6.5 give

$$\Delta = \mathrm{in}(\mathrm{coeff}(xz))\,\mathrm{in}(\mathrm{coeff}(x^2z)) - \mathrm{in}(\mathrm{coeff}(x^3))\,\mathrm{in}(\mathrm{coeff}(z^2)) = \mathrm{in}(\alpha_5)(\mathrm{in}(\beta_3)+\mathrm{in}(\beta_4))^2 \neq 0.$$

From the Newton subdivisions, we see that all bounded edges of both XZ-projections have tropical multiplicity one, so both planar re-embeddings are faithful on the minimal skeleta. Since all legs on $\mathrm{Trop}\,V(\tilde{g}')$ have also multiplicity one, we conclude that the XZ-projection for the refined modification is also faithful on the extended skeleton.

As with Type (I), the tropicalization (6.8) maps the legs of $\Sigma(\mathcal{X})$ marked by α_2 and α_5 isometrically onto the leg adjacent to v_1 and v_4 in the cells σ_1 and σ_2. Since $m_{\mathrm{trop}}(v_2) = 2$, the legs marked with α_3 and α_4 are mapped isometrically onto the leg adjacent to v_2, so these tropicalizations in $\mathbb{R}^3$ are not faithful on the extended skeleta. This can be repaired in dimension four by a vertical modification along $X = \omega_4$, via the ideal

$$J = I_{g,\tilde{f}} + \langle u - (x - \alpha_4)\rangle \subset K[x^{\pm}, y^{\pm}, z^{\pm}, u^{\pm}]. \tag{6.9}$$

The tropical curve $\mathrm{Trop}\,V(J)$ in $\mathbb{R}^4$ is obtained from $\mathrm{Trop}\,V(I_{g,\tilde{f}})$ by four simple operations:

(i) points $p = (p_1, p_2, p_3)$ in $\mathrm{Trop}\,V(I_{g,\tilde{f}})$ with $p_1 < \omega_4$ lift to points of the form (p, ω_4);
(ii) points $p = (p_1, p_2, p_3)$ in $\mathrm{Trop}\,V(I_{g,\tilde{f}})$ with $p_1 > \omega_4$ lift to points (p, p_1);
(iii) the vertex v_3 in $\mathrm{Trop}\,V(J)$ has coordinates $(\omega_4,\ 2\omega_4 + \omega_5/2,\ 2\omega_4 + \omega_5/2, \omega_4)$;
(iv) the multiplicity two leg with direction $(0, -1, 0)$ adjacent to v_3 splits into two multiplicity one legs ℓ_3 and ℓ_4, with directions $(0, -1, 0, 0)$ and $(0, -1, 0, -2)$: these are the images of the corresponding legs in $\Sigma(\mathcal{X})$ under the tropicalization map. Indeed,

$$\mathrm{in}_{\ell_3}(J) = \langle -x^2\,\mathrm{in}(\alpha_5)(x - \mathrm{in}(\alpha_3))u, u - x + \mathrm{in}(\alpha_4), z + \mathrm{in}(\beta_5\beta_4\beta_3)x - \mathrm{in}(\beta_5)x^2\rangle,$$
$$\mathrm{in}_{\ell_4}(J) = \langle y^2 - x^2\,\mathrm{in}(\alpha_5)(x - \mathrm{in}(\alpha_3))u, -x + \mathrm{in}(\alpha_4), z + \mathrm{in}(\beta_5\beta_4\beta_3)x - \mathrm{in}(\beta_5)x^2\rangle.$$

These two identities follow from standard Gröbner bases techniques over valued fields, in particular [41, Proposition 2.6.1, Corollary 2.4.10]. Notice that the UY-projection and its Newton subdivision can be easily obtained by the change of variables $u = x + \alpha_4$. Indeed, the result is a hyperelliptic genus two curve covering $\mathbb{P}^1$, whose six branch points have negative valuations $-\infty, \omega_4, \omega_4, \omega_4, \omega_5$ and ∞. As a consequence, we subdivide its Newton polytope along an edge joining y^2 and u^4. Similar reasoning applies to the UZ-projection. □

6.3. Proof for Type (IV)

The XY-and XZ-projections from Table 6.1 confirm that the two tropical space curves contain no points in σ_4. Furthermore, both curves can be obtained from their XZ-projections by attaching a leg in the direction $(0,-1,0)$ to the vertices v_1, v_2 and v_3. The leg attached to v_3 has multiplicity two, and it is the image of the legs marked with α_4 and α_5 in $\Sigma(\mathcal{X})$. The legs marked with α_2 and α_3 are mapped isometrically onto the legs adjacent to v_1 and v_2 in σ_1. Both curves have a multiplicity two leg ℓ with direction $(0,0,-1)$ attached to v_3:

$$\mathrm{in}_\ell(I_{g,f}) = \mathrm{in}_\ell(I_{g,\tilde{f}}) = \left\langle y^2 - x^3 \prod_{i=4}^{5}(x - \mathrm{in}(\alpha_i)), y + \mathrm{in}(\beta_3\beta_4\beta_5)x - \mathrm{in}(\beta_5)x^2 \right\rangle. \quad (6.10)$$

The vertex v_3 is the image of the unique genus one vertex in the Berkovich skeleton, and it is dual to the unique genus one triangle in the Newton subdivision of g. Furthermore:

Claim 1. *The initial degeneration* $\mathrm{in}_{v_3}(g)$ *defines a smooth elliptic curve in* $(\widetilde{K}^*)^2$.

Indeed, a direct computation and the Type (IV) defining conditions from Table 5.1 reveal

$$\mathrm{in}_{v_3}(g) = y^2 - x^3(x-\mathrm{in}(\alpha_4))(x-\mathrm{in}(\alpha_5)) = x^2((y/x)^2 - x(x-\mathrm{in}(\alpha_4))(x-\mathrm{in}(\alpha_5)), \quad (6.11)$$

so its projectivization is a double cover of $\mathbb{P}^1_{\widetilde{K}}$ branched at four distinguished points.

Remark 6.7. An alternative proof for Claim 1 can be given in terms of j-invariants, by considering the plane cubic curve $\mathcal{X}'$ defined by the truncation g' of g corresponding to all monomials in the triangle dual to v_3 in the Newton subdivision of g. By construction, $\mathrm{Trop}\, V(g')$ is the star of $\mathrm{Trop}\, V(g)$ along v_3. A direct computation with `Singular` and `Sage` (available in the Supplementary material) confirms that for any characteristic of $\widetilde{K}$ other than two, the j-invariant of $\mathcal{X}'$ has non-negative valuation, so $\mathcal{X}'$ has good reduction and the vertex of $\Sigma(\mathcal{X}')$ maps to v_3.

The previous discussion confirms that faithfulness occurs at the level of the minimal skeleta but fails for the extended one, due to the presence of the multiplicity two leg ℓ in σ_2 adjacent to v_3. This can be fixed using a vertical modification and the ideal J from (6.9). The same procedure from Subsection 6.2 allows us to recover $\mathrm{Trop}\, V(J)$ from $\mathrm{Trop}\, V(I_{g,\tilde{f}})$ and $\mathrm{Trop}\, V(I_{g,f})$, where the role of ℓ_3 is replaced by a leg ℓ_5. The following identities hold:

$$\mathrm{in}_{\ell_5}(J) = \langle -x^3(x - \mathrm{in}(\alpha_5))u, u - x + \mathrm{in}(\alpha_4), z + \mathrm{in}(\beta_3\beta_4\beta_5)x - \mathrm{in}(\beta_5)x^2 \rangle,$$
$$\mathrm{in}_{\ell_4}(J) = \langle y^2 - x^3\,\mathrm{in}(\alpha_5)u, -x + \mathrm{in}(\alpha_4), z + \mathrm{in}(\beta_3\beta_4\beta_5)x - \mathrm{in}(\beta_5)x^2 \rangle.$$

The legs ℓ_4 and ℓ_5 adjacent to v_3 have directions $(0,-1,0,-2)$ and $(0,-1,0,0)$ and they are isometric images of the legs in $\Sigma(\mathcal{X})$ marked with α_4 and α_5, respectively. By combining (6.10) with the identity $\mathrm{in}_\ell(J) = \mathrm{in}_\ell(I_{g,\tilde{f}}) + \langle u - x + \mathrm{in}(\alpha_4)\rangle$ we see that the leg ℓ from $\mathrm{Trop}\, V(I_{g,\tilde{f}})$ survives in $\mathrm{Trop}\, V(J)$: it has direction $(0,0,-1,0)$ and multiplicity two. □

6.4. Proof for Type (VI)

From Table 6.1 we see that the vertex v_2 is dual to the unique genus one lattice polygon in the Newton subdivision of g. As in Type (IV), v_2 is the image of the unique genus one vertex in the Berkovich skeleton under the xy- and xz-tropicalizations.

Claim 2. *The initial degeneration* $\mathrm{in}_{v_2}(g)$ *defines a smooth elliptic curve in* $(\widetilde{K}^*)^2$.

Indeed, the conditions from Table 5.1 reveal that $\mathrm{in}_{v_2}(g) = x^2((y/x)^2 - \prod_{i=3}^{5}(x - \mathrm{in}(\alpha_i))$, so its projectivization is a double cover of $\mathbb{P}^1_{\widetilde{K}}$ branched at four distinguished points.

By construction, the naïve tropicalization maps the legs marked with $\alpha_3, \alpha_4, \alpha_5$ in $\Sigma(\mathcal{X})$ isometrically to the leg adjacent to v_2 with direction $(0,-1)$. The next initial form computation reveals that this leg is the projection of a multiplicity three leg ℓ with direction $(0,-1,0)$ adjacent to v_2 which is the image of the aforementioned marked legs in $\Sigma(\mathcal{X})$:

$$\mathrm{in}_\ell(I_{g,f}) = \mathrm{in}_\ell(I_{g,\tilde{f}}) = \langle x^2 \prod_{i=3}^{5}(x - \mathrm{in}(\alpha_i)), z + \mathrm{in}(\beta_3\beta_4\beta_5)x - \mathrm{in}(\beta_5)x^2\rangle. \tag{6.12}$$

As was discussed earlier, the combinatorics of the xz-tropicalizations depend heavily on the genericity of the coefficients of x^3 and x^4 in both $\tilde{g}(x,z)$ and $\tilde{g}'(x,z)$. A careful case-by-case analysis confirms that all vertices have multiplicity one. Furthermore,

$$\mathrm{in}_{v_2}(I_{g,f}) = \mathrm{in}_{v_2}(I_{g,\tilde{f}}) = \langle \mathrm{in}_{v_2}(g), z - y + \mathrm{in}(\beta_3\beta_4\beta_5)x - \mathrm{in}(\beta_5)x^2\rangle.$$

Since all bounded edges also have multiplicity one, we conclude that the xz-tropicalizations are faithful on the minimal skeleton. In what follows, we describe the combinatorics of both space curves in each relevant case and analyze faithfulness on the extended skeleton. The genericity conditions for both x^3 and x^4 are described in Propositions 6.3 and 6.5.

Case 1: generic for x^3. Extended faithfulness cannot be guaranteed since each star of v_2 contains a multiplicity two leg in σ_5 with direction $(0,0,-1)$. The vertex $v_{12} = v'_{12}$ of $\mathrm{Trop}\, V(I_{g,f})$ also has a multiplicity two leg in σ_6 with the same direction.

Case 2: non-generic for x^3, generic for x^4. The two possible xz-tropicalizations are obtained from the Newton subdivision of $\tilde{g}$ and $\tilde{g}'$ in the left and center of Fig. 6.1. They

depend on whether x^3 is marked or not. Both cases were discussed in Remark 6.6. In the marked case, the xz-tropicalization $\operatorname{Trop} V(\tilde{g}')$ is not faithful on the extended skeleton. Indeed, the high multiplicity leg attached to $v_{12} = v'_{12}$ in the direction $(0,0,-1)$ induces an initial degeneration with two distinct reduced components, and faithfulness fails for the extended skeleton. It can be repaired by a vertical modification along this leg and a lift induced by one of these two components.

Similarly, in the unmarked case, Proposition 6.5 shows that the high multiplicity leg attached to v'_{12} in the direction $(0,0,-1)$ induces an initial degeneration with reduced distinct components. So extended faithfulness fails for the xz-tropicalization. Vertical modifications along this leg adapted to these components will repair this situation in dimension three for $I_{g,\tilde{f}}$ and four for $I_{g,f}$.

Finally, the multiplicity of the leg ℓ described in (6.12) and Lemma 3.3 ensure that the leg attached to the vertex v_2 in both xz-tropicalizations is the projection of a single multiplicity two leg in the direction $(0,0,-1)$ attached to v_2. This completes the description of the combinatorics of both space curves.

Case 3: non-generic for both x^3 and x^4. As discussed in Remark 6.6, the Newton subdivision of $\tilde{g}$ cannot be predicted, so we focused on the refined modification and the embedding $I_{g,\tilde{f}}$. The Newton subdivision of $\tilde{g}'$, depicted in the right of Fig. 6.1 shows that no point of $\operatorname{Trop}(I_{g,\tilde{f}})$ lies in the relative interior of σ_4. The star of v_2 consists of the multiplicity three leg ℓ with direction $(0,-1,0)$, the leg ℓ_6 with direction $(2,5,5)$ and two bounded edges with directions $(-1,-1,-1)$ and $(-1,-1,-3)$, respectively. The vertex v_1 is adjacent to a unique leg, with direction $(-2,-1,-1)$. By Proposition 6.5, the vertex v'_{12} is adjacent to a multiplicity two leg with direction $(0,0,-1)$ whose initial degeneration has two distinct reduced components. The xz-tropicalization is not faithful on the extended skeleton. This can be repaired by a vertical modification along $\max\{Z, (5\omega_4 - 3\varepsilon)/2\}$, adapted to one of these components.

As with Type (III), the extended skeleton $\Sigma(\mathcal{X})$ can only be revealed by means of vertical modifications through v_2 designed to separate the images of the legs marked with α_3, α_4 and α_5. We use the ideal

$$J = I_{g,\tilde{f}} + \langle z_3 - (x - \alpha_3), z_4 - (x - \alpha_4)\rangle \subset K[x^{\pm}, y^{\pm}, z^{\pm}, z_3^{\pm}, z_4^{\pm}].$$

The leg ℓ in the star of v_2 in $\operatorname{Trop} V(I_{g,f})$ and $\operatorname{Trop} V(I_{g,\tilde{f}})$ is replaced by three multiplicity one legs (ℓ_3, ℓ_4 and ℓ_5), with directions $(0,-1,0,-2,0)$, $(0,-1,0,0,-2)$, and $(0,-1,0,0,0)$, each coming from the expected marked leg in $\Sigma(\mathcal{X})$. □

6.5. Proof for Type (II)

Throughout this section, and to simplify the exposition, we assume $\operatorname{char} \widetilde{K} \neq 2, 3$. A refinement of our methods will be required in characteristic three.

The Type (II) cone manifests itself as the most combinatorially challenging cell of M_2^{trop}. It is the only case for which the chart σ_4 in the tropical modification of $\mathbb{R}^2$

contains points of the re-embedded tropical curve $\operatorname{Trop} V(I_{g,f})$ in its relative interior. In particular, information from all three coordinate projections is necessary to recover the space curve using Lemma 3.3. Furthermore, as was already observed in Fig. 3.1, depending on the values of the three edge lengths in the theta graph, the YZ-projection of $\operatorname{Trop} V(I_{g,f})$ introduces extra crossings and higher multiplicities that need to be unraveled in the reconstruction process. Here is our main result:

Theorem 6.8. *In Type (II) the tropical curves $\operatorname{Trop} V(I_{g,f})$ come in 13 combinatorial types, depicted in Fig. 6.8. These graphs are determined by a subdivision of the Type (II) cone along its baricenter. Precise coordinates for all vertices are given in* (6.15).

The proof of this result is computational and it involves genericity conditions of the branch points giving each graph. As usual, examples for all cases are provided in the Supplementary material.

The condition $\operatorname{in}(\alpha_3) = \operatorname{in}(\alpha_4)$ characterizing the witness Type (II) region in Table 5.1 suggests a new strategy to determine the combinatorics of $\operatorname{Trop} V(I_{g,f})$ by controlling the value of d_{34}. We introduce a new variable $\beta_{34} := \beta_3 - \beta_4$ and redefine the third branch point as $\alpha_3 := (\beta_4 + \beta_{34})^2$, where $-\operatorname{val}(\beta_{34}) = d_{34} + \operatorname{val}(\alpha_4)/2 = -\operatorname{val}(\alpha_3 - \alpha_4) + \operatorname{val}(\beta_4)$. The hyperelliptic equation becomes $g(x,y) = y^2 - x(x-\beta_2^2)(x-(\beta_4+\beta_{34})^2)(x-\beta_4^2)(x+\beta_5^2)$, and the lifting f from (6.2) of the tropical polynomial F from (3.3) equals

$$f(x,y) = y - \beta_5(\beta_4 + \beta_{34})\beta_4\, x + \beta_5\, x^2.$$

The weight vector $\underline{u} \in \mathbb{R}^4$ encoding the negative valuation of the four parameters equals:

$$\underline{u} := (-\operatorname{val}(\beta_5), -\operatorname{val}(\beta_4), -\operatorname{val}(\beta_{34}), -\operatorname{val}(\beta_2)) = (\omega_5/2, \omega_4/2, d_{34} - \omega_4/2, \omega_2/2). \tag{6.13}$$

We set $u_i = -\operatorname{val}(\beta_i)$ for each $i = 5, 4, 34, 2$ and write the coordinates of $\mathbb{R}^4$ in that order. The Type (II) cone is then determined by the following inequalities:

$$u_5 > u_4, \quad u_4 > u_{34}, \quad \text{and} \quad u_4 > u_2. \tag{6.14}$$

An easy `Sage` computation reveals that the closure of this cone is spanned by three vectors (R_1, R_2 and R_3 in Fig. 6.2) and has a one-dimensional lineality space generated by the all-ones vector. We are solely interested in its interior, since its various proper faces correspond to other curve types in M_2.

On the algebraic side, the interplay between the combinatorics of $\operatorname{Trop} V(I_{g,f})$ and the weight vector $\underline{u}$ is determined by the projection to $\mathbb{R}^4$ of the Gröbner fan of the extended ideal $I_{g,f}K[\beta_5^{\pm}, \beta_4^{\pm}, \beta_{34}^{\pm}, \beta_2^{\pm}, x^{\pm}, y^{\pm}, z^{\pm}]$. Since the computation of this fan with build-in `Sage` functions does not terminate, we turn to Lemma 3.3 and compute $\operatorname{Trop} V(I_{g,f})$ by

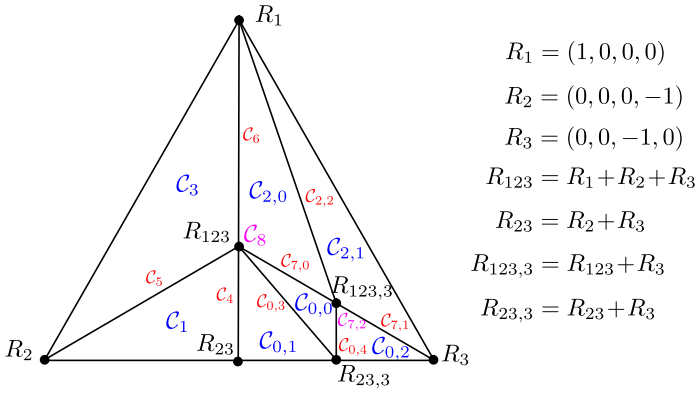

Fig. 6.2. Refined subdivision of the Type (II) cone induced by all possible Newton subdivisions of the yz-projection after removing the one-dimensional lineality space. The first index of each cone reflects the label within the subdivision by leading terms of coefficients as in Table 6.2. The blue cones have maximal dimension four, the red cones have dimension three and the purple cone has dimension two. (For interpretation of the colors in the figure(s), the reader is referred to the web version of this article.)

Table 6.2
From top to bottom: Expected leading terms for all relevant coefficients of $h(y,z)$ (14 total) and $\tilde{g}(x,z)$ (three total) on the nine cones $\mathcal{C}_i$ coarsening the refined subdivision of the Type (II) Cone in Fig. 6.2. Each b_i is the initial form of the parameter β_i.

Monomials	Leading Terms	Weights	Cones
y^4	$2\,b_2^2\,b_5^3$	$\omega_2 + 3\omega_5/2$	[0, 2, 7]
	$2\,b_{34}^2\,b_5^3$	$2d_{34} - \omega_4 + 3\omega_5/2$	[1, 3, 5]
	$2\,b_5^3\,(b_{34}^2 + b_2^2)$	$\omega_2 + 3\omega_5/2$	[4, 6, 8]
y^3z	$-2\,b_4^2\,b_5^3$	$\omega_4 + 3\omega_5/2$	all
y^2z^2, yz^3, z^4	b_5^5 (coeffs 4, -4, 1, resp.)	$5\omega_5/2$	all
y^3	$-b_2^2\,b_4^4\,b_5^4$	$\omega_2 + 2(\omega_4 + \omega_5)$	[0]
	$-b_{34}^2\,b_4^4\,b_5^4$	$2(d_{34} + \omega_5) + \omega_4$	[1]
	$b_2^4\,b_5^6$	$2\omega_2 + 3\omega_5$	[2]
	$b_{34}^4\,b_5^6$	$4d_{34} - 2\omega_4 + 3\omega_5$	[3]
	$-b_4^4\,b_5^4\,(b_{34}^2 + b_2^2)$	$\omega_2 + 2(\omega_4 + \omega_5)$	[4]
	$b_{34}^2\,b_5^4\,(-b_4^2 + b_5\,b_{34})\,(b_4^2 + b_5\,b_{34})$	$2(d_{34} + \omega_5) + \omega_4$	[5]
	$b_5^6\,(b_{34}^2 + b_2^2)^2$	$2\omega_2 + 3\omega_5$	[6]
	$b_2^2\,b_5^4\,(-b_4^2 + b_5\,b_2)\,(b_4^2 + b_5\,b_2)$	$\omega_2 + 2(\omega_4 + \omega_5)$	[7]
	$b_5^4\,(b_{34}^2 + b_2^2)\,(-b_4^4 + b_5^2\,b_{34}^2 + b_5^2\,b_2^2)$	$\omega_2 + 2(\omega_4 + \omega_5)$	[8]
y^2z, yz^2, z^3	$b_2^2\,b_4^2\,b_5^6$ (coeffs 2, -3, 1 resp.)	$\omega_2 + \omega_4 + 3\omega_5$	[0, 2, 7]
	$b_{34}^2\,b_4^2\,b_5^6$ (coeffs -6, 9, -3, resp.)	$2d_{34} + 3\omega_5$	[1, 3, 5]
	$b_4^2\,b_5^6\,(3\,b_{34}^2 - b_2^2)$ (coeffs -2, 3, -1, resp.)	$\omega_2 + \omega_4 + 3\omega_5$	[4, 6, 8]
y^2	$-4\,b_2^2\,b_{34}^2\,b_4^4\,b_5^7$	$2d_{34}+\omega_2+\omega_4+7\omega_5/2$	all
yz, z^2	$b_{34}^2\,b_4^6\,b_5^7$ (coeffs 2, -1, resp.)	$2d_{34}+2\omega_4+7\omega_5/2$	all
y, z	$b_2^2\,b_{34}^2\,b_4^8\,b_5^8$ (coeffs 1, -1, resp.)	$2d_{34}+\omega_2+3\omega_4+4\omega_5$	all
x^4	$-2\,b_4^2$	$2\omega_4$	all
x^3	b_4^4	$2\omega_4$	[0, 1, 4]
	$-b_2^2\,b_5^2$	$\omega_2 + \omega_5$	[2]
	$-b_{34}^2\,b_5^2$	$2d_{34} + \omega_5 - \omega_4$	[3]
	$-(-b_4^2 + b_5\,b_{34})\,(b_4^2 + b_5\,b_{34})$	$2\omega_4$	[5]
	$-b_5^2\,(b_{34}^2 + b_2^2)$	$\omega_2 + \omega_5$	[6]
	$-(-b_4^2 + b_5\,b_2)\,(b_4^2 + b_5\,b_2)$	$2\omega_4$	[7]
	$-(-b_4^4 + b_5^2\,b_{34}^2 + b_5^2\,b_2^2)$	$2\omega_4$	[8]
x^2	$2\,b_2^2\,b_4^2\,b_5^2$	$\omega_2 + \omega_4 + \omega_5$	all

means of the three coordinate projections as we vary $\underline{u}$. In the remainder of this section we describe the interplay between the weight vector $\underline{u}$ and the (x,z)- and (y,z)-subdivisions.

Following earlier notation, we call $\tilde{g}(x,z) = g(x, z + (\beta_4+\beta_{34})\beta_4\beta_5 x - \beta_5 z^2)$ and let $h(y,z)$ be the generator of $I_{g,f} \cap K[y,z]$. The latter is determined by an easy elimination ideal computation using `Singular`, available in the Supplementary material. Its extremal monomials are y, z, y^5 and z^5. The coefficients of both $\tilde{g}$ and h lie in $\mathbb{Z}[\beta_5, \beta_4, \beta_{34}, \beta_2]$. The first column of Table 6.2 shows the 17 terms of both polynomials with non-monomial coefficients. The second column shows the factorization of the leading terms of these non-monomial coefficients for each of the nine cones in Lemma 6.9 and justifies our characteristic assumption on $\widetilde{K}$. The $\underline{u}$-weights give the expected heights of all relevant coefficients of $\tilde{g}$ and h (indicated in the third column.) The table also provides the precise conditions on the initial forms of $\beta_5, \beta_4, \beta_{34}$ and β_2 under which these heights are lower than expected.

The (y,z)- and (x,z)-Newton subdivisions of $I_{g,f}$ will be determined by the valuations of these 17 coefficients. The answer will vary with $\underline{u}$ in a piecewise linear fashion. At first glance, the domains of linearity are determined by the common refinement of the Type (II) cone in $\mathbb{R}^4$ and the Gröbner fan of the product of all these 17 non-monomial coefficients. The latter has f-vector $(1, 21, 54, 35)$, so the refinement is performed by intersecting the Type (II) cone with the 35 chambers in the fan. The next statement describes this naïve subdivision of the Type (II) cone into four triangles determined by the baricenters R_{123} and R_{23} from Fig. 6.2. Its proof is computational, and the required scripts are available in the Supplementary material.

Lemma 6.9. *The Gröbner fans of all 17 non-monomial coefficients of $\tilde{g}$ and h induce a subdivision of the Type (II) cone into nine cones. Following Fig. 6.2 they are:*

$$\mathcal{C}_0 := \mathbb{R}_{>0}\langle R_{23}, R_{123}, R_3\rangle \oplus \mathbb{R}\cdot\mathbf{1}, \quad \mathcal{C}_1 := \mathbb{R}_{>0}\langle R_{23}, R_{123}, R_2\rangle \oplus \mathbb{R}\cdot\mathbf{1}, \quad \mathcal{C}_2 := \mathbb{R}_{>0}\langle R_1, R_{123}, R_3\rangle \oplus \mathbb{R}\cdot\mathbf{1},$$
$$\mathcal{C}_3 := \mathbb{R}_{>0}\langle R_1, R_{123}, R_2\rangle \oplus \mathbb{R}\cdot\mathbf{1}, \quad \mathcal{C}_4 := \mathbb{R}_{>0}\langle R_{23}, R_{123}\rangle \oplus \mathbb{R}\cdot\mathbf{1}, \quad \mathcal{C}_5 := \mathbb{R}_{>0}\langle R_{123}, R_2\rangle \oplus \mathbb{R}\cdot\mathbf{1},$$
$$\mathcal{C}_6 := \mathbb{R}_{>0}\langle R_{123}, R_1\rangle \oplus \mathbb{R}\cdot\mathbf{1}, \quad \mathcal{C}_7 := \mathbb{R}_{>0}\langle R_{123}, R_3\rangle \oplus \mathbb{R}\cdot\mathbf{1}, \quad \mathcal{C}_8 := \mathbb{R}_{>0}\langle R_{123}\rangle \oplus \mathbb{R}\cdot\mathbf{1}.$$

In what follows we discuss the combinatorics of the Newton subdivisions of $\tilde{g}$. The next result summarizes our findings, depicted in Fig. 6.3:

Proposition 6.10. *There are eight combinatorial types of unmarked Newton subdivisions of $\tilde{g}$. The monomial x^3 in $\tilde{g}(x,z)$ is the sole responsible for non-generic behavior, which only occurs in the cells $\mathcal{C}_i$ for $i = 5, 6, 7, 8$.*

Proof. By Table 6.1, the Newton subdivision of $\tilde{g}$ is determined by all possible subdivisions of the parallelogram $\mathcal{P}$. To find the generic subdivision on each cell, we take as a sample weight vector $\underline{u}$ the average of its spanning rays. We compute an example of parameters $\beta_5, \ldots, \beta_2$ with coordinatewise negative valuation $\underline{u}$ and pick initial forms $b_i = \mathrm{in}(\beta_i)$ ensuring the corresponding leading terms in Table 6.2 do not vanish. We compute the corresponding plane tropical curve and its dual subdivision with

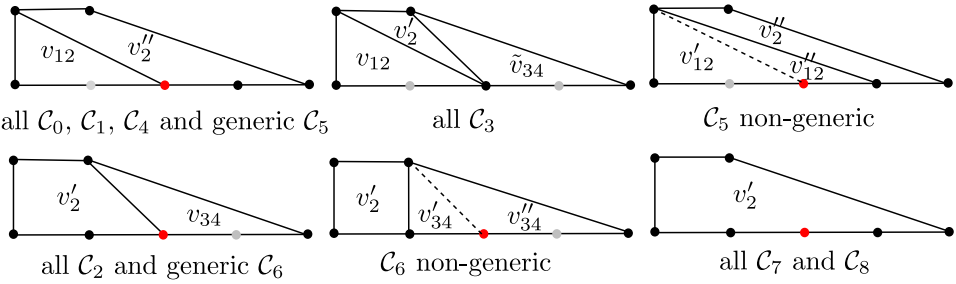

Fig. 6.3. All eight subdivisions of the parallelogram $\mathcal{P}$ from Table 6.1. The generic and non-generic behavior of x^3 on the four relevant cells are indicated by a red dot. The dashed lines correspond to two combinatorial types arising for non-generic initial forms. If absent, both vertices agree with v_{12} and v_{34}, accordingly. For non-generic $\mathcal{C}_7$, x^3 is unmarked. (For interpretation of the colors in the figure(s), the reader is referred to the web version of this article.)

the `tropical.lib` package in `Singular`. All examples and scripts are available in the Supplementary material.

To certify that each generic subdivision is valid on the entire cell, we compute explicit formulas for all the vertices dual to polygons in the subdivision, in terms of the weights of the monomials on $\mathcal{P}$ being maximized (these weights are provided in Table 6.2). Finally, the inequalities defining each of the nine cells confirm that these vertices maximize the same monomials for every weight vector in the given cell.

To address non-generic behavior on the cells $\mathcal{C}_5, \mathcal{C}_6, \mathcal{C}_7$ and $\mathcal{C}_8$, we need only to focus on the monomial x^3. We list all possible subdivisions of $\mathcal{P}$ that can arise by lowering x^3 and construct numerical examples showing which ones are realized. □

Since the linear inequalities between the expected heights of each relevant monomial in $h(y,z)$ can vary within each cell, the methods used for $\tilde{g}$ will not suffice to determine all possible Newton subdivisions of h. A refined subdivision of the Type (II) cone induced by a subdivision of $\mathcal{C}_0$, $\mathcal{C}_2$ and the relative interior of their common facet $\mathcal{C}_7$ will be required to address this point and the effect of non-generic choices of β-parameters.

To this end, we construct nine polynomials h_i for $i = 0, \ldots, 8$, obtained by replacing each coefficient of h by its leading term on the corresponding cone $\mathcal{C}_i$. We compute the Gröbner fan $\mathscr{G}_i$ of each h_i in $\mathbb{R}^6$, and intersect each $\mathcal{C}_i$ with the projection of all maximal cells in $\mathscr{G}_i$ to the four β-coordinates. These calculations are easily performed since each fan has at most 16 chambers and lineality space $\mathbb{R} \cdot \mathbf{1}$. The result of this subdivision process is depicted in Fig. 6.2.

Next, we describe all possible Newton subdivisions of h. As with Proposition 6.10, the proof is computational in nature and requires a careful analysis for non-generic cases.

Proposition 6.11. *Each cell in Fig. 6.2 will give rise to one generic subdivision of $h(y,z)$, with further possibilities if genericity conditions are detected in Table 6.2. Figs. 6.4 through 6.7 depict all possible outcomes, grouped conveniently.*

Before providing the details of the proof for each cell, we point out some common features of the various subdivisions and clarify notation. In all cases, we only indicate vertices of $\operatorname{Trop} V(I_{g,f})$ rather than false crossings arising from certain parallelograms (seen, for example, in the subdivision of Q_1 in Fig. 6.6.) False crossings may also appear from a polygon with at least two parallel edges when a vertex in σ_6 maps to the interior of an edge or leg in σ_4. This is seen in the polygon Q_4 in the same figure: the YZ-projection of the vertex v_{12} in σ_6 lies in the projection of the leg with direction $(0,0,-1)$ adjacent to the vertex v_{21} in σ_4.

In addition to these false crossings, the YZ-projection has other undesirable effects: we will see vertices in σ_4 hidden in edges of $\operatorname{Trop} V(h)$, overlapping of vertices, as well as higher multiplicity edges and legs coming in two flavors:

(i) Multiplicity one edges and legs inherit higher multiplicities in the yz-tropicalization due to the push-forward formula for multiplicities. This occurs for the leg with direction $(2,5,5)$ in σ_3 adjacent to v_4 which inherits multiplicity 5 in $\operatorname{Trop} V(h)$.
(ii) Two edges or legs (one in σ_4 and one in σ_6) overlap in the yz-tropicalization, and their multiplicities get added accordingly. This will always be the case for the edges joining z^4 and y^2z^2 in all Newton subdivisions of h. On the tropical side, this was observed already in Fig. 3.1.
(iii) Vertices in σ_4 lie in relative interiors of edges in $\operatorname{Trop} V(h)$. This occurs for the vertex v_2 and the cells $\mathcal{C}_{0,i}$: v_2 maximizes the edge between z^4 and y^2z^2 in Fig. 6.4.
(iv) A vertex in σ_4 and one in σ_6 become the same vertex in $\operatorname{Trop} V(h)$. This will be indicated in all figures by equalities between labeling vertices dual to a given polygon.

Proof of Proposition 6.11. To determine the generic subdivisions we proceed by direct computation, as in the proof of Proposition 6.10. The results for each one of the 17 cells are shown in Figs. 6.4 through 6.7, where superscripts *gen* indicate generic parameters.

Next, we discuss the labeling of all polygons in the generic subdivisions. By Lemma 3.3, we can place the vertices of $\operatorname{Trop} V(I_{g,f})$ we already know from Table 6.1 and Fig. 6.3 as duals to polygons or edges in the subdivision. The remaining unlabeled polygons correspond to either false crossings or vertices in σ_4. The false crossings correspond to parallelograms, and we leave them blank. The others get labeled with blue vertices of the form v_{2i} with $i = 0,1$ to emphasize that they come from σ_4.

In order to determine all non-generic subdivisions, we look for vanishing of expected leading terms in Table 6.2 that will lower the corresponding monomials. In most cases, the resulting special subdivisions (marked with the superscript *sp* on the figures) will differ from the generic ones in only a few polygons. We treat each cell separately to predict these special behaviors and construct numerical examples to confirm these potential subdivisions do occur.

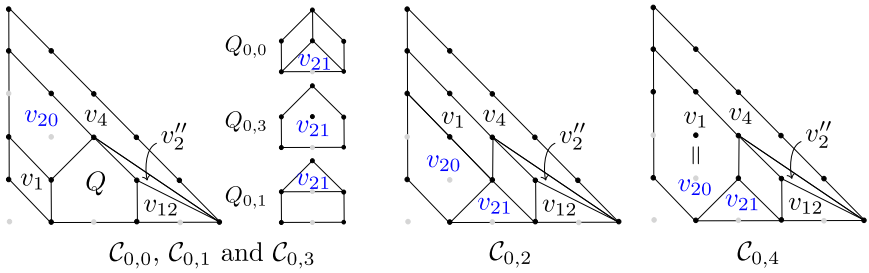

Fig. 6.4. All possible subdivisions corresponding to weight vectors in the cells $\mathcal{C}_{0,i}$ for $i = 0, \dots, 4$. The polygon $Q_{0,i}$ indicates the subdivision of the polygon Q on $\mathcal{C}_{0,i}$. Unlabeled polygons correspond to false crossings. Blue vertices come from σ_4. The notation on the remaining vertices is compatible with that of Table 6.1 and Fig. 6.3. (For interpretation of the colors in the figure(s), the reader is referred to the web version of this article.)

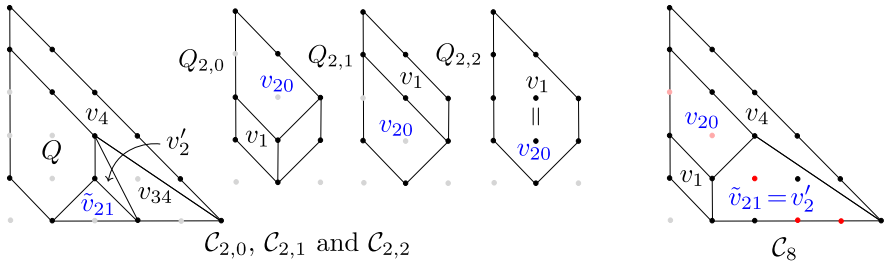

Fig. 6.5. All possible subdivisions for the cells $\mathcal{C}_{2,i}$ for $i = 0, 1, 2$ and $\mathcal{C}_8$. Red (respectively pink) dots indicate marked (resp. unmarked) monomials whose behavior varies with the genericity conditions. (For interpretation of the colors in the figure(s), the reader is referred to the web version of this article.)

We start with the cell $\mathcal{C}_4$. The monomials affected are y^4 (if $b_{34}^2 = -b_2^2$), and y^2, yz^2 and z^3 (if $3b_{34}^2 = b_2^2$). From Fig. 6.6 we see that lowering any of these four monomials will have no effect on the generic subdivision since these points were already unmarked (the unmarking of y^4 was indicated in pink). Therefore, there will be a single Newton subdivision for $\mathcal{C}_4$, namely the generic one.

Special subdivisions on the cell $\mathcal{C}_5$ are determined by the behavior of y^3 whenever $b_4^2 = \pm b_5 b_{34}$. This monomial is marked in Q_5^{gen}, as seen in Fig. 6.6. When the height of this monomial is reduced, an edge between yz and y^4 arises. Furthermore, with the exception of y^3, the heights of all points in the triangle T with vertices y, yz and y^4 are known from Table 6.2. Depending on the height of y^3, there will be two possible subdivisions: either T is a polygon in the subdivision, or it gets divided along an edge between y^3 and yz. Numerical examples confirm that both cases do occur.

The cell $\mathcal{C}_6$ has the same defining genericity conditions as $\mathcal{C}_4$, with the addition that y^4 drops height whenever y^3 does. Since y^2 is marked, the lowering of the monomials z^3, y^2z and yz will not change the subdivision, so we can disregard this genericity condition, and only require $b_{34}^2 = -b_2^2$ for special behavior.

Furthermore, since y^3 and y^4 are both marked in Q_6^{gen} as we see in Fig. 6.6, for special parameters, an edge joining y^2 and y^2z^2 will appear and give rise to a tri-

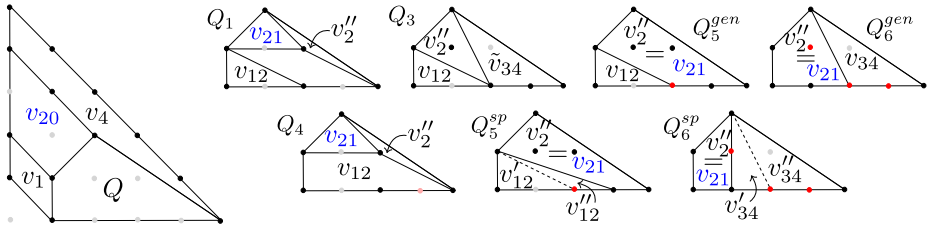

Fig. 6.6. All possible subdivisions for the cells $\mathcal{C}_i$ for $i = 1, 3, 4, 5, 6$. The polygon Q gets subdivided differently on each cell. The subscript *gen* correspond to generic parameters $\beta_5, \beta_4, \beta_{34}$ and β_2, whereas the superscript *sp* indicate special ones. As with Fig. 6.3, dotted lines correspond to extra possible subdivisions. When absent, the corresponding vertices agree.

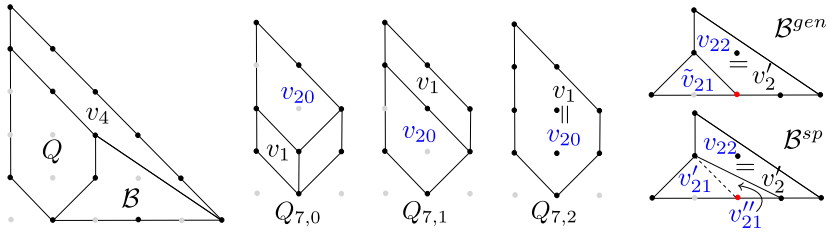

Fig. 6.7. All possible subdivisions for the cells $\mathcal{C}_{7,i}$ for $i = 0, 1, 2$.

angle T with vertices y^2, y^2z^2 and y^5. We claim that T can only be further subdivided by an edge between y^2z^2 and y^3 leading to the two possibilities for Q_6^{sp} shown in the figure. The reason for this lies in Lemma 3.3 and Proposition 6.10. Since $v_{12} = (2\omega_4 + \omega_5/2, \omega_2 + \omega_4 + \omega_5/2)$, this vertex lies in $\sigma_4 \cap \sigma_5$. Therefore, all cells in a subdivision of T will come from vertices in σ_5, namely the vertices v'_{34} and v''_{34} in Fig. 6.3. Unless these two agree, the edge between them in $\operatorname{Trop} V(\tilde{g})$ is dual to an edge with slope -2 in a subdivision of T. By convexity, there is only one option for such an edge.

The analysis of non-genericity for the cells $\mathcal{C}_{7,i}$ with $i = 0, 1, 2$ is simpler that earlier cases since only the monomial y^3 imposes restrictions on the parameters. Only if $b_4^2 = \pm b_2 b_5$ this monomial will be lower than expected. If so, due to the marking of y^4 in the polygon $\mathcal{B}^{gen}$ from Fig. 6.7, an edge between y^2z and y^4 will appear for special parameters. Depending on the height of y^3, we will have one extra edge joining y^2z and y^3. This yields the two possible configurations $\mathcal{B}^{sp}$ in the figure.

Finally, we discuss the subdivisions for non-generic parameters coming from $\mathcal{C}_8$. The same six monomials from $\mathcal{C}_6$ are responsible for special choices of parameters. Since these six monomials were not vertices in the generic subdivision in Fig. 6.5, lowering them will not alter the subdivision, except for unmarking y^3 and y^4 accordingly. Thus, the generic and the special Newton subdivisions agree for $\mathcal{C}_8$. This concludes our proof. □

Formulas for all vertices in $\operatorname{Trop} V(I_{g,f})$ can be given in terms of the vertices v_1, v_2, v_4 from (6.4) (where $\omega_3 = \omega_4$) and the weight vector $(\omega_5, \omega_4, d_{34}, \omega_2)$ from Table 5.1:

$$\begin{aligned}
v_{12} &:= v_1 + (\omega_5 - \omega_2)/2\,(1,1,0), & v_2'' &:= v_2 - (\omega_5 - \omega_4)(0,0,1),\\
v_{34} &:= v_4 - (\omega_5 - \omega_2)/2\,(1,2,3), & v_{12}' &:= v_{12} - \varepsilon'(1,1,0),\\
\tilde{v}_{34} &:= v_4 - (\omega_5 + \omega_4 - 2d_{34})/2\,(1,2,3), & v_{12}'' &:= v_2'' - 2\varepsilon'(1,1,3),\\
v_{20} &:= v_2 - (\omega_4 - d_{34})(0,1,1), & v_{34}' &:= v_2' + 2\varepsilon(1,2,0),\\
v_{21} &:= v_2'' - (3\omega_4 + 2\omega_5 - 2d_{34})/2\,(0,1,1), & v_{34}'' &:= v_{34} - \varepsilon(1,2,3),\\
\tilde{v}_{21} &:= v_2' - (\omega_4 + \omega_2 - 2d_{34})/2\,(0,1,1), & v_{21}' &:= v_{21} + \varepsilon''(0,1,-1),\\
v_2' &:= v_2 - (\omega_4 - \omega_2)(0,0,1), & v_{21}'' &:= v_2' - 2\varepsilon''(0,1,2),
\end{aligned} \tag{6.15}$$

where $0 \le \varepsilon \le (\omega_5 + \omega_2 - 2\omega_4)/6$, $0 \le \varepsilon' \le (2\omega_4 - \omega_5 - \omega_2)/6$ and $0 \le \varepsilon'' \le (\omega_5 + 2d_{34} - \omega_4)/6$. Whenever the value of ε is maximal, we get $v_{34}' = v_{34}''$. Similarly, when ε' and ε'' are maximal, it follows that $v_{12}' = v_{12}''$ and $v_{21}' = v_{21}''$, respectively.

Proof of Theorem 6.8. The result follows by combining Lemma 3.3 with Propositions 6.10 and 6.11. It is worth noticing that $\mathcal{C}_{0,i}$, $\mathcal{C}_1$, and $\mathcal{C}_4$ give tropical curves in $\mathbb{R}^3$ with the same combinatorial type (indicated in Fig. 6.8 by the cell $\mathcal{C}_{014}$). Fig. 3.1 corresponds to a graph in $\mathcal{C}_{014}$. Each special configuration leads to two cells $\mathcal{C}_i^{sp}$ and $\mathcal{C}_i^{sp_2}$ for $i = 5, 6, 7$. The latter is obtained when $v_{12}' = v_{12}''$, $v_{34}' = v_{34}''$ and $v_{21}' = v_{21}''$, respectively. □

A simple computation shows that $\operatorname{in}_v(I_{g,f})$ is reduced and irreducible for all vertices and edges in $\operatorname{Trop} V(I_{g,f})$. We conclude that the tropical skeleton is isometric to the minimal Berkovich skeleton, as predicted by Theorem 1.2. Faithfulness at the level of the extended skeleta can be achieved via the vertical modification (6.9) as in Type (III).

Example 6.12 *(Example 3.4 revisited).* As was shown in Fig. 3.1, the curve from Example 3.4 is of Type (II). It lies in the witness region $\Omega^{(II)}$ with branch points

$$\alpha_1 = \infty,\ \alpha_2 = (3\,t^5)^2,\ \alpha_3 = (11\,t^2 + 5\,t^7)^2,\ \alpha_4 = (11\,t^2)^2,\ \alpha_5 = (1 + t^2)^2 \text{ and } \alpha_6 = 0.$$

By construction, we have natural choices for square-roots of the relevant branch points, namely $\beta_2 = 3\,t^5$, $\beta_3 = 11\,t^2 + 5\,t^7$, $\beta_4 = 11\,t^2$ and $\beta_5 = 1 + t^2$. We re-embed our naïve tropicalization via the following algebraic lift from (6.2) of $F = \max\{Y, -4 + X, 2X\}$:

$$f(x,y) = y - 11\,t^2(1 + t^2)(11\,t^2 + 5\,y^7)\,x + (1 + t^2)\,x^2.$$

Since $\beta_{34} = \beta_3 - \beta_4 = -5\,t^7$, the weight vector $\underline{u}$ from (6.13) becomes

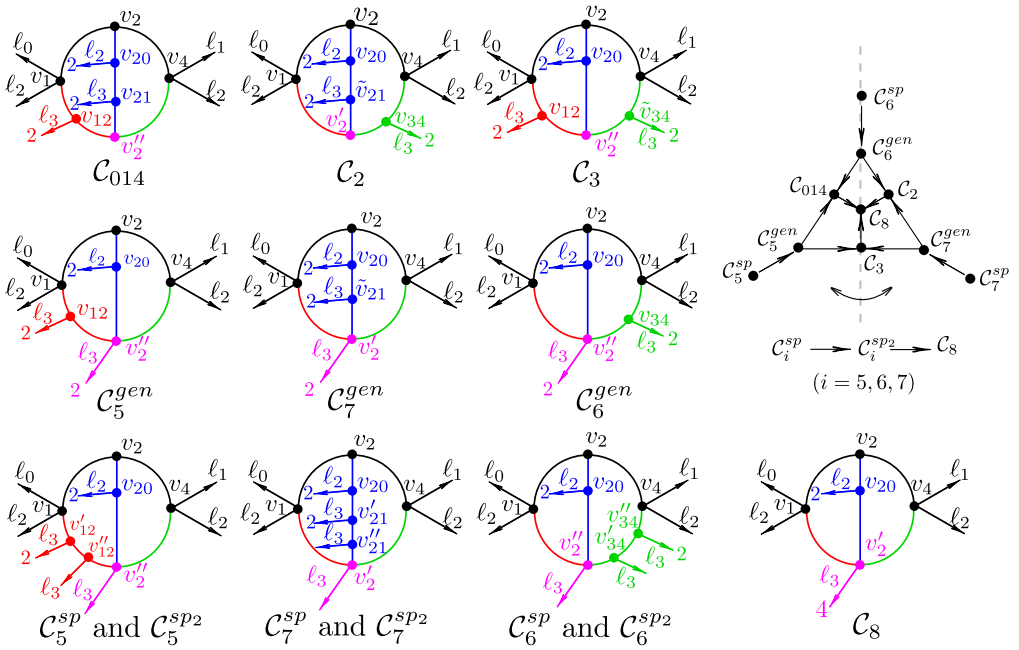

Fig. 6.8. All combinatorial types of $\operatorname{Trop} V(I_{g,f})$ and their (symmetric) poset of specializations, where $\mathcal{C}_i^{sp_2}$ is obtained from $\mathcal{C}_i^{sp}$ by making the two vertices v'_{kl} and v''_{kl} agree (the adjacent leg ℓ_3 has multiplicity 3). The four leg directions are $\ell_0 = -(2,1,1)$, $\ell_1 = (2,2,5)$, $\ell_2 = -e_2$ and $\ell_3 = -e_3$.

$$\underline{u} = (0,-2,-7,-5) = -2\,\mathbf{1} + 5/3\,R_{123} + 1/3\,R_{123,3} + 4/3\,R_{23,3}$$

so it lies in the cell $\mathcal{C}_{0,0}$ from Fig. 6.2. The top left graph in Fig. 6.8 shows the tropical curve $\operatorname{Trop} V(I_{g,f})$, in agreement with Fig. 3.1. Since $\underline{\omega} = (\omega_5, \omega_4, d_{34}, \omega_2) = (0,-4,-9,-10)$, expression (6.4) gives us the vertices $v_1 = (-10,-14,-14)$, $v_2 = v_3 = (-4,-8,-8)$ and $v_4 = (0,0,0)$. We use (6.15) to determine all remaining vertices: $v_{12} = (-5,-9,-14)$, $v_2'' = (-4,-8,-12)$, $v_{20} = (-4,-13,-13)$, and $v_{21} = (-4,-11,-15)$. ⋄

6.6. Types (V) and (VII)

As discussed earlier in this section, these are the only two types of curves whose naïve tropicalization is faithful on the minimal skeleton. As Fig. 6.9 shows, these tropical curves have high-multiplicity legs with direction $(0,-1)$. They are the images of four legs on the source curves in Fig. 1.2. For Type (VII), the unique multiplicity four leg adjacent to v_1 is the isometric image of the legs of $\Sigma(\mathcal{X})$ marked with $\alpha_2, \ldots, \alpha_5$. For Type (V), the legs marked with α_2 and α_3 are mapped isometrically onto the multiplicity two leg adjacent to v_1, while the legs marked with α_4 and α_5 are mapped to the corresponding vertical leg adjacent to v_3. In both cases, the legs marked with α_1 and α_6 are mapped isometrically to the legs with directions $(-2,-1)$ and $(2,5)$, respectively. The next result

Fig. 6.9. From left to right: Naïve tropicalizations for Types (V) and (VII) via Newton subdivisions, following the notation from Table 6.1.

discusses the behavior of the vertices of the Berkovich skeleta under tropicalization, where $v_1 = (\omega_2, 3\omega_2/2 + \omega_4)$ and $v_4 = (\omega_4, 5\omega_4/2)$:

Lemma 6.13. *The initial degeneration of the vertex v_1 of $\mathrm{Trop}V(f)$ for Type (VII) is a smooth genus two curve over $\widetilde{K}$. The vertex is the image of the unique genus two vertex of the extended skeleton of $\mathcal{X}^{\mathrm{an}}$ under the naïve tropicalization map.*

Proof. A simple computation gives $\mathrm{in}_{v_1}(g) = y^2 - x\prod_{i=2}^{5}(x - \mathrm{in}(\alpha_i))$. Table 5.1 ensures that this initial degeneration is a genus two hyperelliptic curve branched at six distinct points: 0, $\mathrm{in}(\alpha_2), \ldots, \mathrm{in}(\alpha_5)$ and ∞ in $\mathbb{P}^1_{\widetilde{K}}$. Therefore, it is smooth. The second claim follows directly by continuity and the earlier description of the images of all legs. □

Lemma 6.14. *The initial degenerations of both vertices of $\mathrm{Trop}V(g)$ for Type (V) are smooth genus one curves over $\widetilde{K}$. These vertices are the images of the genus one vertices of the extended skeleton of $\mathcal{X}^{\mathrm{an}}$ under the naïve tropicalization map.*

Proof. A direct computation gives $\mathrm{in}_{v_1}(g) = y^2 - \mathrm{in}(\alpha_4)\,\mathrm{in}(\alpha_5)x(x - \mathrm{in}(\alpha_2)(x - \mathrm{in}(\alpha_3))$. By Table 5.1 we conclude that $\mathrm{in}_{v_1}(g)$ defines an elliptic curve over $\widetilde{K}$, since it is a double cover of $(\widetilde{K}^*)^2$ branched at four distinct points: 0, $\mathrm{in}(\alpha_2)$, $\mathrm{in}(\alpha_3)$ and ∞ in $\mathbb{P}^1_{\widetilde{K}}$. Expression (6.11) computed for Type (IV) is also valid for Type (V), so $\mathrm{in}_{v_3}(g)$ is a smooth genus one curve in $(\widetilde{K}^*)^2$.

Since the images of the legs marked with α_2 and α_3 meet at v_1, we see that v_1 is the image of the corresponding genus one vertex. Similar arguments prove the claim for v_3. □

Remark 6.15. Techniques from Remark 6.7 can be used here to show that the vertices of $\mathrm{Trop}\,V(g)$ have genus one. Computations available in the Supplementary material confirm that the valuations of the j-invariants of the restriction of g to the triangles dual to v_1 and v_3 are non-negative for any characteristic of $\widetilde{K}$ other than two.

As discussed earlier, the naïve tropicalization is not faithful on the extended skeleta. We overcome this via vertical modifications along the tropical polynomials $\mathrm{trop}(x - \alpha_2)$ and $\mathrm{trop}(x - \alpha_4)$. Our next result show that these methods yield faithfulness for these tropical curves in dimensions four and five. The Supplementary material provides examples illustrating this technique for both types.

Proposition 6.16. *Let $\mathcal{X}$ be of Type (VII). Then, the embedding $\mathcal{X} \hookrightarrow (K^*)^5$ given by*

$$J = \langle g, z_i - (x - \alpha_i) \colon \ i = 2, 3, 4 \rangle \subset K[x^{\pm}, y^{\pm}, z_2^{\pm}, z_3^{\pm}, z_4^{\pm}], \tag{6.16}$$

induces a faithful tropicalization for the extended skeleton with respect to $\alpha_1, \ldots, \alpha_6$. The tropical curve $\operatorname{Trop} V(J)$ has one vertex and six legs, and all tropical multiplicities are one.

Proof. The result follows from the Fundamental Theorem of Tropical Geometry [41, Theorem 3.2.5] after parameterizing $\mathcal{X}(K)$ by the maps:

$$K \ni x \mapsto (x, \pm\Big(x \prod_{i=2}^{5} (x - \alpha_i)\Big)^{1/2}, x - \alpha_2, x - \alpha_3, x - \alpha_4). \tag{6.17}$$

We claim that $\operatorname{Trop} V(J)$ has a single vertex $v = \omega_2(1, 5/2, 1, 1, 1)$ and six legs ℓ_i $(i = 1, \ldots, 6)$ with directions $(-2, -1, 0, 0, 0)$, $(0, -1, -2, 0, 0)$, $(0, -1, 0, -2, 0)$, $(0, -1, 0, 0, -2)$, $(0, -1, 0, 0, 0)$ and $(2, 5, 2, 2, 2)$. By construction, all tropical multiplicities equal one. Indeed, standard Gröbner bases arguments from [41, Proposition 2.6.1, Corollary 2.4.10] ensure that the initial degeneration of the first and last legs equal

$$\operatorname{in}_{\ell_1}(J) = \langle y^2 + x \operatorname{in}(\alpha_5) \prod_{i=2}^{4} z_i,\ z_j - \operatorname{in}(\alpha_j) \colon j = 2, 3, 4 \rangle,\ \operatorname{in}_{\ell_6}(J) = \langle y^2 - x^5,\ z_j - x \colon j = 2, 3, 4 \rangle.$$

Similarly, the initial degenerations with respect to the legs ℓ_2, ℓ_3 and ℓ_4 are

$$\operatorname{in}_{\ell_i}(J) = \langle y^2 - x z_2 z_3 z_4 (x - \operatorname{in}(\alpha_5)), x - \operatorname{in}(\alpha_i), z_j - (x - \operatorname{in}(\alpha_j)) \colon j = 2, 3, 4, j \neq i \rangle \ (i = 2, 3, 4),$$

while $\operatorname{in}_{\ell_5}(J) = \langle x z_2 z_3 z_4 (x - \operatorname{in}(\alpha_5)), z_j - (x - \operatorname{in}(\alpha_j)) \colon j = 2, 3, 4 \rangle$. We conclude that all six initial degenerations are reduced and irreducible, so $m_{\text{trop}}(\ell_i) = 1$ for all $i = 1, \ldots, 6$.

Finally, $\operatorname{in}_v(J) = \langle y^2 - x z_2 z_3 z_4 (x - \operatorname{in}(\alpha_5)), z_j - (x - \operatorname{in}(\alpha_j)) \colon j = 2, 3, 4 \rangle$, so $m_{\text{trop}}(v) = 1$ as well. A direct computation from (6.17) shows that each leg in $\operatorname{Trop} V(J)$ is the isometric image of the corresponding marked leg of $\Sigma(\mathcal{X})$ under the new tropicalization. □

Proposition 6.17. *Let $\mathcal{X}$ be of Type (V). Then, the embedding $\mathcal{X} \hookrightarrow (K^*)^4$ given by*

$$J = \langle g, z_2 - (x - \alpha_2), z_4 - (x - \alpha_4) \rangle \subset K[x^{\pm}, y^{\pm}, z_2^{\pm}, z_4^{\pm}], \tag{6.18}$$

induces a faithful tropicalization of the extended Berkovich skeleton of $\mathcal{X}$ with respect to the six branch points $\alpha_1, \ldots, \alpha_6$.

Proof. We use the same techniques from Proposition 6.16 and apply two successive vertical modifications, starting from $\operatorname{trop}(x - \alpha_4)$ followed by $\operatorname{trop}(x - \alpha_2)$. In particular,

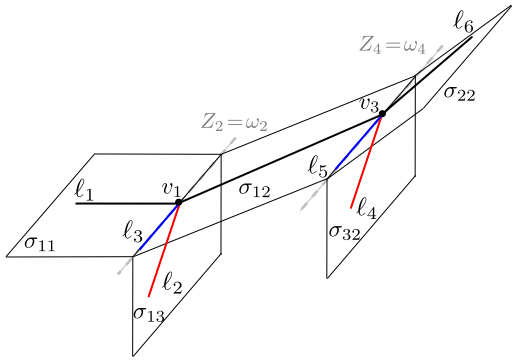

$$\sigma_{11} := \{X \leq Z_2 = \omega_2, Z_4 = \omega_4\}$$
$$\sigma_{13} := \{X = \omega_2 \geq Z_2, Z_4 = \omega_4\}$$
$$\sigma_{12} := \{X = Z_2 \geq \omega_2, Z_4 = \omega_4\}$$
$$\sigma_{32} := \{X = Z_2 = \omega_4 \geq Z_4\}$$
$$\sigma_{22} := \{X = Z_2 = Z_4 \geq \omega_4\}$$

Fig. 6.10. Extended faithfulness for Type (V) via two vertical modifications.

$$\mathrm{in}_{v_1}(J) = \langle \mathrm{in}_{v_2}(g(x,y)), z_2-(x-\alpha_2), z_4+\alpha_4\rangle, \quad \mathrm{in}_{v_3}(J) = \langle \mathrm{in}_{v_3}(g(x,y)), z_2-x, z_4-(x-\alpha_4)\rangle.$$

Both initial degenerations are smooth by Lemma 6.14.

The vertical modification techniques described in [20, Lemma 2.2, Proposition 2.3] allow us to determine $\mathrm{Trop}\, V(J)$ by means of the planar XY-, Z_2Y- and Z_4Y-projections. The ambient tropical surface $\mathrm{Trop}\, V(\langle z_2 - (x-\alpha_2), z_4 - (x-\alpha_4)\rangle)$ consists of five two-dimensional cells and it is depicted in Fig. 6.10 together with $\mathrm{Trop}\, V(J)$. As expected, $\mathrm{Trop}\, V(J)$ consists of two four-valent vertices $v_1 = (\omega_2, 3\omega_2/2 + \omega_4, \omega_2, \omega_4)$, and $v_3 = (\omega_4, 5\omega_4/2, \omega_4, \omega_4)$, joined by an edge with direction $(2,3,2,0)$, with six legs $\ell_1, \ldots, \ell_6$. They are the isometric image of the six marked legs of the extended skeleta and their directions are: $\ell_1 = (-2,-1,0,0)$, $\ell_2 = (0,-1,-2,0)$, $\ell_3 = \ell_5 = (0,-1,0,0)$, $\ell_4 = (0,-1,0,-2)$ and $\ell_6 = (2,5,2,2)$. Similar computations to the ones done in the proof of Proposition 6.16 reveal that all tropical multiplicities equal one. □

7. Igusa invariants and their tropicalizations

In 1960, Igusa introduced three invariants j_1, j_2, j_3 (called *absolute Igusa invariants*) characterizing isomorphism classes of smooth genus two curves when $\mathrm{char}\, \widetilde{K} \neq 2$ [33]. These invariants can be expressed as rational functions (with integer coefficients) in the pairwise differences of the six branch points defining the hyperelliptic equation (1.1).

It is worth noticing that a curve $\mathcal{X}$ with Igusa invariants in K need not be defined over K but rather over a field extension. A concrete algorithm for constructing the curve from these invariants was developed by Mestre [42]. For alternative methods involving Hilbert and Siegel moduli spaces that are better suited for computations over finite fields, as well as applications to Cryptography we refer to [39].

In order to give precise formulas for j_1, j_2 and j_3 we first construct four homogeneous polynomials A, B, C and D in u and the six branch points $\alpha_1, \ldots, \alpha_6$. Up to an automorphism of $\mathbb{P}^1$ we may assume none of the branch points lies at infinity. We write

$$\Delta_{ij} := (\alpha_i - \alpha_j)^2 \quad \text{for } i < j, \tag{7.1}$$

and set the homogeneous degree eight polynomial A in $\mathbb{Z}[u, \alpha_1, \ldots, \alpha_6]$ to be

$$A := u^2 \sum_{\{\{i,j\},\{k,l\},\{m,n\}\}} \Delta_{ij}\,\Delta_{kl}\,\Delta_{mn}\,, \tag{7.2}$$

where we sum over the 15 tripartitions of $[6] = \{1, \ldots, 6\}$. Similarly, set

$$B := u^4 \sum_{\{\{i,j,k\},\{l,m,n\}\}} (\Delta_{ij}\,\Delta_{jk}\,\Delta_{ki})\,(\Delta_{lm}\,\Delta_{mn}\,\Delta_{nl})\,, \tag{7.3}$$

where we sum over the ten partitions of $[6]$ into two sets of size three. We define C as

$$C := u^6 \sum_{\substack{\{\{i,j,k\},\{l,m,n\}\}\\ \{\{i,l\},\{j,m\},\{k,n\}\}}} (\Delta_{ij}\,\Delta_{jk}\,\Delta_{ki})\,(\Delta_{lm}\,\Delta_{mn}\,\Delta_{nl})\,(\Delta_{il}\,\Delta_{jm}\,\Delta_{kn}), \tag{7.4}$$

where we sum over the 60 ways of defining a pair consisting of a partition $[6] = U_1 \sqcup U_2$ into two sets of size 3 and an ordered tripartition where each pair contains exactly one element from U_1. We interpret this indexing set as a labeling of a Type (V) tree T with six leaves, as in Table 5.1. Each set U_i correspond to the leaves attached to each of the two vertices of the tree. The planar embedding of T is relevant since the differences Δ_{il}, Δ_{jm} and Δ_{kn} in each summand of C corresponding to mirror leaves on each side of the tree. This description will be used frequently to compute $-\operatorname{val}(C)$.

Finally, we let D be the square of the discriminant of the right hand side of (1.1), i.e.

$$D := u^{10} \prod_{1 \le i < j \le 6} \Delta_{ij}. \tag{7.5}$$

The polynomials A, B and C have 141, 1 531 and 8 531 terms, respectively.

Definition 7.1. The three *Igusa invariants* of the smooth hyperelliptic curve $\mathcal{X}$ equal

$$j_1(\mathcal{X}) := \frac{A^5}{D}\,, \quad j_2(\mathcal{X}) := \frac{A^3\,B}{D}\,, \quad \text{and} \quad j_3(\mathcal{X}) := \frac{A^2\,C}{D}. \tag{7.6}$$

Notice that $j_1, j_2, j_3 \in \mathbb{Q}(\alpha_1, \ldots, \alpha_6)$. Furthermore, an easy calculation shows that applying an automorphism on the target $\mathbb{P}^1$ of the hyperelliptic cover, and changing the equation (1.1) defining $\mathcal{X}$ accordingly, yields the same three invariants.

Our objective in this section is to study the behavior of the three Igusa invariants under tropicalization and prove the first half of Theorem 1.4. The second half is discussed in Section 8. We start by defining the tropical Igusa functions $j_i^{\mathrm{trop}} : M_2^{\mathrm{trop}} \to \mathbb{R}_{\ge 0}$. As it occurs with genus one curves and their tropical j-invariant [37], the construction involves

a genericity assumption. The precise hypersurfaces to avoid for each combinatorial type are discussed in the proof of Theorem 7.3 and are listed in the Supplementary material.

Definition 7.2. Given a genus two abstract tropical curve Γ we define its three *tropical Igusa invariants* as $j_i^{\mathrm{trop}}(\Gamma) := -\mathrm{val}(j_i(\mathcal{X}))$ for $i = 1, 2, 3$ for a generic smooth genus two algebraic lift $\mathcal{X}$ of Γ.

Note that a generic algebraic lift $\mathcal{X}$ of Γ is given by generic values α_i which are chosen using Table 5.1. By construction, in the non-generic case, the negative valuations will be lower than expected. Although it is not evident from the definition, our first result shows that these three tropical Igusa functions indeed depend solely on Γ, rather than on the isomorphism class of $\mathcal{X}$. Furthermore, they define piecewise linear functions on M_2^{trop} with domains of linearity given by the seven cones describing all combinatorial types. Here is the precise statement addressing the first half of Theorem 1.4:

Theorem 7.3. *Let $\mathcal{X}$ be a genus two hyperelliptic curve defined over K with* $\mathrm{char}\,\widetilde{K} \neq 2, 3$. *The tropical Igusa functions equal*

(i) $j_1^{trop}(\Gamma) = L_1 + 12L_0 + L_2$, $j_2^{trop}(\Gamma) = j_3^{trop}(\Gamma) = L_1 + 8L_0 + L_2$ *if Γ is a dumbbell curve,*
(ii) $j_1^{trop}(\Gamma) = j_2^{trop}(\Gamma) = j_3^{trop}(\Gamma) = L_1 + L_0 + L_2$ *if Γ is a theta curve,*

where L_0, L_1, L_2 denote the lengths on each curve, as in Fig. 2.1. All three formulas remain valid under specialization and yield well-defined piecewise linear maps on the moduli space M_2^{trop} with domains of linearity corresponding to the seven combinatorial types.

Remark 7.4. The previous result shows that the three tropical Igusa functions do not characterize tropical curves of genus two, not even within a fixed combinatorial type and should not be considered tropical analogs of Igusa invariants. Indeed, the second and third tropical Igusa functions agree on each cone in M_2^{trop}, and all three agree on the cone of theta curves. In particular, we cannot recover the length data for each tropical curve from these three functions.

We would like to comment on the relation of this result with [32]. In [33], Igusa introduced ten projective invariants of smooth genus two curves, and the three specific quotients j_1, j_2 and j_3. Whenever these quotients do not vanish, they determine a unique point in M_2 (a smooth curve of genus two) over a field of characteristic different than two. In particular, these invariants become coordinates on M_2. Our work describes to which extent their tropicalizations fail to be coordinates on M_2^{trop}. Building on earlier work of Liu [40], [32] shows that the set of ten invariants suffices to characterize the type and lengths of the tropicalization Γ. One should take into account that in [32], the ten

invariants are expressed in terms of the coefficients of the hyperelliptic equation (1.1), while our three quotients are written in terms of the branch points.

Proof of Theorem 7.3. Consider a generic lift $\mathcal{X}$ of our tropical curve Γ. This means, a tuple of generic branch points $\alpha_1, \ldots, \alpha_6$ in K^* whose valuations satisfy the conditions described in Table 5.1 and yield the metric graph Γ. Furthermore, we assume $\operatorname{val}(\alpha_1) = 0$, and $u = 1$ since u plays no role when defining each $j_i(\mathcal{X})$. By expression (7.6), the tropical Igusa functions of Γ equal:

$$\begin{cases} -\operatorname{val}(j_1(\mathcal{X})) = -5\operatorname{val}(A) + \operatorname{val}(D)\,, \\ -\operatorname{val}(j_2(\mathcal{X})) = -3\operatorname{val}(A) - \operatorname{val}(B) + \operatorname{val}(D)\,, \\ -\operatorname{val}(j_3(\mathcal{X})) = -2\operatorname{val}(A) - \operatorname{val}(C) + \operatorname{val}(D). \end{cases} \tag{7.7}$$

We treat each invariant separately, analyzing the contributions of each summand in the definition of the four polynomials A, B, C, and D, and checking for potential cancellations of the expected initial terms. The proof is completed by discussing the behavior of each maximal cells of M_2^{trop} separately in two lemmas below.

The genericity conditions on $\mathcal{X}$ are imposed so that the initial forms of each polynomial have the expected valuation after specializing them at the initial forms of each branch point. The two maximal cells in M_2^{trop} require no genericity assumptions, since the leading terms of all polynomials involved are monomials.

Type (I) cells: For a Type (I) curve, the negative valuation of each A, B, C, D is obtained by computing the initial term on each of these four polynomials with respect to the weight vector $\underline{\omega} := (\omega_1, \ldots, \omega_6) \in \mathbb{R}^6$ with $\omega_1 < \ldots < \omega_6$. Lemma 7.5 ensures that

$$\begin{aligned} -\operatorname{val}(A) &= 2(\omega_4 + \omega_5 + \omega_6), & -\operatorname{val}(C) &= 6(\omega_5 + \omega_6) + 4\omega_4 + 2\omega_3, \\ -\operatorname{val}(B) &= 4(\omega_5 + \omega_6) + 2(\omega_3 + \omega_4), & -\operatorname{val}(D) &= 2\omega_2 + 4\omega_3 + 6\omega_4 + 8\omega_5 + 10\,\omega_6. \end{aligned} \tag{7.8}$$

Combining these values with (7.7) and the formulas for L_0, L_1 and L_2 from Table 5.1 gives:

$$\begin{aligned} j_1^{\mathrm{trop}}(\Gamma) &= 10(\omega_4 + \omega_5 + \omega_6) - (2\omega_2 + 4\omega_3 + 6\omega_4 + 8\omega_5 + 10\omega_6) \\ &= 4\omega_4 + 2\omega_5 - 2\omega_2 - 4\omega_3 = 2(\omega_5 - \omega_4) + 6(\omega_4 - \omega_3) + 2(\omega_3 - \omega_2) \\ &= L_1 + 12L_0 + L_2\,, \\ j_2^{\mathrm{trop}}(\Gamma) &= 6(\omega_4 + \omega_5 + \omega_6) + 4(\omega_5 + \omega_6) + 2(\omega_3 + \omega_4) - (2\omega_2 + 4\omega_3 + 6\omega_4 + 8\omega_5 + 10\omega_6) \\ &= 2\omega_5 + 2\omega_4 - 2\omega_3 - 2\omega_2 = 2(\omega_5 - \omega_4) + 4(\omega_4 - \omega_3) + 2(\omega_3 - \omega_2) \\ &= L_1 + 8L_0 + L_2\,, \\ j_3^{\mathrm{trop}}(\Gamma) &= 4(\omega_4 + \omega_5 + \omega_6) + 6(\omega_6 + \omega_5) + 4\,\omega_4 + 2\,\omega_3 - (2\omega_2 + 4\omega_3 + 6\omega_4 + 8\omega_5 + 10\omega_6) \\ &= L_1 + 8L_0 + L_2 = j_2^{\mathrm{trop}}(\Gamma)\,. \end{aligned}$$

Type (II) cells: Following Table 5.1, the weights for Type (II) curves satisfy

$$\omega_1 < \omega_2 < \omega_3 = \omega_4 < \omega_5 < \omega_6 \text{ and } -d_{34} := \operatorname{val}(\alpha_3 - \alpha_4) > -\omega_3. \tag{7.9}$$

For this reason, in order to determine the valuations of A, B, C and D we consider the factor Δ_{34} as a new variable α_{34}^2, and replace each variable α_4 by $\alpha_{34} + \alpha_3$ in all four polynomials. A similar strategy was used in Subsection 6.5. We denote the new polynomials by

$$A', B', C', D' \in \mathbb{Z}[\alpha_1, \alpha_2, \alpha_3, \alpha_{34}, \alpha_5, \alpha_6]. \tag{7.10}$$

A computation with `Sage` (available in the Supplementary material) shows that A', B' and C' have 177, 1 911 and 11 745 terms, respectively.

The weight of the new variable α_{34} equals d_{34}. We replace our weight vector in $\mathbb{R}^6$ by $\underline{\omega} = (\omega_1, \omega_2, \omega_3, d_{34}, \omega_5, \omega_6)$. By construction, the negative valuation of each A, B, C, D agrees with that of A', B', C' and D'. The later equals the $\underline{\omega}$-weight of the initial form of A', B', C' and D', respectively. Lemma 7.6 ensures that

$$\begin{aligned} -\operatorname{val}(A) &= 2(\omega_3 + \omega_5 + \omega_6)\,, \quad -\operatorname{val}(C) = 6(\omega_3 + \omega_5 + \omega_6)\,, \\ -\operatorname{val}(B) &= 4(\omega_3 + \omega_5 + \omega_6)\,, \quad -\operatorname{val}(D) = 2\omega_2 + 8\omega_3 + 2d_{34} + 8\omega_5 + 10\,\omega_6. \end{aligned} \tag{7.11}$$

We conclude that $-5\operatorname{val}(A) = -3\operatorname{val}(A) - 2\operatorname{val}(B) = -2\operatorname{val}(A) - 3\operatorname{val}(C)$. The formulas for the lengths L_0, L_1, and L_2 from Table 5.1 yield

$$\begin{aligned} j_1^{\mathrm{trop}}(\Gamma) = j_2^{\mathrm{trop}}(\Gamma) &= j_3^{\mathrm{trop}}(\Gamma) \\ &= 10(\omega_3 + \omega_5 + \omega_6) - (2\omega_2 + 8\omega_3 + 2d_{34} + 8\omega_5 + 10\omega_6) \\ &= 2\omega_5 + 2\omega_3 - 2\omega_2 - 2d_{34} = 2(\omega_5 - \omega_3) + 2(\omega_3 - \omega_2) + 2(\omega_3 - d_{34}) \\ &= L_1 + L_0 + L_2\,. \end{aligned}$$

Type (III) through (VII) cells: In order to prove the statement for lower dimensional cells, we first note that the substitution A, B, C, D for A', B', C', D' has no impact when computing their valuations on Type (I). Indeed, the weight $\underline{\omega} = (\omega_1, \omega_2, \omega_3, d_{34}, \omega_5, \omega_6) \in \mathbb{R}^6$ satisfies $d_{34} = \omega_4$ and $\operatorname{in}(\alpha_{34}) = \operatorname{in}(\alpha_4)$.

We fix a lower dimensional cell in M_2^{trop} and pick the weight vector $\underline{\omega}$ in $\mathbb{R}^6$, where the fourth entry equals ω_4, as described in Table 5.1. Consider a sequence of weight vectors $(\underline{\omega}^{(n)})_{n\in\mathbb{N}}$ corresponding to a Type (I) curve specializing to $\underline{\omega}$. By continuity and the characterization of Gröbner fans of homogeneous polynomials [22], we conclude that the $\underline{\omega}^{(n)}$-initial terms for A, B, C and D are present in the corresponding $\underline{\omega}$-initial terms. Therefore, as long as the initial forms of each polynomial do not vanish after evaluating them at $\operatorname{in}(\underline{\alpha})$, the formulas for the Tropical Igusa functions on Type (I) remain valid for the lower dimensional types: the valuation of each polynomial is the expected one. The

proof involving Type (II) sequences is similar since $\omega_4^{(n)} = d_{34}^{(n)} \to \omega_3$ if we approach a curve of Type (III), (VI) or (VII). □

The following two lemmas are used in the proof of Theorem 7.3 as well as in Section 8. They can be verified via `Macaulay2` computations by choosing appropriate weight vectors in $\mathbb{R}^6$. The required scripts are available in the Supplementary material. For completeness, we provide alternative non-computational proofs that help understand the behavior of these polynomials under tropicalization. They justify the need to exclude $\operatorname{char} \widetilde{K} = 3$.

Lemma 7.5. *Assume* $\operatorname{char} \widetilde{K} \neq 2, 3$. *Given a weight vector* $\underline{\omega} = (\omega_1, \ldots, \omega_6) \in \mathbb{R}^6$ *in the relative interior of a Type (I) cell in* M_2^{trop}, *we have*

$$\operatorname{in}_{\underline{\omega}}(A) = 6\alpha_4^2\alpha_5^2\alpha_6^2,\ \operatorname{in}_{\underline{\omega}}(B) = 4\alpha_3^2\alpha_4^2\alpha_5^4\alpha_6^4,\ \operatorname{in}_{\underline{\omega}}(C) = 8\alpha_3^2\alpha_4^4\alpha_5^6\alpha_6^6 \text{ and } \operatorname{in}_{\underline{\omega}}(D) = \alpha_2^2\alpha_3^4\alpha_4^6\alpha_5^8\alpha_6^{10}.$$

Proof. By Table 5.1, the weight vector $\underline{\omega} = (\omega_1, \ldots, \omega_6)$ corresponding to Type (I) curves satisfies $\omega_1 < \omega_2 < \ldots < \omega_6$. Since D is given as a product of all expressions Δ_{ij} from (7.1), and $\operatorname{val}(\alpha_i) > \operatorname{val}(\alpha_j)$ for $i < j$, we get $\operatorname{val}(\Delta_{ij}) = -2\omega_j$ for $i < j$, thus

$$-\operatorname{val}(D) = 2\omega_2 + 4\omega_3 + 6\omega_4 + 8\omega_5 + 10\omega_6, \quad \text{and} \quad \operatorname{in}_{\underline{\omega}}(D) = \alpha_2^2\alpha_3^4\alpha_4^6\alpha_5^8\alpha_6^{10}.$$

The computation for $\operatorname{in}_{\underline{\omega}}(A)$ is more involved, since it requires determining the initial term of each summand in A and checking for potential cancellations. Each summand $\Delta_{ij}\Delta_{kl}\Delta_{mn}$ of A in expression (7.2) has valuation $-2(\omega_j+\omega_l+\omega_n)$ for $i < j, k < l, m < n$. The conditions on the parameters ω_i ensure that the minimal valuation is attained for the six tripartitions of the form $\{\{i,4\},\{k,5\},\{m,6\}\}$. The coefficient associated to $\alpha_4^2\alpha_5^2\alpha_6^2$ on each of these summands equals one, so no cancellations occur and this monomial appears in A with coefficient six. Thus, $\operatorname{in}_{\underline{\omega}}(A) = 6\,\alpha_4^2\alpha_5^2\alpha_6^2$ if $\operatorname{val}(6) = 0$.

Next, we analyze the summands in B given in (7.3) to determine the initial term of B with respect to the weight vector $\underline{\omega}$. The conditions on $\underline{\omega}$ ensure that the summand indexed by the partition $\{\{i,j,k\},\{l,m,n\}\}$ has valuation $-2(\omega_j + 2\omega_k + \omega_m + 2\omega_n)$ for $i < j < k$ and $l < m < n$. The minimum valuation is achieved when $k, n \in \{5,6\}$ and $j, m \in \{3,4\}$. The corresponding summands are indexed by the four splits

$$\{1,3,5\} \sqcup \{2,4,6\}\,, \{2,3,5\} \sqcup \{1,4,6\}\,, \{1,4,5\} \sqcup \{2,3,6\} \text{ and } \{2,4,5\} \sqcup \{1,3,6\}.$$

On each summand, the monomial $\alpha_3^2\alpha_4^2\alpha_5^4\alpha_6^2$ has coefficient one, so $\operatorname{in}_{\underline{\omega}}(B) = 4\,\alpha_3^2\alpha_4^2\alpha_5^4\alpha_6^2$.

In order to compute $\operatorname{in}_{\underline{\omega}}(C)$ and $-\operatorname{val}(C)$ we use expression (7.4) and analyze the valuation of all its 60 summands. The minimum valuation equals $-(6(\omega_6+\omega_5)+4\omega_4+2\omega_3)$. This value is obtained for those indices where each element in the pairs $\{5,6\}$ and $\{3,4\}$ belongs to a different set of the split $\{i,j,k\} \sqcup \{l,m,n\}$. Moreover, the elements $4, 5$ and 6 must lie in different pairs in the tripartition $\{\{i,l\},\{j,m\},\{k,n\}\}$. A combinatorial

analysis allows us to assume $1 = i < j < k$ and conclude that the summands with minimum valuation correspond to the eight ordered tuples:

$$\begin{aligned}(i,j,k,l,m,n) = &(1,3,6,4,5,2)\,,\ (1,4,5,6,2,3)\,,\ (1,4,6,5,2,3)\,,\ (1,3,5,4,6,2)\,,\\ &(1,3,6,5,4,2)\,,\ (1,4,5,6,3,2)\,,\ (1,4,6,5,3,2)\,,\ (1,3,5,6,4,2)\,.\end{aligned} \tag{7.12}$$

On these summands, the monomial $\alpha_3^2\alpha_4^4\alpha_5^6\alpha_6^6$ is monic, so $\mathrm{in}_{\underline{\omega}}(C) = 8\,\alpha_3^2\alpha_4^4\alpha_5^6\alpha_6^6$. □

Lemma 7.6. *Let $A', B', C', D' \in \mathbb{Z}[\alpha_1, \alpha_2, \alpha_3, \alpha_{34}, \alpha_5, \alpha_6]$ be the polynomials in (7.10). Given a weight vector $\underline{\omega} = (\omega_1, \omega_2, \omega_3, d_{34}, \omega_5, \omega_6) \in \mathbb{R}^6$ inducing a point in the relative interior of a Type (II) cell in M_2^{trop}, we have*

$$\begin{aligned}\mathrm{in}_{\underline{\omega}}(A') &= 8\,\alpha_3^2\alpha_5^2\alpha_6^2\,,\ \ \mathrm{in}_{\underline{\omega}}(C') = 8\,\alpha_3^6\alpha_5^6\alpha_6^6\,,\\ \mathrm{in}_{\underline{\omega}}(B') &= 4\,\alpha_3^4\alpha_5^4\alpha_6^4\,,\ \ \mathrm{in}_{\underline{\omega}}(D') = \alpha_2^2\alpha_3^8\alpha_{34}^2\alpha_5^8\alpha_6^{10}.\end{aligned}$$

Proof. We start with D'. Since the weight vector $\underline{\omega}$ satisfies (7.9), formula (7.5) implies

$$-\mathrm{val}(\Delta_{ij}) = \begin{cases} 2d_{34} & \text{if } (i,j) = (3,4),\\ 2\,\omega_j & \text{if } j \neq 4, \\ 2\,\omega_3 & \text{if } j = 4, i < 3,\end{cases} \qquad \text{for } i < j,$$

because $-\mathrm{val}(\alpha_{34}+\alpha_3-\alpha_j) = \omega_{\max\{j,3\}}$ for $j \neq 3, 4$. We conclude that $-\mathrm{val}(D') = 2\,\omega_2 + 8\,\omega_3 + 2\,d_{34} + 8\,\omega_5 + 10\,\omega_6$. Furthermore, the term realizing this valuation is $\alpha_2^2\alpha_3^8\alpha_{34}^2\alpha_5^8\alpha_6^{10}$, hence it equals $\mathrm{in}_{\underline{\omega}}(D')$.

To compute $\mathrm{in}_{\underline{\omega}}(A')$ we proceed analogously. For each tripartition not involving $\{3,4\}$, the valuation of the corresponding summand equals $-2(\omega_j + \omega_l + \omega_n)$, assuming $i < j$, $k < l$, and $m < n$. As in Type (I), the minimum is achieved at $-2(\omega_3 + \omega_5 + \omega_6)$, when $j = 3$ or 4, $l = 5$, and $n = 6$, namely for the 8 tripartitions

$$\{\{1,*\},\{2,5\},\{*,6\}\},\ \{\{1,*\},\{2,6\},\{*,5\}\},\ \{\{1,5\},\{2,*\},\{*,6\}\},\ \{\{1,6\},\{2,*\},\{*,5\}\}.$$

Notice that since $\mathrm{in}_{\underline{\omega}}(\alpha_{34} + \alpha_3) = \mathrm{in}_{\underline{\omega}}(\alpha_3)$, it is easy to verify that the coefficient of $\alpha_3^2\alpha_5^2\alpha_6$ on these eight summands equals 1.

On the contrary, if $\{3,4\}$ is a pair in the tripartition (say the middle one), the valuation of each such summand equals $-2(\omega_j + d_{34} + \omega_n)$, which is strictly larger than $-2(\omega_3 + \omega_5 + \omega_6)$. We conclude that $\mathrm{in}_{\underline{\omega}}(A') = 8\,\alpha_3^2\alpha_5^2\alpha_6$.

We proceed similarly for the polynomial B', distinguishing between splits where 3 and 4 belong to different subsets or not. In the first case, there are four summands realizing the minimum valuation $-2(2\omega_3 + 2\omega_5 + 2\omega_6)$, corresponding to the splits where 5 and 6 also are in different subsets. They all contribute one monomial $\alpha_3^4\alpha_5^4\alpha_6^4$ to B', each with coefficient 1.

On the contrary, if 3 and 4 lie in the same subset, the minimum valuation for these summands is $-2(\omega_2 + d_{34} + 2\omega_5 + 2\omega_6)$ and it is obtained when 5 and 6 are in different subsets (as in Type (I)). The conditions on $\underline{\omega}$ ensure that $\omega_2 + d_{34} < 2\omega_3$, so $\mathrm{in}_{\underline{\omega}}(B') = 4\alpha_3^4\alpha_5^4\alpha_6^4$.

Finally, we compute $\mathrm{in}_{\underline{\omega}}(C')$. For each summand of C' corresponding to a split with 3 and 4 in different subsets, the valuation is the same as the one computed for Type (I). The expected valuation is $-6(\omega_6 + \omega_5 + \omega_3)$ and it is attained at the eight tuples below:

$$(i,j,k,l,m,n) = (1,3,6,4,5,2)\,,\ (1,4,5,6,2,3)\,,\ (1,4,6,5,2,3)\,,\ (1,3,5,4,6,2)\,,$$
$$(1,3,6,5,2,4)\,,\ (1,4,5,3,6,2)\,,\ (1,4,6,3,5,2)\,,\ (1,3,5,6,2,4)\,.$$

The first group corresponds to the four tuples on the top row of (7.12) since the variable α_{34} does not appear on those summands. The second group correspond to tuples where 4 is opposed to 5 or 6 but this loss is compensated by 3 winning over 1 and 2. Notice that these terms did not contribute for the Type (I) cell. Collectively, these eight tuples contribute the monomial $8\,\alpha_3^6\alpha_5^6\alpha_6^6$.

For the remaining 24 summands in C', where 3 and 4 lie in the same set, the possible $\underline{\omega}$-initial forms are $\alpha_6^6\alpha_5^4\alpha_{34}^2\alpha_3^4\alpha_2^2$, $\alpha_6^6\alpha_5^6\alpha_{34}^2\alpha_3^2\alpha_2^2$, and $\alpha_6^6\alpha_5^4\alpha_{34}^2\alpha_3^6$. Their valuation is strictly bigger that $-6(\omega_6 + \omega_5 + \omega_3)$, therefore $\mathrm{in}_{\underline{\omega}}(C') = 8\alpha_3^6\alpha_5^6\alpha_6^6$. □

In the rest of this section, we discuss the behavior of the tropical Igusa invariants when $\mathrm{char}\,\widetilde{K} = 3$. Notice that in this case, we cannot predict the valuation of the polynomial A on the relative interior of the Type (I) cell, since the initial form of A in Lemma 7.5 has a coefficient with non-zero valuation.

Theorem 7.7. *Let* $\mathrm{char}\,\widetilde{K} = 3$ *and* Γ *be a curve of Type (I), (IV) or (V). Then:*

(1) *If* $1 - \omega_4 \leq \omega_3$, *then the formulas for all* $j_i^{trop}(\Gamma)$ *from Theorem 7.3 hold.*
(2) *If* $1 - \omega_4 > \omega_3$, *then* $j_1^{trop}(\Gamma) = j_2^{trop}(\Gamma) = L_1 + 2L_0 + L_2$, *whereas* $j_3^{trop}(\Gamma) = L_1 + 4L_0 + L_2$.

If Γ *is a (specialization of a) Type (II) curve, the formulas from Theorem 7.3 hold.*

Proof. If Γ is a Type (II) curve, or a specialization thereof, the formulas for all initial forms in Lemma 7.6 remain valid in characteristic 3. Therefore, the same genericity assumptions imposed in Theorem 7.3 yield the formulas for the tropical Igusa invariants for these curves.

In what remains, we treat the remaining three types: (I), (IV) and (V). As discussed above, the initial form of A will not have a uniform value on each of these cones when $\mathrm{char}\,\widetilde{K} = 3$. We bypass this difficulty by writing A as an integer combination of four polynomials with coefficients ± 1 and disjoint supports, comparing the valuation of their initial forms, and considering possible ties and cancellations. A calculation available on

the Supplementary material yields $A = 4A_4 + 6A_6 + 12A_{12} + 120A_{120}$. Any $\underline{\omega}$ in the relative interior of the Type (I), (IV) or (V) cells gives

$$\begin{aligned} \mathrm{in}_{\underline{\omega}}(A_4) &= -\alpha_6^2\alpha_5^2\alpha_4\alpha_3\,, & \mathrm{in}_{\underline{\omega}}(A_{12}) &= \alpha_6^2\alpha_5\alpha_4\alpha_3\alpha_2\,, \\ \mathrm{in}_{\underline{\omega}}(A_6) &= \alpha_6^2\alpha_5^2\alpha_4^2\,, & \mathrm{in}_{\underline{\omega}}(A_{120}) &= -\alpha_6\alpha_5\alpha_4\alpha_3\alpha_2\alpha_1. \end{aligned} \tag{7.13}$$

Since $\omega_1 < \omega_2 < \ldots < \omega_6$ in Type (I), we conclude that $\mathrm{in}_{\underline{\omega}}(A_6) > \mathrm{in}_{\underline{\omega}}(A_{12}), \mathrm{in}_{\underline{\omega}}(A_{120})$ so we need only compare the weights of A_4 and $6A_6$. There are two cases to analyze:

Case 1: If $1-\omega_4 \leq -\omega_3$, our genericity assumptions ensure that $\mathrm{val}(6\alpha_4 - 4\alpha_3) = 1-\omega_4$. Thus $\mathrm{val}(A)$ is the one predicted in Lemma 7.5. The formulas for the tropical Igusa invariants described in Theorem 7.3 remain valid in this setting.

Case 2: If $1 - \omega_4 > -\omega_3$, we conclude that $\mathrm{in}_{\underline{\omega}}(A) = 4\,\mathrm{in}_{\underline{\omega}}(A_4)$, and so $-\mathrm{val}(A) = 2\omega_6 + 2\omega_5 + \omega_4 + \omega_3$. The expressions for $\mathrm{val}(B)$, $\mathrm{val}(C)$, and $\mathrm{val}(D)$ obtained from Lemma 7.5 and arithmetic manipulations as in the proof of Theorem 7.3 yield the desired expressions for the Igusa invariants on the Type (I) cone. □

Remark 7.8. If $1 - \omega_4 = -\omega_3$ and $\mathrm{in}(6\alpha_4) = \mathrm{in}(-4\alpha_3)$ the above methods do not allow us to compute $-\mathrm{val}(A)$. We bypass this difficulty by using three Laurent monomials in the 3 Igusa invariants where the polynomial A is canceled out. Lemma 7.5 yields:

$$\begin{aligned} 5j_2^{\mathrm{trop}}(\Gamma) - 3j_1^{\mathrm{trop}}(\Gamma) &= 2\,\mathrm{val}(D) - 5\,\mathrm{val}(B) = 2L_1 + 4L_0 + 2L_2\,, \\ 3j_3^{\mathrm{trop}}(\Gamma) - 2j_1^{\mathrm{trop}}(\Gamma) &= 3\,\mathrm{val}(D) - 5\,\mathrm{val}(C) = 3L_1 + 16L_0 + 3L_2\,, \\ 3j_3^{\mathrm{trop}}(\Gamma) - 2j_2^{\mathrm{trop}}(\Gamma) &= \mathrm{val}(D) + 2\,\mathrm{val}(B) - 3\,\mathrm{val}(C) = L_1 + 8L_0 + L_2. \end{aligned}$$

The matrix describing the three integer linear combination of j_1^{trop}, j_2^{trop} and j_3^{trop} has rank two, so we can only express the last two invariants in terms of j_1^{trop}.

8. A new Igusa invariant

As was shown in Remark 7.4, the fact that the tropical Igusa functions do not yield coordinates on M_2^{trop} raises a natural question: can we replace j_1, j_2, j_3 by an alternative set of three algebraic invariants better suited for tropicalization? Given the expressions in Theorem 7.3 we propose to replace j_3 with a linear expression in j_1, j_2, j_3 whose initial form corresponding to a weight vector of Type (I) or (II) appears as a result of a cancellation in the initial forms of the j_i's. In other words, we aim to compute a Khovanskii basis of the ring of invariants of M_2.

The computation of $\mathrm{val}(A), \mathrm{val}(B)$ and $\mathrm{val}(C)$ on Types (I) and (II) in expressions (7.8) and (7.11) gives the linear relation

$$-\mathrm{val}(A) - \mathrm{val}(B) = -\mathrm{val}(C).$$

Therefore, a cancellation might be produced among leading terms via the expressions

$$Q_\lambda := A\,B - \lambda C \quad \text{(for Type (I))} \qquad \text{and} \qquad Q'_\lambda := A'\,B' - \lambda C' \quad \text{(for Type (II))}\,, \tag{8.1}$$

for suitable $\lambda \in K^*$. For generic choices of λ, a `Sage` calculation shows that $Q_\lambda \in \mathbb{Q}[\alpha_1, \alpha_2, \alpha_3, \alpha_4, \alpha_5, \alpha_6]$ has 12 567 terms, whereas $Q'_\lambda \in \mathbb{Q}[\alpha_1, \alpha_2, \alpha_3, \alpha_{34}, \alpha_5, \alpha_6]$ has 11 891.

By Lemmas 7.5 and 7.6 we know that for $\operatorname{char} \widetilde{K} \neq 2, 3$:

$$\begin{aligned} &\text{On Type (I):} && \operatorname{in}_{\underline{\omega}}(A)\ \operatorname{in}_{\underline{\omega}}(B) = 24\,\alpha_3^2\alpha_4^4\alpha_5^6\alpha_6^6 = 3\ \operatorname{in}_{\underline{\omega}}(C) && \text{so} \quad \lambda = 3\,. \\ &\text{On Type (II):} && \operatorname{in}_{\underline{\omega}'}(A')\ \operatorname{in}_{\underline{\omega}'}(B') = 32\,\alpha_3^6\alpha_5^6\alpha_6^6 = 4\ \operatorname{in}_{\underline{\omega}'}(C') && \text{so} \quad \lambda = 4. \end{aligned} \tag{8.2}$$

These relations shows which values of λ will produce cancellations between the $\underline{\omega}$-leading terms of AB and C in Q_λ and Q'_λ. This choice yields a new Igusa invariant in Type (I):

$$j'_3 := \frac{Q_3 A^2}{D} = \frac{A^3 B}{D} - 3\frac{A^2 C}{D} = j_2 - 3j_3.$$

The tropicalization of j'_3 equals $-\operatorname{val}(j_3)$ and it is determined by the $\underline{\omega}$-initial form of Q_3. A `Macaulay2` computation finds the initial terms:

$$\operatorname{in}_{\underline{\omega}}(Q_3) = 8\,\alpha_6^6\alpha_5^6\alpha_4^3\alpha_3^3, \quad \text{so} \ -\operatorname{val}(Q_3) = 6(\omega_6 + \omega_5) + 3(\omega_4 + \omega_3).$$

Combining this expression with (7.8) and the length formula from Table 5.1 yields

$$\begin{aligned} j_3'^{\,\mathrm{trop}} &= 6(\omega_6 + \omega_5) + 3(\omega_4 + \omega_3) + 4(\omega_4 + \omega_5 + \omega_6) - (2\omega_2 + 4\omega_3 + 6\omega_4 + 8\omega_5 + 10\,\omega_6) \\ &= 2\omega_5 + \omega_4 - \omega_3 - 2\omega_2 = 2(\omega_5 - \omega_4) + 3(\omega_4 - \omega_3) + 2(\omega_3 - \omega_2) = L_1 + 6L_0 + L_2\,. \end{aligned}$$

The new function $j_3'^{\,\mathrm{trop}}$ fails to provide new length data for Type (I) curves. For this reason, we turn to the Type (II) cell and work with Q_4, as predicted by (8.1). We set:

$$j_4 := \frac{Q_4 A^2}{D} = \frac{A^3 B}{D} - 4\frac{A^2 C}{D} = j_2 - 4j_3. \tag{8.3}$$

By construction $j_4^{\mathrm{trop}} = j_3^{\mathrm{trop}}$ on Type (I) curves if $\operatorname{char} \widetilde{K} \neq 2, 3$.

Since we are interested in the behavior of j_4^{trop} on the Type (II) cell, we work with Q'_4 instead of Q_4. A `Sage` calculation reveals that $Q'_4 \in \mathbb{Q}[\alpha_1, \alpha_2, \alpha_3, \alpha_{34}, \alpha_5, \alpha_6]$ has 11 379 terms. The possible weight vectors $\underline{\omega} = (\omega_1, \omega_2, \omega_3, d_{34}, \omega_5, \omega_6) \in \mathbb{R}^6$ giving Type (II) curves form a six-dimensional open cone in $\mathbb{R}^6$, whose closure we denote by Θ.

The possible valuations of Q_4 are determined by the Gröbner fan of Q'_4. A `Sage` computation shows that its f-vector equals $(1, 32, 174, 396, 420, 168)$. We are interested in the intersection of the Gröbner fan of Q'_4 with the relative interior of the cone Θ. The following lemma shows that Θ gets subdivided into three maximal pieces

$$\Theta_0 := \Theta \cap \{d_{34} \geq \omega_2,\, \omega_5 + d_{34} \geq 2\omega_3\}\,,\ \Theta_1 := \Theta \cap \{2\omega_3 \geq \omega_5 + \omega_2,\, 2\omega_3 \geq \omega_5 + d_{34}\},$$
$$\Theta_2 := \Theta \cap \{\omega_2 \geq d_{34},\, \omega_5 + \omega_2 \geq 2\omega_3\}\,. \tag{8.4}$$

Lemma 8.1. *The pieces Θ_0, Θ_1 and Θ_2 in (8.4) determine the $\underline{\omega}$-initial form of Q_4':*

$$\mathrm{in}_{\underline{\omega}}(Q_4') = \begin{cases} -8\alpha_6^6\alpha_5^6\alpha_{34}^2\alpha_3^4 & \text{if} \quad \underline{\omega} \in \operatorname{rel\,int}(\Theta_0)\,, \\ -8\alpha_6^6\alpha_5^4\alpha_3^8 & \text{if} \quad \underline{\omega} \in \operatorname{rel\,int}(\Theta_1)\,, \\ -8\alpha_6^6\alpha_5^6\alpha_3^4\alpha_2^2 & \text{if} \quad \underline{\omega} \in \operatorname{rel\,int}(\Theta_2)\,. \end{cases}$$

On the intersection of Θ_i and Θ_j, the initial form is obtained by adding the forms for each piece. On the triple intersection, the initial form equals the sum of the three forms.

Proof. The proof is computational, and all the required `Sage` scripts are included in the Supplementary material. Since the computation of the Gröbner fan of Q_4 using `Sage` halts, we replace Q_4' by the sum of its extremal monomials and calculate its Gröbner fan. We then compute the intersection of this fan with Θ and check that only three of its maximal cones intersect Θ in dimension six. We consider a sample interior point in the relative interior of each piece (e.g. the sum of its extremal rays) and determine the initial forms of Q_4' on each Θ_i using `Macaulay2`. The equalities defining Θ_i are determined by `Sage`. The last claim in the statement follows from the defining properties of Gröbner fans. □

The pieces Θ_0, Θ_1 and Θ_2 have a natural interpretation in terms of length data:

Lemma 8.2. *Given $i = 0, 1, 2$, the inequalities defining Θ_i single out the minimal edge length L_i of the corresponding theta graph.*

In particular, the subdivision (8.4) of Θ is compatible with the automorphisms of this cone induced by permutations of the underlying theta graph. The proof of this result follows from the length formulas in Table 5.1. Below is the main result in this section:

Theorem 8.3. *Let $\mathcal{X}$ be a curve in M_2, defined over K with* $\operatorname{char} \widetilde{K} \neq 2$, *and generic with respect to its (abstract) tropicalization Γ. The tropical Igusa function j_4^{trop} equals*

(i) $j_4^{trop}(\Gamma) = j_3^{trop}(\Gamma)$ *if Γ is a dumbbell curve, and*
(ii) $j_4^{trop}(\Gamma) = L_0 + L_1 + L_2 - \min\{L_0, L_1, L_2\}$ *if Γ is a theta curve,*

where L_0, L_1, L_2 denote the lengths on each curve as in Fig. 2.1. The formulas remain valid under specialization and yield well-defined piecewise linear maps on M_2^{trop}.

Proof. The formula for Type (I) will depend on the characteristic of $\widetilde{K}$ and will be obtained from Theorems 7.3 and 7.7. A simple inspection shows that in all cases $j_4^{\mathrm{trop}} \leq j_3^{\mathrm{trop}}$. The genericity of $\mathcal{X}$ ensures that no cancellations occur and thus, $j_{4\overset{\circ}{\circ}\!-\!\overset{\circ}{\circ}}^{\mathrm{trop}} = j_{3\overset{\circ}{\circ}\!-\!\overset{\circ}{\circ}}^{\mathrm{trop}}$.

To prove the statement on the Type (II) cell, we notice that j_4 differs from j_3 by replacing C' with Q_4', so $j_4^{\mathrm{trop}} = j_3^{\mathrm{trop}} + \mathrm{val}(C') - \mathrm{val}(Q_4')$. Lemma 8.1 and (7.11) gives

$$\mathrm{val}(C')-\mathrm{val}(Q_4') = \begin{cases} -6(\omega_6+\omega_5+\omega_3)+6(\omega_6+\omega_5)+2d_{34}+4\omega_3 = -L_0 & \text{if } \underline{\omega} \in \Theta_0, \\ -6(\omega_6+\omega_5+\omega_3)+6\omega_6+4\omega_5+8\omega_3 = -L_1 & \text{if } \underline{\omega} \in \Theta_1, \\ -6(\omega_6+\omega_5+\omega_3)+6(\omega_6+\omega_5)+4\omega_3+2\omega_2 = -L_2 & \text{if } \underline{\omega} \in \Theta_2. \end{cases}$$

By Lemma 8.2 and Theorem 7.3 we conclude that on Type (II) curves

$$j_{4\overset{\circ}{\textcircled{\circ}}}^{\mathrm{trop}} = j_{3\overset{\circ}{\textcircled{\circ}}}^{\mathrm{trop}} - \min\{L_0, L_1, L_3\} = L_0 + L_1 + L_2 - \min\{L_0, L_1, L_3\}.$$

Analogous arguments as the ones provided in the proof of Theorem 7.3 and the genericity of $\mathcal{X}$ ensure that the given formulas are valid under specialization. □

The Igusa functions j_1, j_2, j_4 characterize isomorphism types in M_2. The tropical Igusa functions $j_1^{\mathrm{trop}}, j_2^{\mathrm{trop}}$ and j_4^{trop} allow us to recover partial length data for each point in M_2^{trop}, once we determine the combinatorial type of the curve using Theorem 1.1 and Table 5.1. The methods presented in this section will not produce a complete set of tropical invariants on M_2^{trop}. Indeed, we have exploited the unique relation among the valuations of A, B, and C to build j_4 and no further combination of A, B, C would produce a cancellation of initial terms. It remains an interesting challenge to develop an alternative approach to generate a new algebraic invariant on M_2 inducing the missing tropical invariant on each cell of M_2^{trop}.

Acknowledgments

We wish to thank Claus Fieker, Michael Joswig, Lars Kastner, Ralph Morrison, Sam Payne, Padmavathi Srinivasan, Bernd Sturmfels and Annette Werner for very fruitful conversations. We thank the two anonymous referees for useful suggestions on an earlier version of this paper. The first author was supported by an Alexander von Humboldt Postdoctoral Research Fellowship (Germany), an NSF postdoctoral fellowship DMS-1103857 and an NSF Standard Grant DMS-1700194 (USA). The second author was supported by the DFG transregional collaborative research center grant SFB-TRR 195 "Symbolic Tools in Mathematics and their Application", INST 248/235-1 (Germany).

Part of this project was carried out during the 2013 program on *Tropical Geometry and Topology* at the Max-Planck Institut für Mathematik in Bonn (Germany), where the second author was in residence, and during the 2016 major program on *Combinatorial Algebraic Geometry* at the Fields Institute in Toronto (Canada), where both authors

were in residence. The authors would like to thank both institutes for their hospitality, and for providing excellent working conditions.

References

[1] D. Abramovich, L. Caporaso, S. Payne, The tropicalization of the moduli space of curves, Ann. Sci. Éc. Norm. Supér. (4) 48 (4) (2015) 765–809.
[2] L. Allermann, J. Rau, First steps in tropical intersection theory, Math. Z. 264 (3) (2010) 633–670.
[3] M. Baker, S. Norine, Harmonic morphisms and hyperelliptic graphs, Int. Math. Res. Not. IMRN (15) (2009) 2914–2955.
[4] M. Baker, S. Payne, J. Rabinoff, On the structure of non-Archimedean analytic curves, in: Tropical and Non-Archimedean Geometry, in: Contemp. Math., vol. 605, Amer. Math. Soc., Providence, RI, 2013, pp. 93–121.
[5] M. Baker, S. Payne, J. Rabinoff, Nonarchimedean geometry, tropicalization, and metrics on curves, Algebraic Geom. 3 (1) (2016) 63–105.
[6] V.G. Berkovich, Spectral Theory and Analytic Geometry over Non-Archimedean Fields, Mathematical Surveys and Monographs, vol. 33, Amer. Math. Soc., Providence, RI, 1990.
[7] L.J. Billera, S.P. Holmes, K. Vogtmann, Geometry of the space of phylogenetic trees, Adv. in Appl. Math. 27 (4) (2001) 733–767.
[8] B. Bolognese, M. Brandt, L. Chua, From curves to tropical Jacobians and back, in: Combinatorial Algebraic Geometry, in: Fields Inst. Commun., vol. 80, Fields Inst. Res. Math. Sci, Toronto, ON, 2017, pp. 21–45.
[9] M. Brandt, P.A. Helminck, Tropical superelliptic curves, arXiv:1709.05761, 2017.
[10] S. Brodsky, M. Joswig, R. Morrison, B. Sturmfels, Moduli of tropical plane curves, Res. Math. Sci. 2 (2015) 4, 31.
[11] E. Brugallé, I. Itenberg, G. Mikhalkin, K. Shaw, Brief introduction to tropical geometry, in: Proceedings of the Gökova Geometry–Topology Conference 2014, Gökova Geometry/Topology Conference (GGT), Gökova, 2015, pp. 1–75.
[12] E.A. Brugallé, L.M. López de Medrano, Inflection points of real and tropical plane curves, J. Singul. 4 (2012) 74–103.
[13] A. Buchholz, H. Markwig, Tropical covers of curves and their moduli spaces, Commun. Contemp. Math. 17 (1) (2015) 1350045, 27.
[14] L. Caporaso, Algebraic and tropical curves: comparing their moduli spaces, in: Handbook of Moduli. Vol. I, in: Adv. Lect. Math. (ALM), vol. 24, Int. Press, Somerville, MA, 2013, pp. 119–160.
[15] L. Caporaso, Gonality of algebraic curves and graphs, in: Algebraic and Complex Geometry, in: Springer Proc. Math. Stat., vol. 71, Springer, Cham, 2014, pp. 77–108.
[16] R. Cavalieri, M. Chan, M. Ulirsch, J. Wise, A moduli stack of tropical curves, arXiv:1704.03806, 2017.
[17] R. Cavalieri, H. Markwig, D. Ranganathan, Tropicalizing the space of admissible covers, Math. Ann. 364 (3–4) (2016) 1275–1313.
[18] M. Chan, Combinatorics of the tropical Torelli map, Algebra Number Theory 6 (6) (2012) 1133–1169.
[19] M. Chan, Tropical hyperelliptic curves, J. Algebraic Combin. 37 (2) (2013) 331–359.
[20] M.A. Cueto, H. Markwig, How to repair tropicalizations of plane curves using modifications, Exp. Math. 25 (2) (2016) 130–164.
[21] W. Decker, G.-M. Greuel, G. Pfister, H. Schönemann, Singular 4-1-0 — A computer algebra system for polynomial computations, http://www.singular.uni-kl.de, 2016.
[22] K. Fukuda, A.N. Jensen, R.R. Thomas, Computing Gröbner fans, Math. Comp. 76 (260) (2007) 2189–2212 (electronic).
[23] A. Gathmann, M. Kerber, H. Markwig, Tropical fans and the moduli spaces of tropical curves, Compos. Math. 145 (1) (2009) 173–195.
[24] E. Gawrilow, M. Joswig, polymake: a framework for analyzing convex polytopes, in: G. Kalai, G.M. Ziegler (Eds.), Polytopes — Combinatorics and Computation, Birkhäuser, 2000, pp. 43–74.
[25] L. Gerritzen, M. van der Put, Schottky Groups and Mumford Curves, Lecture Notes in Mathematics, vol. 817, Springer, Berlin, 1980.
[26] A. Gibney, D. Maclagan, Equations for Chow and Hilbert quotients, Algebra Number Theory 4 (7) (2010) 855–885.

[27] E.Z. Goren, K.E. Lauter, Genus 2 curves with complex multiplication, Int. Math. Res. Not. IMRN 5 (2012) 1068–1142.
[28] D.R. Grayson, M.E. Stillman, Macaulay2, a software system for research in algebraic geometry. Available at http://www.math.uiuc.edu/Macaulay2/, 2009.
[29] A. Gross, Correspondence theorems via tropicalizations of moduli spaces, Commun. Contemp. Math. 18 (3) (2016) 1550043, 36.
[30] W. Gubler, J. Rabinoff, A. Werner, Skeletons and tropicalizations, Adv. Math. 294 (2016) 150–215.
[31] W. Gubler, J. Rabinoff, A. Werner, Tropical skeletons, Ann. Inst. Fourier (Grenoble) 67 (5) (2017) 1905–1961.
[32] P. Helminck, Tropical Igusa invariants and torsion embeddings, arXiv:1604.03987.
[33] J. Igusa, Arithmetic variety of moduli for genus two, Ann. of Math. (2) 72 (1960) 612–649.
[34] I. Itenberg, G. Mikhalkin, E. Shustin, Tropical Algebraic Geometry, second edition, Oberwolfach Seminars, vol. 35, Birkhäuser Verlag, Basel, 2009.
[35] A.N. Jensen, Gfan, a software system for Gröbner fans and tropical varieties. Available at http://www.math.tu-berlin.de/~jensen/software/gfan/gfan.html, 2009.
[36] A.N. Jensen, H. Markwig, T. Markwig, `tropical.lib`. A SINGULAR 3.0 library for computations in tropical geometry, http://www.math.uni-tuebingen.de/user/keilen/en/tropical.html, 2007.
[37] E. Katz, H. Markwig, T. Markwig, The j-invariant of a plane tropical cubic, J. Algebra 320 (10) (2008) 3832–3848.
[38] M. Kerber, H. Markwig, Counting tropical elliptic plane curves with fixed j-invariant, Comment. Math. Helv. 84 (2) (2009) 387–427.
[39] K. Lauter, T. Yang, Computing genus 2 curves from invariants on the Hilbert moduli space, J. Number Theory 131 (5) (2011) 936–958.
[40] Q. Liu, Courbes stables de genre 2 et leur schéma de modules, Math. Ann. 295 (2) (1993) 201–222.
[41] D. Maclagan, B. Sturmfels, Introduction to Tropical Geometry, Graduate Studies in Mathematics, vol. 161, American Mathematical Society, Providence, RI, 2015.
[42] J.-F. Mestre, Construction de courbes de genre 2 à partir de leurs modules, in: Effective Methods in Algebraic Geometry, Castiglioncello, 1990, in: Progr. Math., vol. 94, Birkhäuser Boston, Boston, MA, 1991, pp. 313–334.
[43] G. Mikhalkin, Tropical geometry and its applications, in: International Congress of Mathematicians. Vol. II, Eur. Math. Soc., Zürich, 2006, pp. 827–852.
[44] G. Mikhalkin, Moduli spaces of rational tropical curves, in: Proceedings of Gökova Geometry–Topology Conference 2006, Gökova Geometry/Topology Conference (GGT), Gökova, 2007, pp. 39–51.
[45] S. Payne, Analytification is the limit of all tropicalizations, Math. Res. Lett. 16 (3) (2009) 543–556.
[46] Q. Ren, S.V. Sam, B. Sturmfels, Tropicalization of classical moduli spaces, Math. Comput. Sci. 8 (2) (2014) 119–145.
[47] J. Richter-Gebert, B. Sturmfels, T. Theobald, First steps in tropical geometry, in: Idempotent Mathematics and Mathematical Physics, in: Contemp. Math., vol. 377, Amer. Math. Soc., Providence, RI, 2005, pp. 289–317.
[48] D. Speyer, B. Sturmfels, The tropical Grassmannian, Adv. Geom. 4 (3) (2004) 389–411.
[49] W. Stein, Sage Mathematics Software (Version 6.8), http://www.sagemath.org, 2015.
[50] J. Tevelev, Compactifications of subvarieties of tori, Amer. J. Math. 129 (4) (2007) 1087–1104.
[51] I. Tyomkin, Tropical geometry and correspondence theorems via toric stacks, Math. Ann. 353 (3) (2012) 945–995.
[52] T. Wagner, Faithful tropicalization of Mumford curves of genus two, Beitr. Algebra Geom. 58 (1) (2017) 47–67.